Continuum, Inc.

CALCULATION OF FLOW ABOUT POSTS AND POWERHEAD MODEL

Final Report CI-FR-D101-07

Contract No. NAS8-35506

Prepared For:

National Aeronautics and Space Administration
George C. Marshall Space Flight Center
Marshall Space Flight Center, AL 35812

Prepared By:

Continuum, Inc.
1500 Perimeter Parkway
Suite 125
Huntsville, AL 35806

1.0 Forward and Summary

This document was prepared by personnel at Continuum, Inc. of Huntsville, Alabama in fulfillment of Contract No. NAS8-35506 for the National Aeronautics and Space Administration, George C. Marshall Space Flight Center.

The material contained herein was produced by Continuum in support of the NASA mission under the direction of Mr. G.A. Wilhold of NASA/MSFC. In this effort various studies were performed using Continuum's computational fluid dynamics computer program, CONTINUSYS, (formerly named VAST). Many reports and presentations have been made under this procurement. In this document those efforts which have been reported elsewhere will be summarized and included as appendices.

The study encompassed a wide range of problems of interest to NASA and demonstrate the power and utility of a mature CFD capability.

2.0 Technical Discussion

A large number of computational fluid mechanics (CFD) problems of interest to NASA were investigated under this contract. Some of these efforts were of considerable magnitude, while others were minor. Of the primary studies, most have been documented elsewhere and will simply be summarized here. The previous documentation has been included as appendices for further clarification/information. The primary studies were:

- The analysis of the turnaround duct/hot gas manifold/transfer tubes (fuel side) of the SSME (references cited).
- The analysis of the LOX-T ("hot dog") manifold (oxidizer side) of the SSME (references cited).
- The analysis of hydrogen accumulation in the Vandeburg flame trench (references cited).
- Modification of the Intel/VT241 systems to accommodate the EADS and PLOT 3D (documented here).

Additionally, many other investigations were performed whose results were delivered to the cognizant NASA personnel as working information. Some of these efforts involved:

- Numerous axisymmetric solutions for the turnaround duct to investigate various configurations.
- Studies involving erosion of the SRB nozzle - both standard environments and postulations of surface aberrations which, once induced, might worsen or propagate.
- Postulation of defects and resultant flow field solutions for several other potential failures and failure modes.

These efforts remain undocumented due to the exploratory/educational nature of the problems/solutions. With regard to the failure analyses, all analyses were negative and therefore of no permanent value.

Additionally, consultation and assistance was provided to NASA/MSFC personnel in numerous flow solutions using the CONTINUSYS code. These efforts are also undocumented.

2.1 Hot Gas Manifold Analysis

Several three dimensional analyses of the hot gas manifold (including turnaround and transfer ducts) were conducted using the CONTINUSYS code during the course of this study. Results from these efforts have been presented in several reports and papers. Further documentation can be found in References 1-5.

The computation of the fluid flow in the HPFTP turbine exhaust system, consisting of the turnaround duct, hot gas manifold and transfer tube, was performed using CONTINUSYS. The configuration analyzed consisted of the First Manned Orbital Flight (FMOF) version of the turnaround duct, the "phase 3" two duct hot gas manifold and the "Version B" transfer tube which includes the flow separator. The effects of turbine-induced swirl were considered negligible, hence a plane of symmetry between the two transfer tubes was incorporated.

The turnaround duct consists of an annular passage which has an 180 deg. turn in the axial direction. This duct conveys hot turbine exhaust gases from the turbine rotors to the manifold. The hot gas manifold consists of a spherically shaped bowl which collects the flow from the turnaround duct and sends it to the two transfer tubes. The transfer tubes are passages with elliptical cross sections and contoured inlets which transfer the hot gases to the engine main injector assembly. It is the flow environment in the exit plane of the transfer tubes that is required to analyze the flow about the LOX posts. The flow environment in the transfer tube exit planes was determined by analyzing the fluid flow in the turnaround duct, hot gas manifold and transfer tubes. Flow conditions at the exit from the turbine were used as fixed known conditions and the flow through the system was computed using CONTINUSYS.

The effects of turbine swirl were neglected, allowing the assumption of symmetry between the transfer tubes. This permitted the problem to be analyzed using only one half of the actual system. The system was modeled with a three dimensional grid network containing 10,724 nodes. This grid, considered the minimum necessary to achieve a qualitative result, is depicted in Figure A. The struts and posts in the exit region of the turnaround duct have been darkened to clarify their locations.

The boundary conditions on the inlet plane of the turnaround duct were specified by NASA. Sinusoidal pressure and velocity distributions based on test data were also supplied. A wall friction type turbulence model was used to determine the effects of turbulence on the system. The turbulent fluid flow environment in the HPFTP hot gas exhaust system was analyzed using CONTINUSYS in order to describe the environment near the LOX posts. The analysis predicted non-uniform swirl patterns in the transfer tube exit plane which may influence LOX post structural integrity. The results of the analysis will be used to define the fluid flow environment near single and multiple LOX posts in support of NASA's LOX post analyses.

An example of the grid distribution typical of the three dimensional analyses is given below.

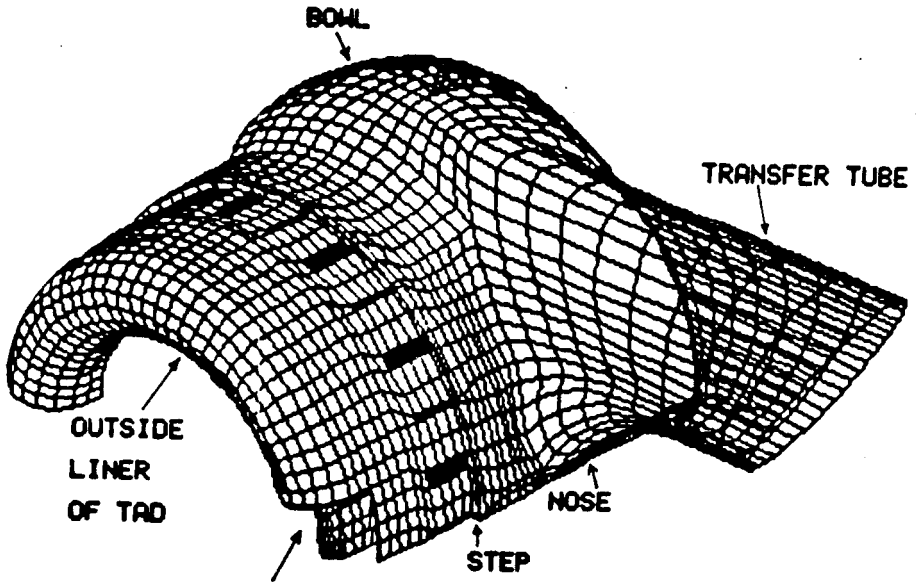

This very complex three dimensional fluid flow problem was analyzed using Continuum's CM-1000 workstation and a CRAY computer. All problem definition tasks and graphic displays were performed interactively on the workstation. The CRAY supercomputer was accessed directly from the workstation and was used to execute the CONTINUSYS code in its vectorized form. Use of the workstation concept greatly facilitated and accelerated problem definition and execution, mainly due to the interactive editing and graphics capabilities of the workstation.

2.2 LOX-T Manifold Analysis

Structural problems in the SSME LOX-T ("hot dog") manifold have occurred in some engines. An analysis of the configuration was conducted in an attempt to explain why cracks appeared in the vanes and whether the LOX-T design was responsible for a vibratory phenomena noticed in the engine.

An exploratory analysis was conducted which was two dimensional. The intent was to explore and understand, at a minimum cost, the flow in the "hot dog" and to compare the resuls with a water table experiment which had been conducted on a similar two dimensional approximation to the manifold.

The problem geometry and grid discretization is shown below.

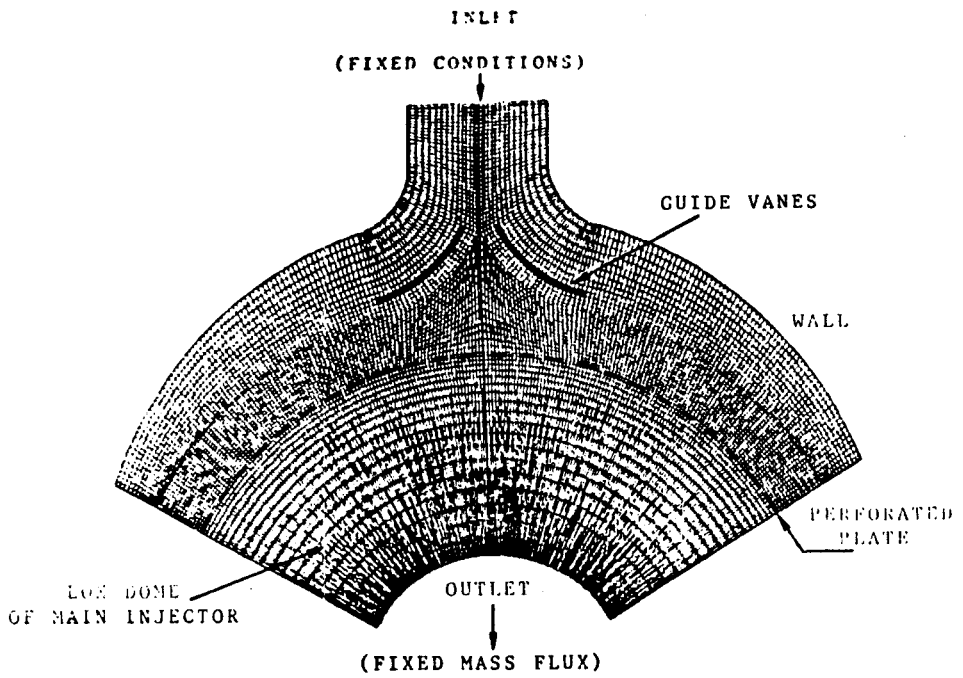

The flow enters through the inlet pipe as shown, is deflected by the guide vanes, and enters the manifold through a perforated plate. The entire investigation is discussed in Reference 6. In the referenced investigation vortical flow is calculated to exist between the guide vanes and the perforated plate and even downstream of the perforated plate. Force coefficients were calculated for the guide vanes and delivered to NASA. This information was, in turn, given to another contractor for a flutter analysis.

Based on the analysis, it did not appear that the previously mentioned vibratory phenomena was due to vortical flow/shedding in the LOX-T. A full three dimensional analysis should be undertaken to verify this tentative conclusion which was, of course, based on a two dimensional approximation.

2.3 Hydrogen Accumulation in the Vandenburg Flame Trench

This study effort investigated the hazard potential of hydrogen accumulation in the flame trench during an SSME shutdown. The flame trench and the grid discretization of the trench and surrounding region are depicted below.

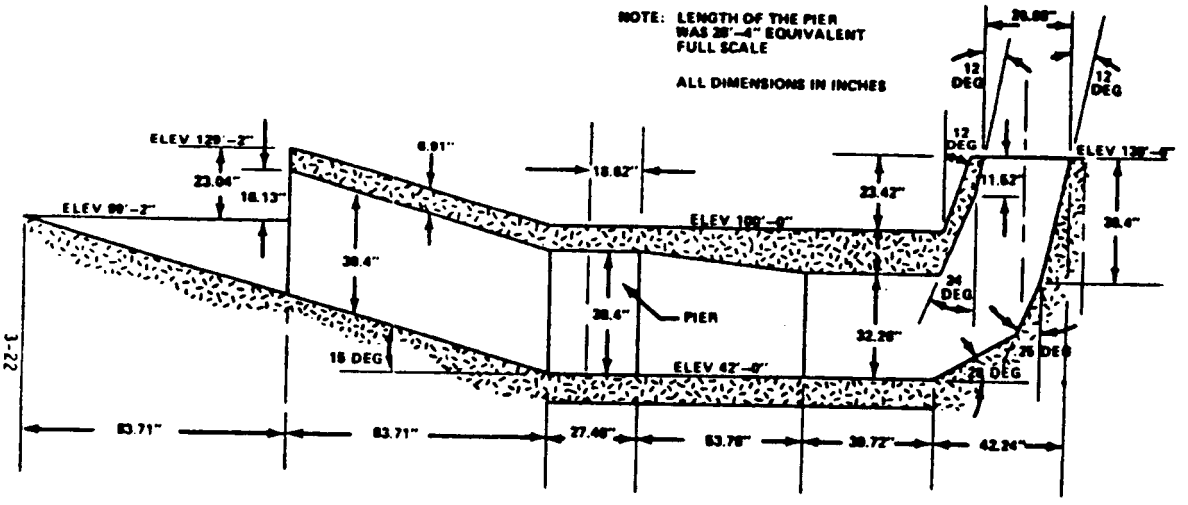

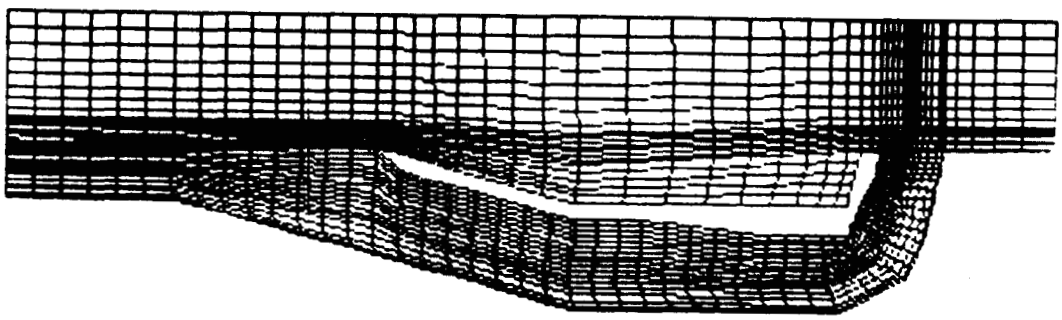

2D FLAME TRENCH GRID DEFINITION

In the simulation a 34 knot wind blowing from the right hand side was assumed as a worst case. The plume was allowed to flow for one second, then the oxidizer flow was turned off, but the hydrogen continued to flow for an additional 1.5 seconds. Reference 7 discusses the situation in greater detail, but the primary conclusion is that a hazardous situation may occur if some positive steps are not taken to alleviate this situation. The most obvious is to remove the flame trench cover.

2.4 CONTINUSYS/EADS/PLOT3-D Interface Task

Continuum performed two tasks which allowed NASA to better utilize the capabilities of the CONTINUSYS code in conjunction with the Engineering Analysis and Data System (EADS) facility at Marshall Center. These two tasks were to interface NASA's Intel CM1000 workstation to the EADS network and to provide a compatibility between the CONTINUSYS code and the NASA-Ames PLOT3D graphics code. The work accomplished for each of these tasks is discussed individually.

2.4.1 CM1000 - EADS Interface

Continuum modified NASA's Intel CM1000 workstation to allow it to interface with the EADS network. The workstation design included the capability to interface with a

remote mainframe computer by allowing the workstation to appear as a remote job entry (RJE) station to the mainframe. RJE interfaces to mainframe computers traditionally utilize a communications protocol to transfer data over communications lines in a predictable, verifiable manner. Although the CM1000 workstation previously had been equipped with a communication capability, that capability utilized the 200UT communications protocol to provide communications with NASA-Ames. The EADS system does not support the 200UT protocol for RJE operations, but instead supports the 3780 protocol. The task thus became one of providing a 3780 interface from the CM1000 while maintaining the 200UT interface capability.

The 3780 interface capability was provided using a protocol converter, an external electronics device which would perform all of the protocol formatting and transmission interaction tasks and relieve the Intel processor of these functions. This approach was the same as had been succussfully used with the 200UT protocol. The A/S-2G protocol converter from the Black Box Corporation was selected. This converter was installed between the Intel of the CM1000 and a Bus Interface Unit connected to the EADS network, thus providing a direct connection from the CM1000 to the EADS network. To maintain communications capability with NASA-Ames, the 3780 protocol converter was connected to the Intel through a data selector switch. This switch, through which the 200UT protocol converter was also routed, allows the user to physically connect either of the protocol converters to the Intel in a simple manner, depending on the site with which communications is desired.

Although the communications protocol functions were provided through a protocol converter, a software handler needed to be developed to interface the Intel with the protocol converter. A handler existed for the 200UT protocol converter but was not compatible with the 3780 protocol converter. This handler was successfully developed and installed on the Intel, but with one limitation. Since the Intel hardware as configured in the CM1000 is incapable of controlling the flow of information from the protocol converter, the transmission rate between the protocol converter and the Intel had to be restricted to 1200 baud to prevent data from arriving at the Intel faster than the Intel could process it. Increasing the transmission rate above 1200 baud leads to the eventual overrunning and loss of data between the protocol converter and the Intel.

The CM1000 workstation, being designed to operate as an RJE station interfacing to a

mainframe computer, contains the mechanisms to generate complete job streams for the intended mainframe. Therefore, the CM1000 needed to be customized to be able to generate job streams which were compatible with EADS. This customization was successfully accomplished under this task.

2.4.2 CONTINUSYS - PLOT3D interface

NASA desired the ability to process results from the CONTINUSYS code using the PLOT3D plotting capability developed at NASA-Ames. Having this capability would allow NASA to produce plot results generated by CONTINUSYS, using the plotting facilities being established at Marshall Center and which were based on PLOT3D. The original approach envisioned was that the CONTINUSYS code would be modified to produce data files which were in a format compatible with PLOT3D.

When Continuum investigated the capabilities of the PLOT3D package, it was realized that PLOT3D was more restrictive in types of problems allowed than was the CONTINUSYS code. These restrictions included: PLOT3D allows only one specie of gas, whereas the CONTINUSYS code allows multiple species; and, PLOT3D assumes a fixed gas constant of 1.0 and a fixed ratio of specific heats of 1.4, whereas the CONTINUSYS code allows these quantities to be specified by the user for each problem. Modifying the CONTINUSYS code to conform to these restrictions would severly limit the capability available with the CONTINUSYS code. It was therefore decided to develop a separate code which would function as a translator between CONTINUSYS and PLOT3D.

The translator was successfully developed within a code named CONVRT which was installed on EADS. What follows is a discussion of the operation of CONVRT. The CONVRT code is written in FORTRAN and runs on the EADS Cray, in order to be able to easily access the binary data files created by the CONTINUSYS code. The PLOT3D-compatible data files are formatted data files, conforming to the PLOT3D format

specifications. The CONVRT code, when executed, reads one control card from the standard data input stream. That card should have a (2A1,I5) format, where the two alphabetic fields define the type of translation to be performed and the integer field defines the CONTINUSYS step number to be processed if checkpoint data is being translated. The translation types available and the files used by CONVRT in each case are as follows.

MP - Convert CONTINUSYS mesh data to PLOT3D grid data. Unit 2 is the input CONTINUSYS mesh data file, unit 4 is the output PLOT3D grid file.

GP - Convert CONTINUSYS geometry data to PLOT3D grid data. Unit 2 is the input CONTINUSYS geometry data file, unit 4 is the output PLOT3D grid file.

CP - Convert CONTINUSYS checkpoint data to PLOT3D checkpoint data. The desired step number must be input on the control card. Unit 2 is the input CONTINUSYS geometry data file, unit 3 is the input CONTINUSYS checkpoint data file, unit 4 is the output PLOT3D checkpoint file.

MV - Convert PLOT3D grid data to CONTINUSYS mesh data. Unit 2 is the input PLOT3D grid data file, unit 4 is the output CONTINUSYS mesh data file.

The following considerations should be made regarding the overcoming of the PLOT3D restrictions noted above. When checkpoint data is converted from a CONTINUSYS analysis containing multiple species, then all of the specie densities are combined to form a composite density and this composite density is placed into the PLOT3D data file. Since the data values contained in the PLOT3D checkpoint data file represent density, momentum, and energy, then any values computed from these are influenced by the gas properties assumed. The gas properties assumed by PLOT3D may not match the gas

properties used by the CONTINUSYS code; therefore, the values of pressure, temperature, and Mach number must be scaled to determine the values plotted by PLOT3D. The appropriate scale factors are as follows.

$$K_T = \frac{(.4)\ (R)}{\gamma - 1}$$

$$K = \frac{.4}{\gamma - 1}$$

$$K_M = \sqrt{\frac{\gamma(\gamma - 1)}{.56}}$$

Note that these scaling factors will not work correctly if the CONTINUSYS problem contains multiple gas species which have differing properties, as the gas properties of the combined gas are not constant throughout the flow field but vary with composition.

3.0 Conclusions

A number of complex computational fluid mechanics problems related to the space shuttle were addressed under this contract. Some of the analyses were exploratory in nature, using the CONTINUSYS code to provide preliminary information to enhance understanding of the problem, while in others the primary thrust was to acquire design information. In all cases the ability to predict information rapidly in these very complex analyses is seen to be an important demonstration of the power and utility of this mature predictive capability.

REFERENCES

1. "Calculation of Flow About Posts and Powerhead Model", P.G. Anderson, et al, Interim Report, CI-IT-0079, January 21, 1985. (Appendix A)

2. "Calculation of Flow About Posts and Powerhead Model", P.G. Anderson et al, Interim Report, December 26, 1985. (Appendix B)

3. "SSME Data Reduction For Comparative Study", T.S. Wang et al, CI-TR-0095, June 27, 1986. (Appendix C)

4. "Turbulent Flow In the Turnaround Duct, Hot Gas Manifold and Transfer Tubes", R.C. Farmer, et al, presented at the third Computational Fluid Dynamics Workshop at George C. Marshall Space Flight Center, June 11, 1985. (Appendix D)

5. "Flow Analysis of SSME HPFTP Exhaust System", P.G. Anderson, presented at the second Computational Fluid Dynamics Workshop at George C. Marshall Space Flight Center, November 28, 1984. (Appendix E)

6. "Flow Analysis of the SSME LOX Manifold", Y.M. Dakhoul, C.M. Seaford, presented at the fourth Computational Fluid Dynamics Workshop at George C. Marshall Space Flight Center, April 8 - 11, 1986. (Appendix F)

7. "Two Dimensional Flame Trench Simulation During Engine Shutoff", T.S. Wang, H.V McConnaughey, presented at the fourth Computational Fluid Dynamics Workshop at George C. Marshall Space Flight Center, April 8 - 11, 1986. (Appendix G).

APPENDIX A

CALCULATION OF FLOW ABOUT POSTS AND POWERHEAD MODEL

Interim Report, Contract NAS8-35506

CI-IR-0079

Prepared For:

National Aeronautics and Space Administration
George C. Marshall Space Flight Center
Marshall Space Flight Center, AL 35812

By:

Peter G. Anderson
Richard C. Farmer

CONTINUUM, Inc.
4715 University Drive
Suite 118
Huntsville, AL 35805

January 21, 1985

TABLE OF CONTENTS

TABLE OF FIGURES

FORWARD

This document was prepared by personnel at Continuum, Inc. for NASA-MSFC under Contract NAS8-35506. This document is an interim report on the first year of work under this contract.

1. INTRODUCTION

1.1 Background

The highly non-uniform flow around the LOX posts in the SSME powerhead has contributed to a long history of failures of the posts. Both pressure and heating loads have caused problems which have resulted in undesirable, but necessary, design modifications such as the use of LOX post flow shields. The geometric complexity of the LOX post flowfield is enormous; 600 posts are fed by the five hot gas discharge ducts from the HPFTP and HPOTP. The posts are fluted to modify the structure of the trailing vortices and are shielded by plates covering pairs of posts in the outermost row. Hot gases flow along the sides of the injector elements into entry ports which conduct the flow through an annulus into the main combustion chamber. The region of posts which are subjected to extreme environments is contained within the region bounded by the exits of the hot gas transfer ducts, the bottom of the oxidizer manifold, and the space above the secondary plate. The hydrogen cavity flow between the primary and secondary plates does not cause severe environments and is not considered further.

Assuming that the flow from the HGM is symmetric about a plane through the center transfer tube, one-half of the region could be modeled at one time. Even the half-plane flow would be too complex to provide a direct numerical solution to the flow field of interest. Continuum has been contracted to address this problem by a phased effort which first models the flow around a single and small clusters (2-10) of posts, second models the velocity field in the cross-flow plane, and third models the entire flow region with a 3-dimensional network-type model. However, the contract has been modified to include a full 3-D numerical solution of the flow field in the high pressure fuel turbopump turnaround duct (TAD), hot gas manifold (HGM) and transfer tubes. The results of this

effort will be used to define boundary conditions for LOX post analyses.

1.2 Objectives

The following sections discuss the work performed under Phase I of the contract as modified to reflect the TAD/HGM/Duct analysis. These sections include a presentation of Continuum's laminar and turbulent boundary layer development in support of the LOX post study and the results of the 3-D HGM analysis.

2. SUMMARY

Continuum has developed shear stress wall functions which will permit viscous analyses without requiring excessive numbers of computational grid points. These wall functions, laminar and turbulent, have been compared to standard Blasius solutions and are directly applicable to the cylinder-in-crossflow class of problems to which the LOX post problem belongs. The results of this work are presented herein.

Continuum has also performed a full 3-D fluid flow analysis of the HPFTP exhaust system which consists of the turnaround duct, 2-duct hot gas manifold and the "Version B" transfer ducts. The results of this analysis are presented in this report.

3. HIGH REYNOLDS NUMBER CROSSFLOW ABOUT A CYLINDER

3.1 Introduction

In order to accurately account for pressure loading and heating to cylinders in crossflow, like for the LOX posts in the powerhead, a detailed flowfield prediction and suitable wall boundary conditions are required. It is impractical to resolve the flowfield in the vicinity of the wall with enough grid points to accurately calculate either the wall friction or heating, therefore a special wall treatment is required. "Wall functions" are commonly used to provide the required boundary conditions; however, care must be exercised in order not to make the wall functions too empirical. The end result is to predict

frictional losses from the detailed flow vectors, not from the mean channel flow. The following procedure was developed and tested with geometrically simple problems to provide the necessary CFD tools for powerhead analysis.

3.2 Laminar Boundary Layers

Laminar boundary layers on a flat plate were analyzed with Continuum's VAST code for constant density and temperature (hence pressure also) conditions. Figure 3-1 shows the results of these analyses compared to the Blasius solution. A mean lateral velocity was used as a boundary condition on the free-stream side of the computational region. The excellent agreement of the VAST solution with the Blasius solution suggests that no significant artificial viscosity effects are present in the solution for this case. Notice that only 15 lateral node points were used for this calculation. Identical results were obtained for a case run with 11 nodes, only one of which was initially in the boundary layer. When 7 nodes were used with a step velocity profile a solution was generated, but the accuracy of this solution was reduced. These results are considered acceptable, and the use of at least one node in the initial boundary layer is reasonable.

3.3 Turbulent Boundary Layer

For turbulent wall flows, including fully developed pipe flows, for a smooth wall the following empirical velocity profiles are valid.

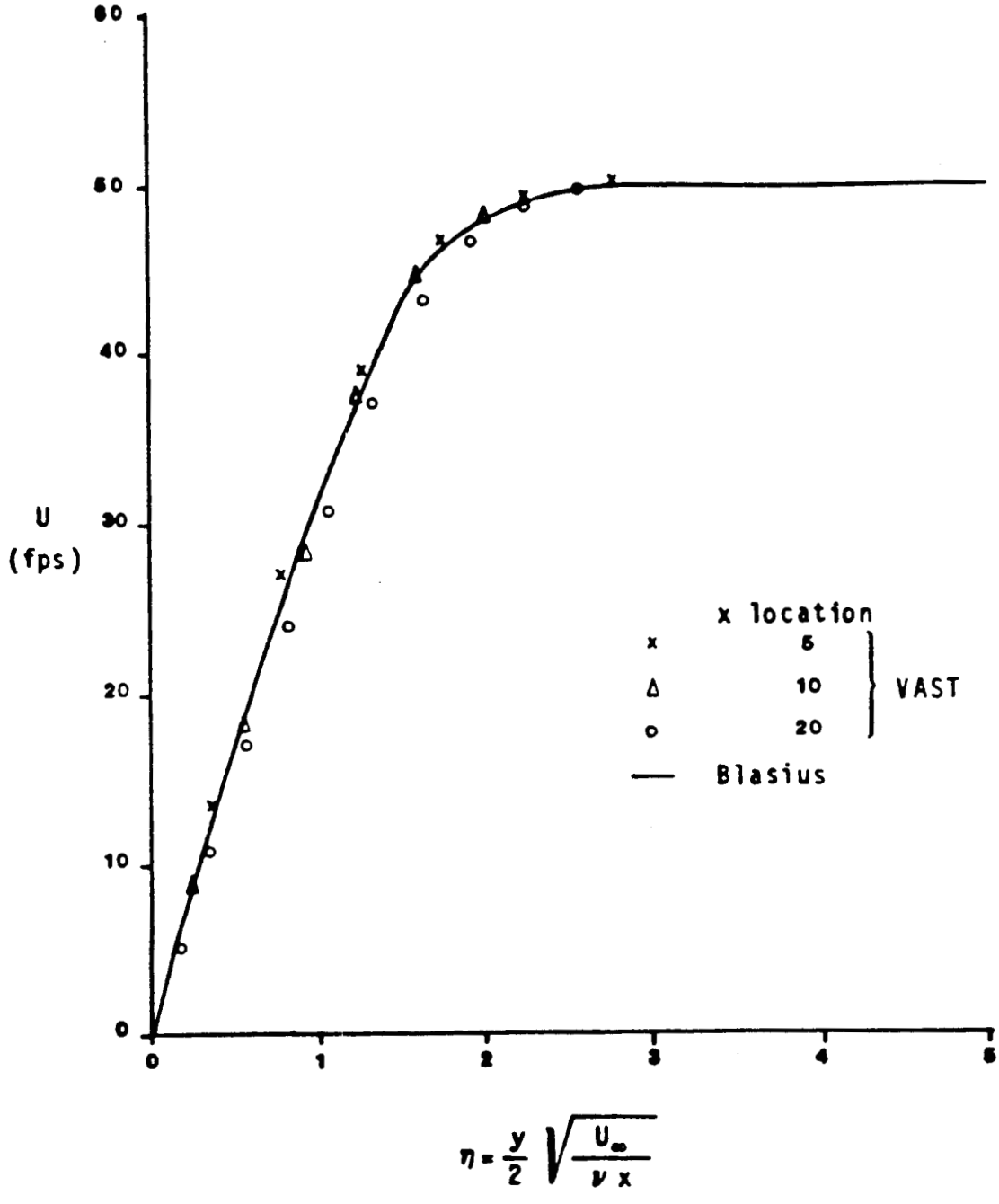

Fig. 3-1 Laminar Boundary Layer on a Flat Plate

$$u^+ = 5.5 + 2.5 \ln(y^+) \quad \text{for } y^+ > 30 \tag{3-1}$$

$$u^+ = -3.05 + 5.0 \ln(y^+) \quad \text{for } 5 < y^+ < 30 \tag{3-2}$$

$$u^+ = y^+ \quad \text{for } y^+ < 5 \tag{3-3}$$

where

$$u^+ = u/u^*$$

$$u^* = (\tau_o/\rho)^{0.5}$$

$$y^+ = (\tau_o/\rho)^{0.5}\, y/\nu$$

Blasius' empirical shear stress relationship is appropriate.

$$\tau_o = 0.0255\, \rho u^2 (\nu/u^* \ell)^{0.25} \tag{3-4}$$

where ℓ = R for pipe flow

$\ell = \delta$ for boundary layers

The boundary layer thickness implied by (3-4) and a 1/7 power-low profile is

$$\delta = 0.376\, X/R_e^{0.2} \tag{3-5}$$

From equation (3-3)

$$\left(\frac{\partial u}{\partial y}\right)_w = \tau_o/\rho = (u^*)^2/\nu \tag{3-6}$$

In terms of real distance from the wall, equation (3-1) represents most of the boundary layer, therefore the following computation procedure is suggested. A fictitous wall is assumed to be 0.0005 feet away from the real wall, and no flow is assumed to occur between the two walls. Equation (3-1) is valid at .0005 feet from the wall; hence, if u is calculated with a slip boundary condition, u^* is determined. Equation (3-6) is used to

calculate the velocity gradient at the wall. Since equation (3-1) is not explicit in u^*, the approximation

$$u^* = 0.1662529\ u^{0.867325}/(y/\nu)^{0.132675} \qquad (3-7)$$

is used. These equations determine the velocity gradient and shear stress at the wall. An eddy viscosity is used to determine both the local shear stress and the variation of this stress with distance from the wall, y.

$$\mu_T = 0.07\ u^* \ell\,(FR) + \mu \qquad (3-8)$$

where

$$FR = (y/0.3\,\ell) \text{ for } 0 < (y/\ell) < 0.3$$
$$FR = 1.0 \text{ for } (y/\ell) > 0.3$$

Equations (3-7) and (3-8) and the momentum equations were used to calculate the turbulent boundary layer over a flat plate between 1 and 2 ft running length over the plate. A turbulent boundary layer was assumed at the leading edge of the plate. The flow was air with a free steam velocity of 100 fps (this is an approximate Reynolds Number of 10^6). By adjusting the constants in equations (3-7) and (3-8), the profile at the end of the plate was predicted to be that shown in Fig. 3-2. The fit is very good, especially near the wall; the calculated wall shear stress is within 5% of the correct answer. This procedure is accurate enough to extend its development to more geometrically complex flows. The reasons for the necessity of adjusting the constants in equations (3-7) and (3-8) and for the lack of better fit at y's near the free stream side of the boundary layer are still under investigation.

Research to continue these analyses until cylinders in cross-flow can be accurately simulated is in progress.

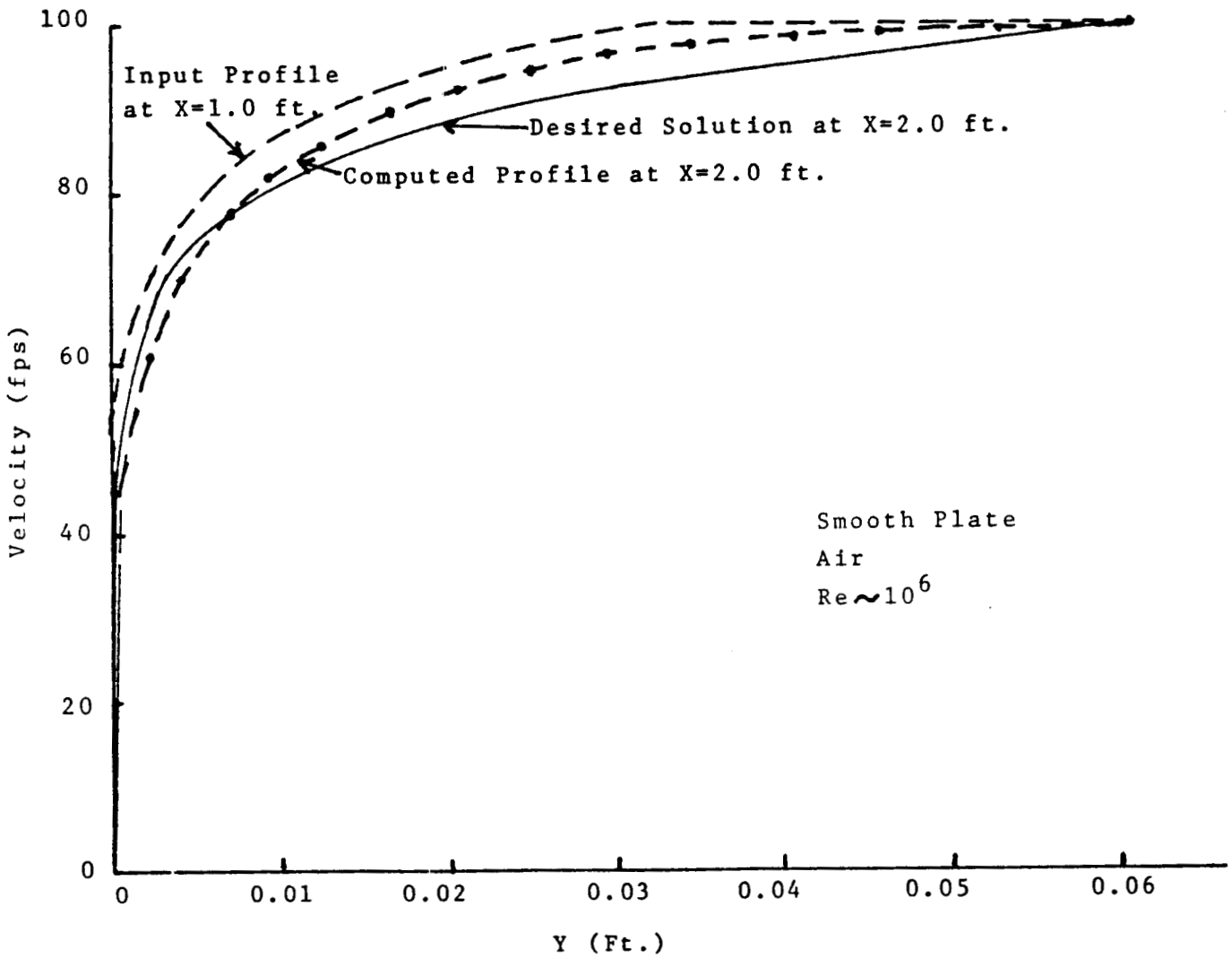

Fig. 3-2 Turbulent Boundary Layer Calculation

4. HGM FLOW ANALYSIS

4.1 Introduction

The analysis of the flow environment surrounding the SSME LOX posts requires a definition of the flow field in the HPFTP transfer tubes exit planes. The exit plane flow is development by defining the flow conditions immediately downstream of the turbine and computing the flow field through the turnaround duct, hot gas manifold and transfer tube. This section discusses the computation of the flow field in the turnaround duct, hot gas manifold and transfer duct for a two-duct configuration.

4.2 Configuration

The configuration analyzed consisted of the FMOF turnaround duct, the "Phase 3" two-duct hot gas manifold and the "Version B" transfer tube which includes the flow separator. The effects of turbine-induced swirl were neglected at the direction of the customer; hence, a plane of symmetry between the 2 transfer tubes was incorporated.

4.3 Flow Conditions at Inlet

The flow conditions at the inlet to the turnaround duct were specified by the customer. The fluid in the system was air at 530°R flowing at 72 lbm/sec. The pressure across the inlet was described by the equation.

$$P = \left[190.0\ 0.98 + 0.0441\ \mathrm{Sin}^2\left(\frac{\phi}{2}\right)\right] \mathrm{psia} \qquad (4\text{-}1)$$

where ϕ is the angular location which ranges from 0° between the transfer tubes and 180° on the plane of symmetry on the side fartherest from the transfer tubes. The velocity profile in the TAD inlet is defined by the equation

$$V = \bar{V}(1.0 + 0.04\ \mathrm{Cos}\phi) \qquad (4\text{-}2)$$

where V is the average velocity of any angle ϕ and $\bar{V}$ is the average velocity over the entire inlet. The velocity has no cross flow component due to the assumption of no turbine-induced swirl. The turbulent viscosity was specified as 10,000 times the molecular viscosity for air.

4.4 Computational Grid

The configuration described in subsection 4.2 was modeled using 10,724 nodal grid points. The grid points depicting the boundaries of the configuration are shown in Figs. 4-1, 4-2. The struts and posts in the turnaround duct have been darkened in to clarify their locations. The computational grid in the plane of symmetry at the 0° (between the transfer tubes) and 180° (far side) positions are shown in Fig. 4-3. The inlet to the turnaround duct has been artifically moved upstream to avoid influencing the flow in the 180° bend by the prescribed inlet flow conditions. Figures 4-1 through 4-3 illustrate that all of the salient features of the configuration have been incorporated into the grid.

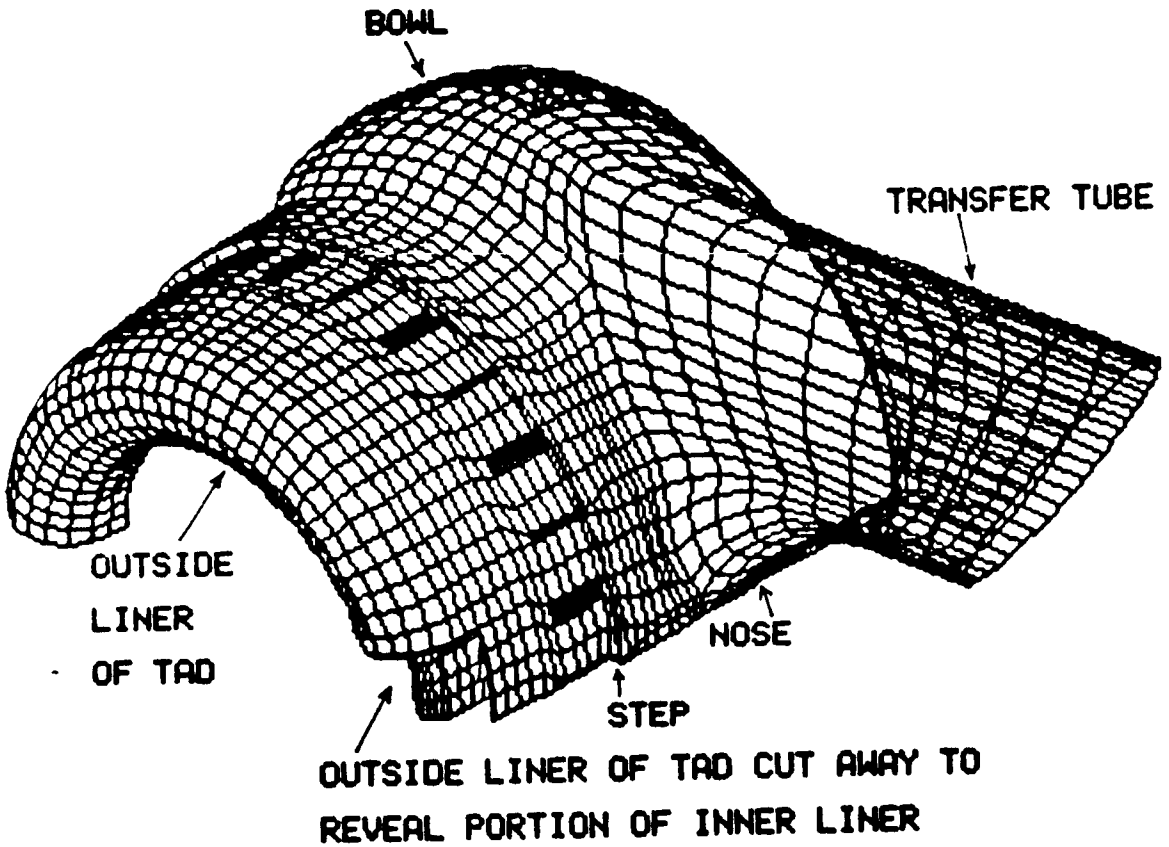

Fig. 4-1 View of Grid From Outside

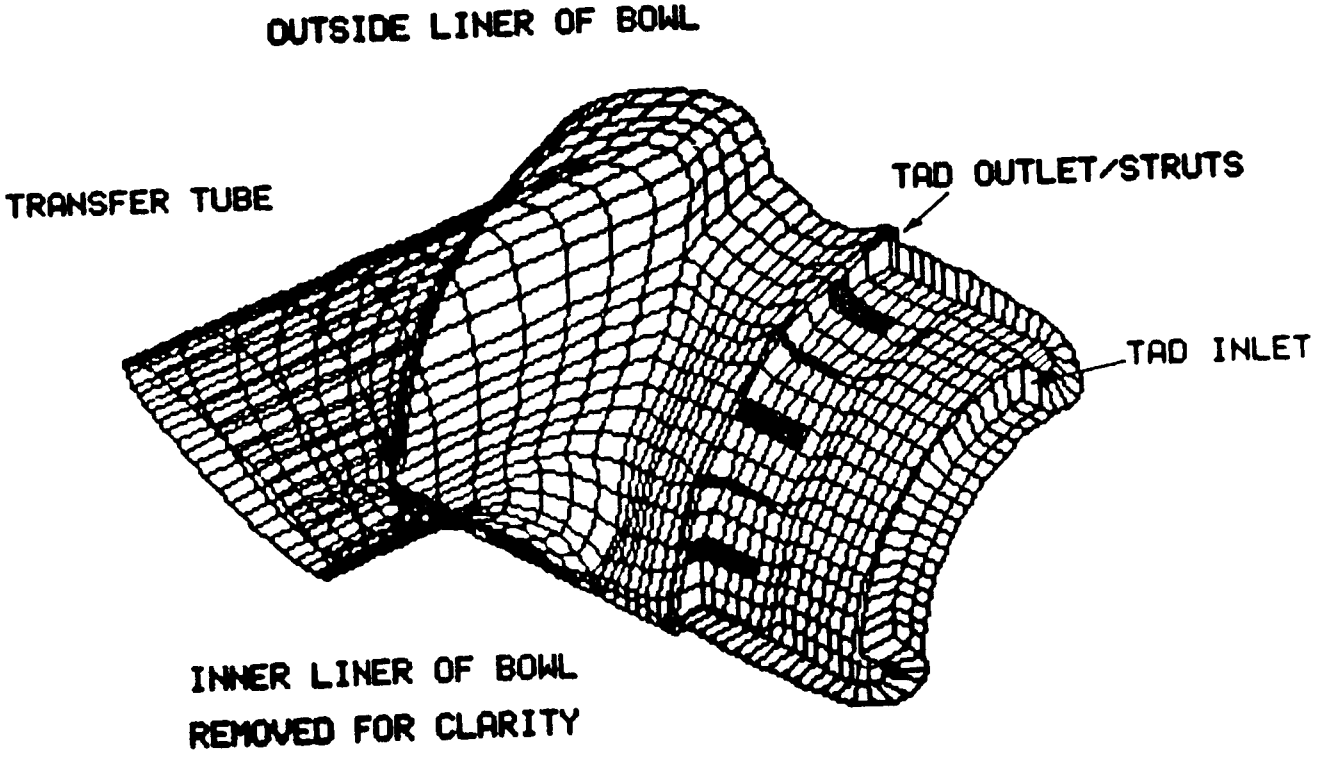

Fig. 4-2 View of Grid From Inside

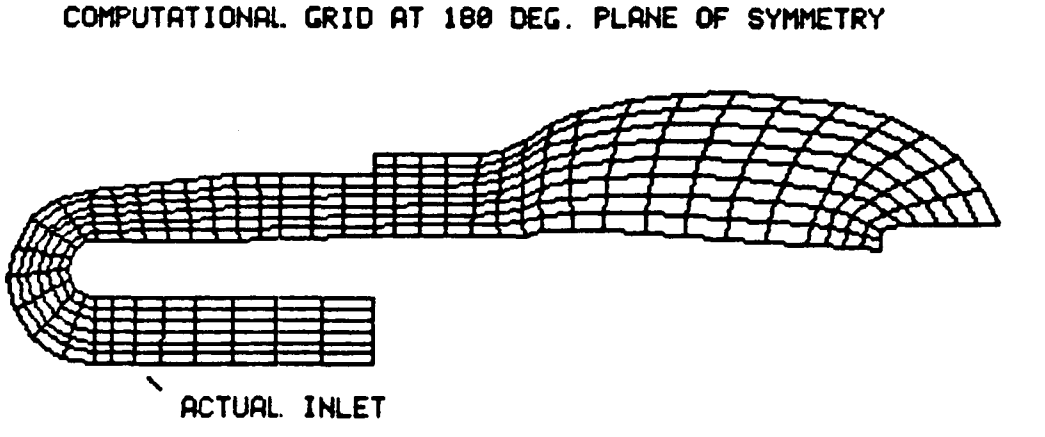

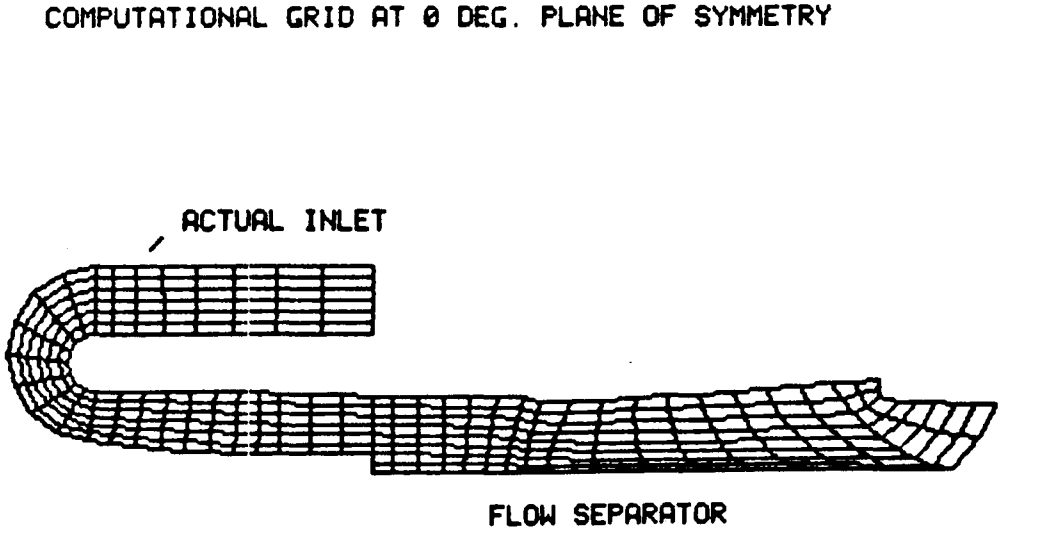

Fig. 4-3 Grids in Plane of Symmetry

4.5 Initial and Boundary Conditions

The inlet conditions prescribed in subsection 4.3 were applied to the artificially displaced inlet shown in Fig. 4-3. The viscosity of 10,000 times the molecular viscosity of air results in a Reynolds Number of 300 to 400 and, hence, laminar flow. Therefore a laminar parabolic velocity profile was superimposed on the average velocity distributed defined by Equation 4-2.

No-slip boundary conditions were specified for all solid walls and tangency, or free-slip, boundary conditions were applied to the plane of symmetry. The mass flow rate in the exit plane of the transfer tube was held fixed at 72 lbm/sec. The total conditions at the inlet were held fixed, thereby allowing spurious signals to pass upstream and out of the problem.

4.6 Results

The flowfield for the TAD, HGM and transfer tube described above was computed using Continuum's VAST code. The problem required 11,000 time steps before a converged solution was obtained. The results of the study were presented in detail to the customer on November 28, 1984. A summary of the results will be discussed in this section.

The total pressure drop through the system is presented in Fig. 4-4 and shows a drop of 18 psi in the 180 bend of the turnaround duct, a 14 psi drop through the struts, and a total drop through the system of 48 psi. Static pressure drop through the system was about 35 psi. The pressure variation in the circumferencial direction in the HGM bowl inlet is shown in Fig. 4-5 and indicates a variation of 30 psi. Exactly how much of this result is affected by the assumed inlet pressure variation (8.38 psi) is unknown but it appears to be small.

The pressure distribution in the cross section in the plane of symmetry between the transfer tubes is presented in contour form in Fig. 4-6. The figure shows significant pressure drops in the 180° bend of the TAD and through the struts. The pressure variation in the bowl is small except in localized areas.

The pressure in the exit plane of the transfer tube varies only about 4 psi, hence, the exit plane pressure distribution is not presented in this discussion. Instead, velocity contours in the transfer tube are presented in Fig. 4-7 to show the nonuniform velocity distribution. A small area of high speed flow appears in the outer and upper portion of the tube.

Figures 4-4 through 4-7 show large pressure gradients in the turnaround duct and small pressure gradients in the transfer tube indicating an improved design over the 3 duct system currently in use.

5. CLOSURE

The analyses of single and multiple LOX posts will be continued. The laminar flow analysis of the TAD/HGM/transfer tubes was completed; the turbulent flow case will be analyzed in the next reporting period.

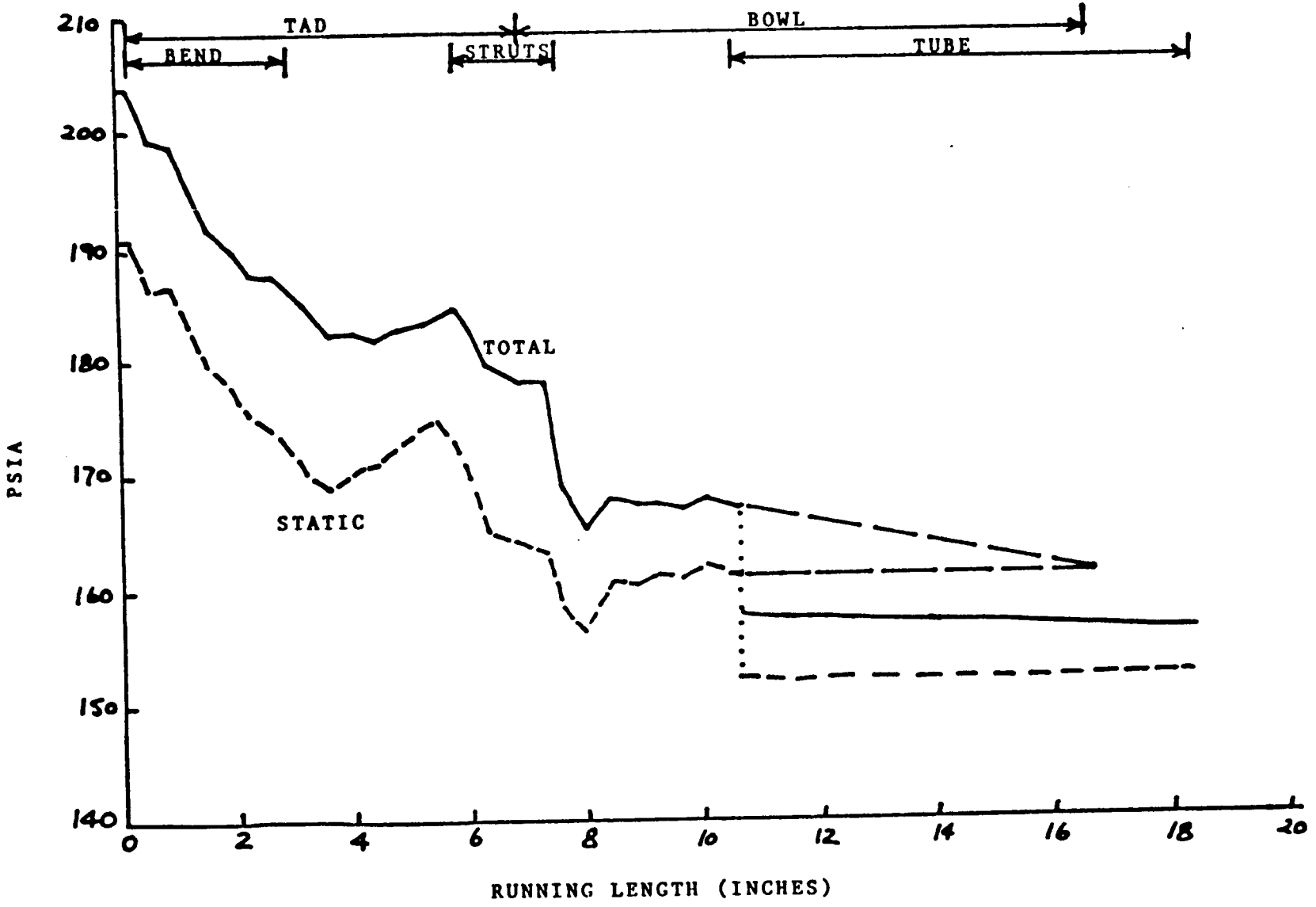

Fig. 4-4 Averaged Pressure in TAD/Bowl/Tube

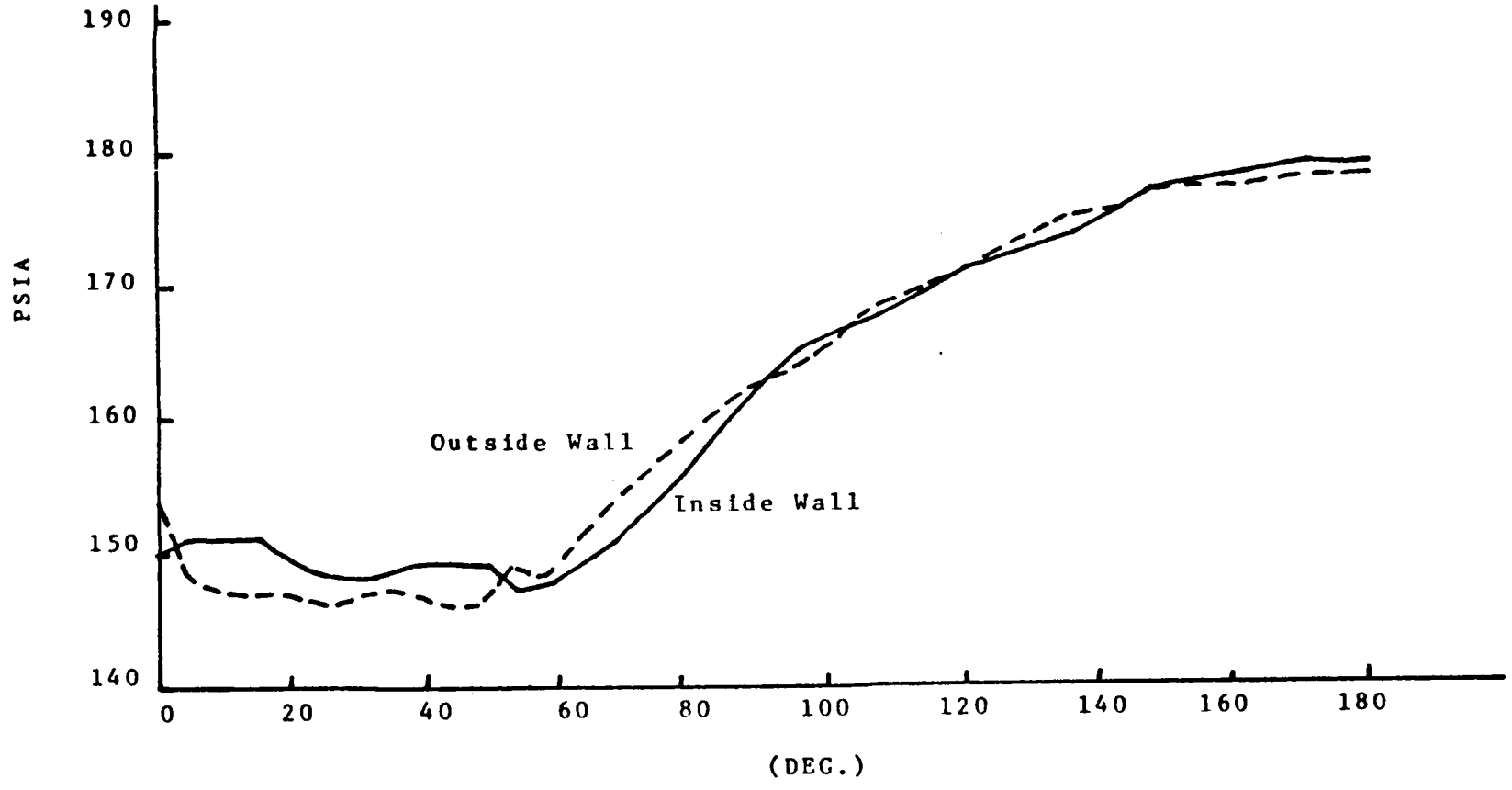

Fig. 4-5 Pressure Variation Around Bowl

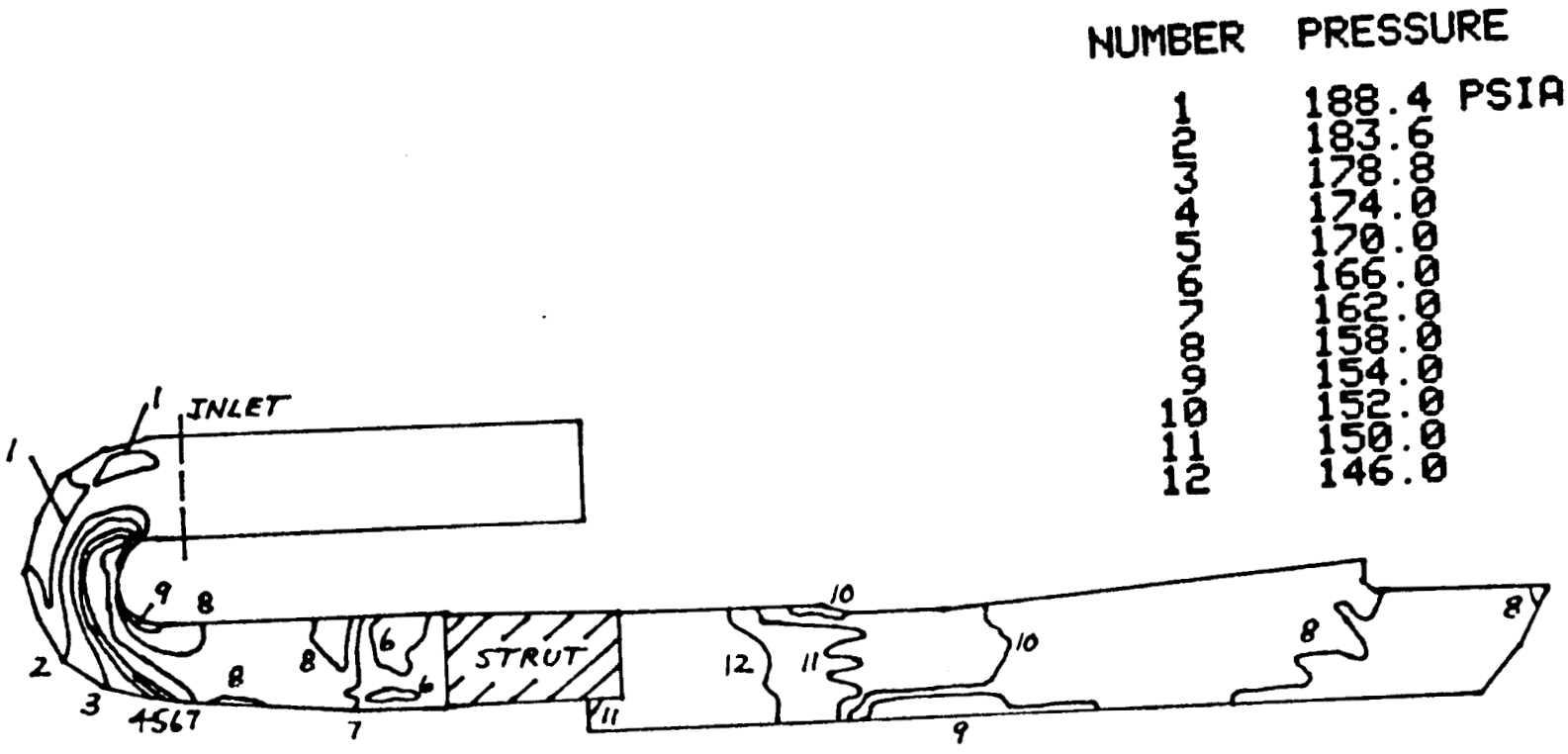

Fig. 4-6 Pressure Contours in TAD/Bowl at 0 Deg.

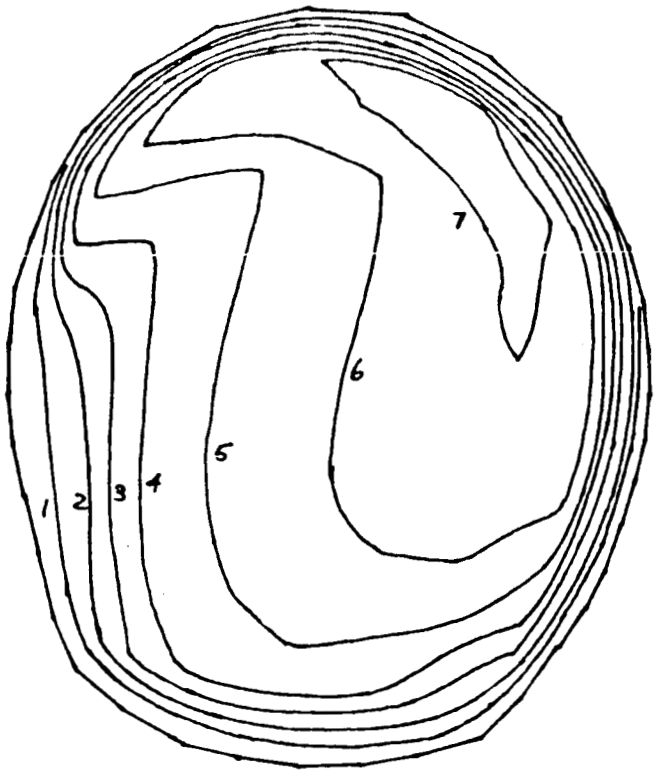

NUMBER	VELOCITY
1	44 FPS
7	308 FPS

Fig. 4-7 Velocity Contours Midway In Transfer Tube
(Looking into Tube from LOX Posts)

APPENDIX B

CALCULATION OF FLOW ABOUT POSTS AND POWERHEAD MODEL

Interim Report, Contract NAS8-35506

Prepared For:

National Aeronautics and Space Administration
George C. Marshall Space Flight Center
Marshall Space Flight Center, AL 35812

By:

Peter G. Anderson
Richard C. Farmer

CONTINUUM, Inc.
4715 University Drive
Suite 118
Huntsville, AL 35805

December 26, 1985

TABLE OF CONTENTS

TABLE OF FIGURES

FORWARD

This document was prepared by personnel at Continuum, Inc. for NASA-MSFC under Contract NAS8-35506. This document is an interim report on the second year of work under this contract.

1. INTRODUCTION

1.1 Background

The highly non-uniform flow around the LOX posts in the SSME powerhead has contributed to a long history of failures of the posts. Both pressure and heating loads have caused problems which have resulted in undesirable, but necessary, design modifications such as the use of LOX post flow shields. The geometric complexity of the LOX post flowfield is enormous; 600 posts are fed by the five hot gas discharge ducts from the HPFTP and HPOTP. The posts are fluted to modify the structure of the trailing vortices and are shielded by plates covering pairs of posts in the outermost row. Hot gases flow along the sides of the injector elements into entry ports which conduct the flow through an annulus into the main combustion chamber. The region of posts which are subjected to extreme environments is contained within the region bounded by the exits of the hot gas transfer ducts, the bottom of the oxidizer manifold, and the space above the secondary plate. The hydrogen cavity flow between the primary and secondary plates does not cause severe environments and is not considered further.

Assuming that the flow from the HGM is symmetric about a plane through the center transfer tube, one-half of the region could be modeled at one time. Even the half-plane flow would be too complex to provide a direct numerical solution to the flow field of interest. Continuum has been contracted to address this problem by a phased effort which first models the flow around a single and small clusters (2-10) of posts, second models the velocity field in the cross-flow plane, and third models the entire flow region with a 3-dimensional network-type model. However, the contract has been modified to include a full 3-D numerical solution of the flow field in the high pressure fuel turbopump turnaround duct (TAD), hot gas manifold (HGM) and transfer tubes. The results of this effort will be used to define boundary conditions for LOX post analyses.

1.2 Objectives

The following sections discuss the work performed under Phase I of the contract as modified to reflect the TAD/HGM/Duct analysis. Continuum's laminar and turbulent boundary layer development in support of the LOX post study and the results of the laminar 3-D HGM analysis were presented in Reference 1. The following sections present the turbulent 3-D HGM results.

2. SUMMARY

Continuum has developed shear stress wall functions which will permit viscous analyses without requiring excessive numbers of computational grid points. These wall functions, laminar and turbulent, have been compared to standard Blasius solutions and are directly applicable to the cylinder-in-crossflow class of problems to which the LOX post problem belongs. The results of this work were presented in Reference 1.

Continuum has also performed a full 3-D turbulent fluid flow analysis of the HPFTP exhaust system which consists of the turnaround duct, 2-duct hot gas manifold and the "Version B" transfer ducts. The results of this analysis are presented in this report.

3. HGM FLOW ANALYSIS

3.1 Introduction

The analysis of the flow environment surrounding the SSME LOX posts requires a definition of the flow field in the HPFTP transfer tubes exit planes. The exit plane flow is development by defining the flow conditions immediately downstream of the turbine and computing the flow field through the turnaround duct, hot gas manifold and transfer tube. This section discusses the computation of the turbulent flow field in the turnaround duct, hot gas manifold and transfer duct for a two-duct configuration.

3.2 Configuration

The configuration analyzed consisted of the FMOF turnaround duct, the "Phase 3" two-duct hot gas manifold and the "Version B" transfer tube which includes the flow separator. The effects of turbine-induced swirl were neglected at the direction of the customer; hence, a plane of symmetry between the 2 transfer tubes was incorporated.

3.3 Flow Conditions at Inlet

The flow conditions at the inlet to the turnaround duct were specified by the customer. The fluid in the system was air at 530°R flowing at 72 lbm/sec. The pressure across the inlet was described by the equation.

$$P = 190.0 \left[0.98 + 0.0441 \, Sin^2\left(\frac{\phi}{2}\right)\right] psia \qquad (3\text{-}1)$$

where ϕ is the angular location which ranges from 0° between the transfer tubes and 180° on the plane of symmetry on the side fartherest from the transfer tubes. The velocity profile in the TAD inlet is defined by the equation

$$V = \bar{V}(1.0 + 0.04\ \mathrm{Cos}\phi) \qquad (3\text{-}2)$$

where V is the average velocity at any angle ϕ and $\bar{V}$ is the average velocity over the entire inlet. The velocity has no cross flow component due to the assumption of no turbine-induced swirl. The turbulent wall function model presented in Ref. 1 was used in this analysis.

3.4 Computational Grid

The configuration described in subsection 3.2 was modeled using 10,724 nodal grid points. The grid points depicting the boundaries of the configuration are shown in Figs. 3-1, 3-2. The struts and posts in the turnaround duct have been darkened in to clarify their locations. The computational grid in the plane of symmetry at the 0° (between the transfer tubes) and 180° (far side) positions are shown in Fig. 3-3. The inlet to the turnaround duct has been artifically moved upstream to avoid influencing the flow in the 180° bend by the prescribed inlet flow conditions. Figures 3-1 through 3-3 illustrate that all of the salient features of the configuration have been incorporated into the grid.

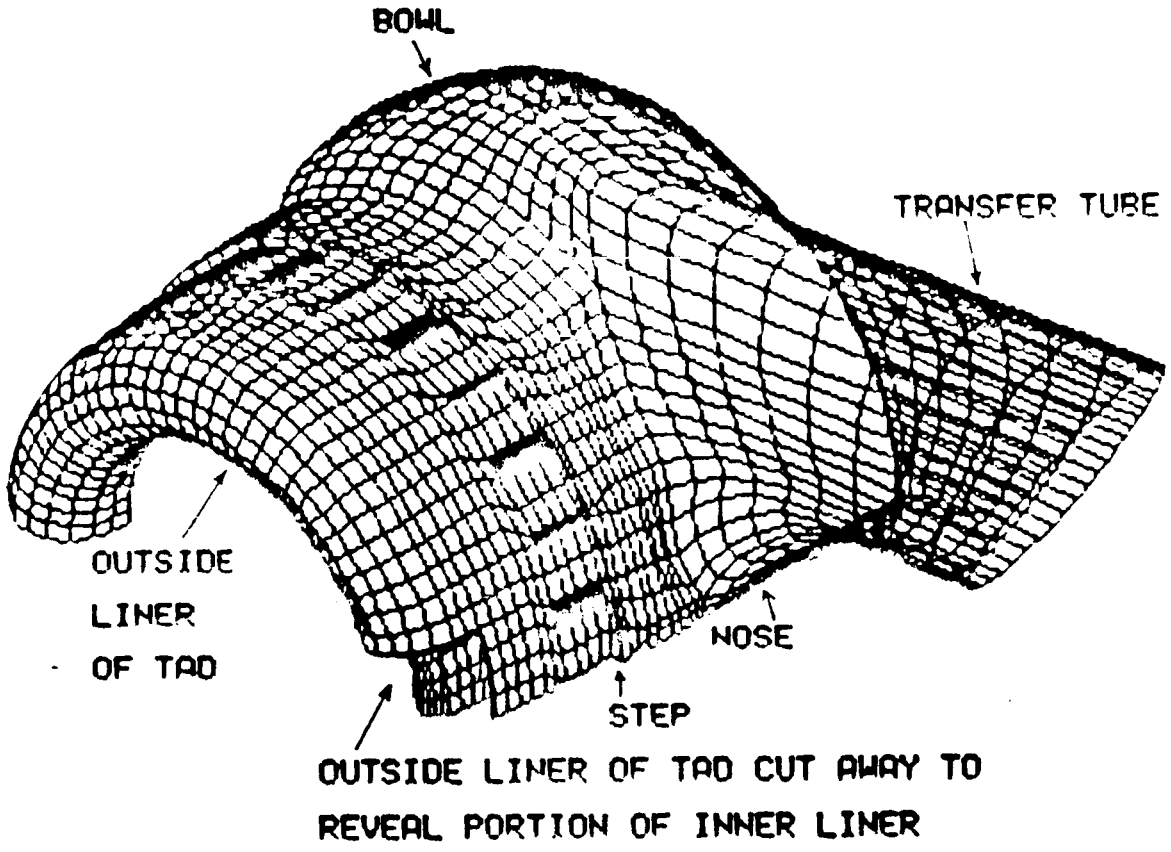

Fig. 3-1 View of Grid From Outside

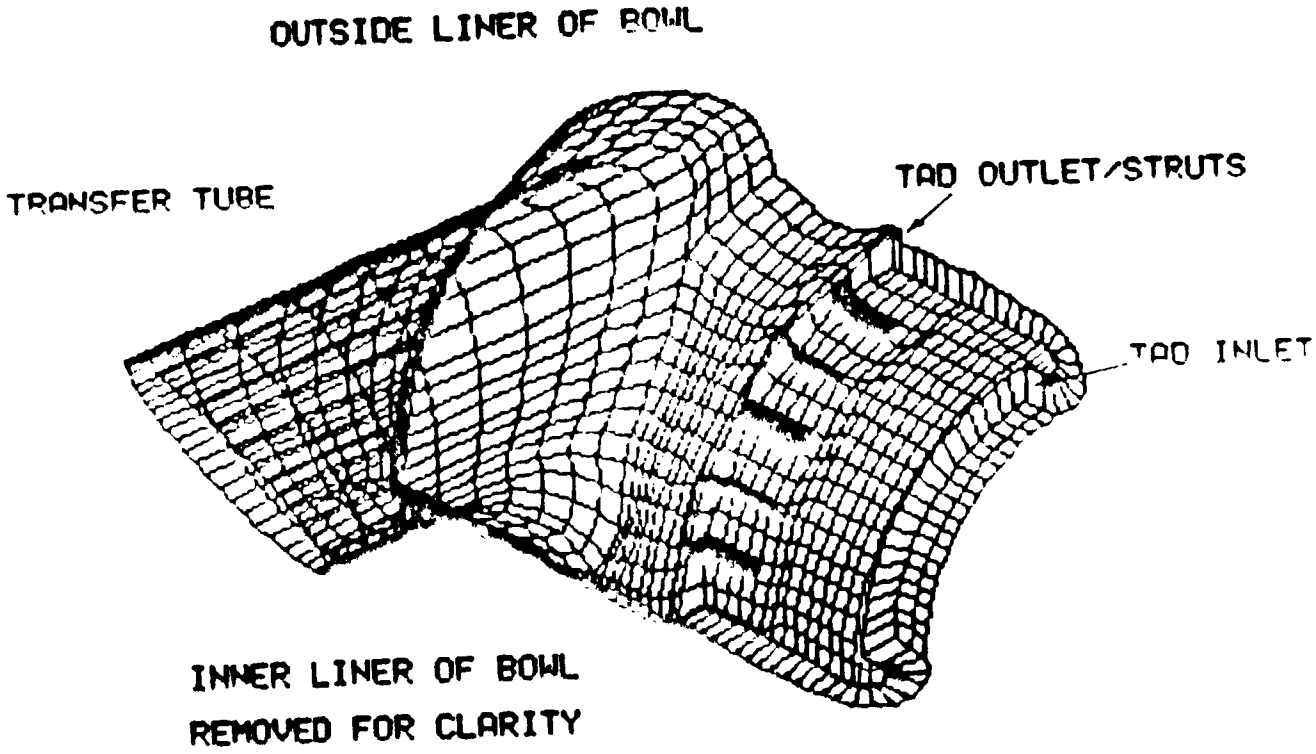

Fig. 3-2 View of Grid From Inside

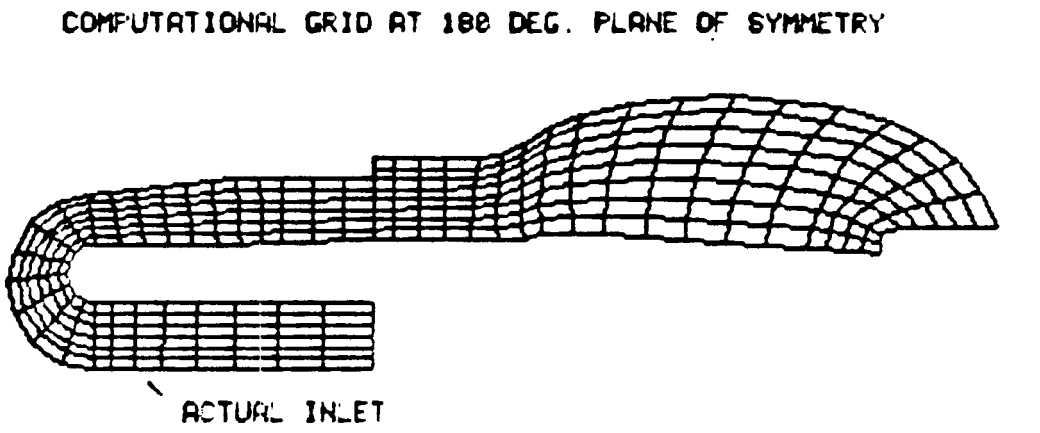

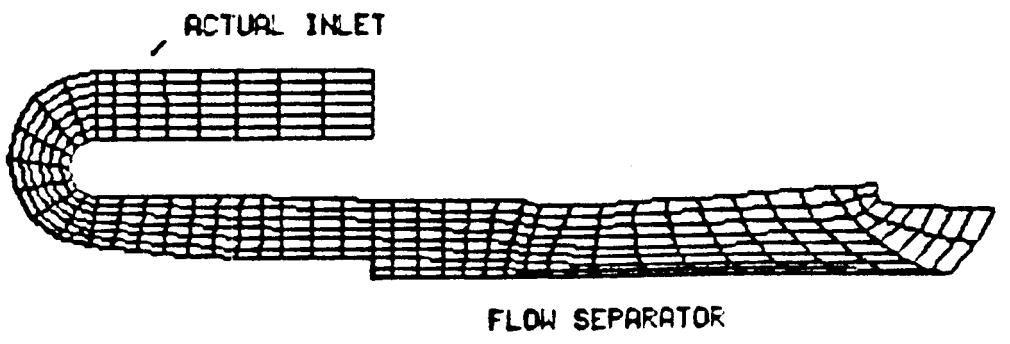

Fig. 3-3 Grids in Plane of Symmetry

3.5 Initial and Boundary Conditions

The inlet conditions prescribed in subsection 3.3 were applied to the artificially displaced inlet shown in Fig. 3-3. A turbulent "plug flow" velocity profile was superimposed on the average velocity distributed defined by Equation 3-2.

Turbulent wall function boundary conditions were specified for all solid walls and tangency, or free-slip, boundary conditions were applied to the plane of symmetry. The mass flow rate in the exit plane of the transfer tube was held fixed at 72 lbm/sec. The total conditions at the inlet were held fixed, thereby allowing spurious signals to pass upstream and out of the problem.

3.6 Results

The flowfield for the TAD, HGM and transfer tube described above was computed using Continuum's VAST code. Previously, a pseudo-laminar calculation was reported for this same configuration where in properties for air were used except 10^4 times the real viscosity was used as a crude representation of turbulence. The problem was started with the pseudo-laminar solution as the initial guess and required 8,000 time steps before a converged solution was obtained. The results of the study were presented in detail to the customer in September , 1985. A summary of the results will be discussed in this section.

The total pressure drop through the system for the pseudo-laminar and turbulent cases are presented in Fig. 3-4 and shows a drop of about 20 psi for the turbulent case as opposed to 48 psi for the pseudo-laminar case.

AVERAGED PRESSURES IN TAD/HGM/TT

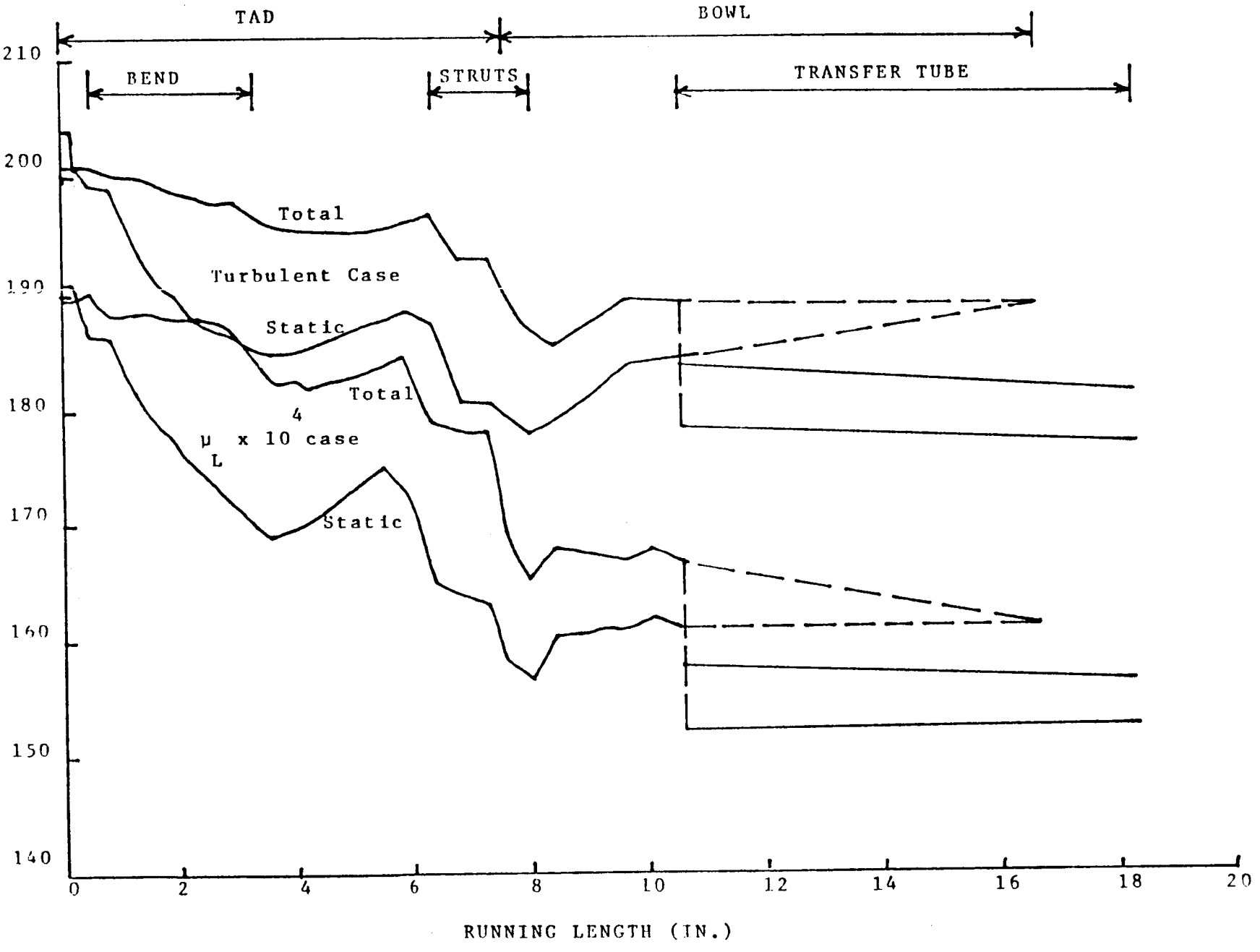

Figure 3-4 - Averaged Pressure

Three flow features were significantly different between the laminar and turbulent cases. The flow downstream of the 180° degree bend in the TAD exhibits more deceleration for the pseudo-laminar case than for the turbulent case (Fig. 3-5) and the recirculation in the HGM bowl is less pronounced for the laminar case (Fig. 3-5). Also, the direction of swirl in the transfer tube is reversed between the laminar and turbulence cases (Fig. 3-6). These differences indicate the importance of simulating, as nearly as possible, the correct flow regime when analyzing problems such as the TAD/HGM/Tube problem.

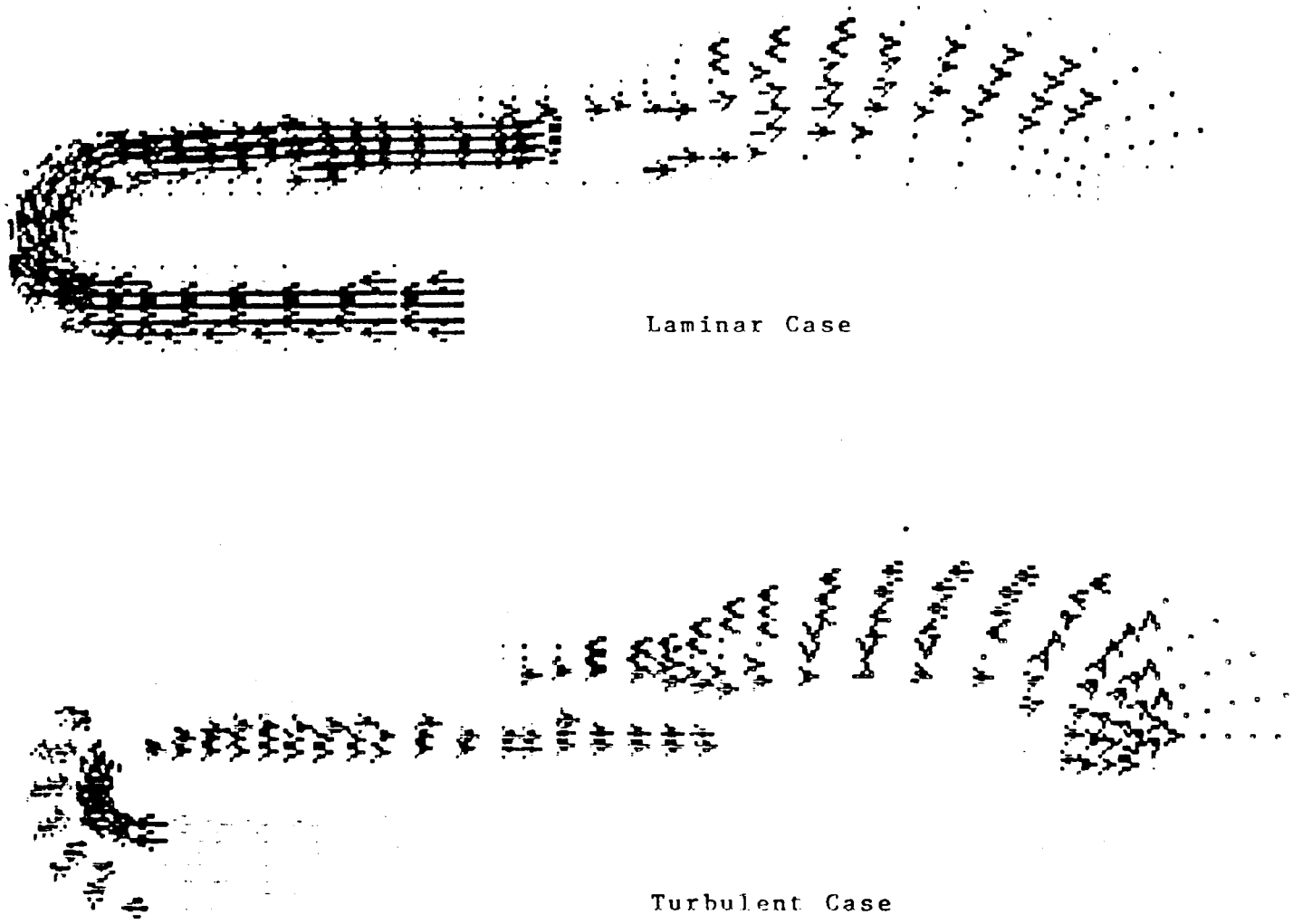

Fig. 3-5 - Velocity Vectors in 180 Plane of Symmetry

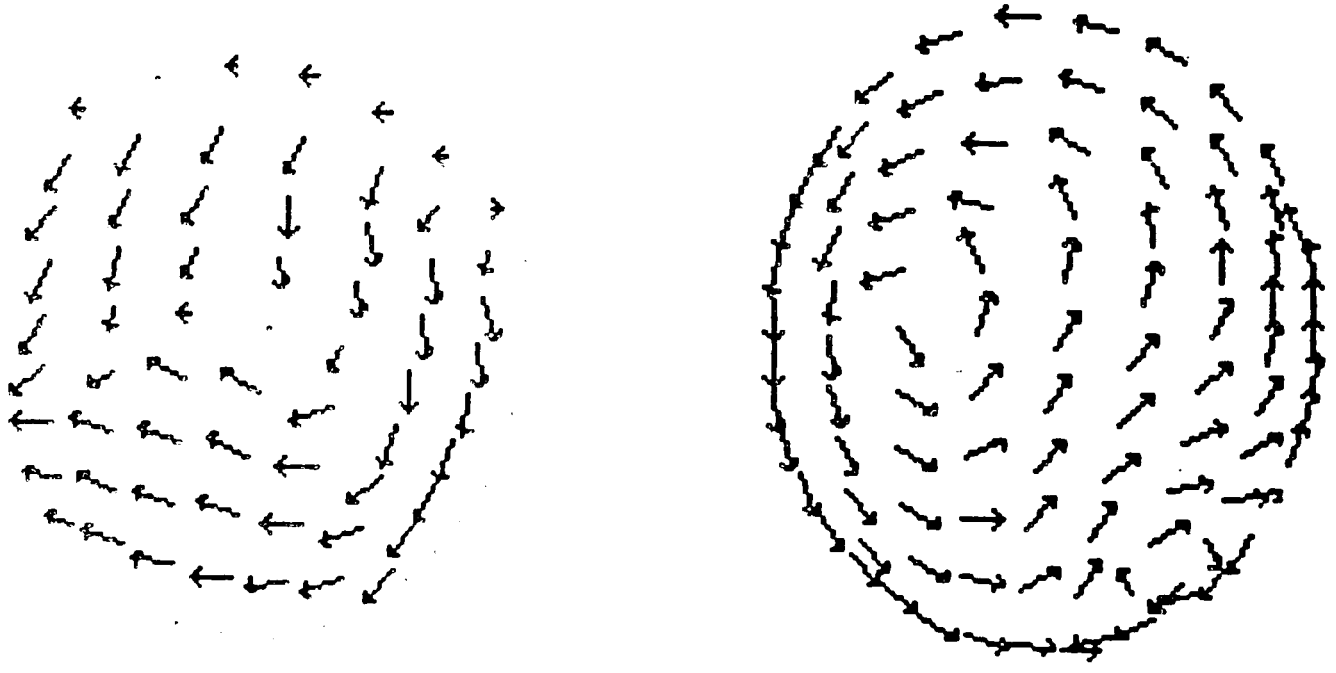

Laminar Case

Turbulent Case

Fig. 3-6 - Velocity Vectors in Exit Plane of Transfer Duct

5. CLOSURE

The analyses of single and multiple LOX posts will be continued using the results of the above analyses as boundary conditions for LOX post simulations.

6. REFERENCES

1. Anderson, P. G., and Farmer, R.C., "Calculation of Flow About Posts and Powerhead Model, Interim Report, Contract NAS8-35506", Continuum, Inc., report CI-IR-0079, December 1984.

APPENDIX C

SSME HGM DATA REDUCTION FOR COMPARATIVE STUDY

Contract NAS8-35506

CI-TR-0095

Prepared For:

National Aeronautics and Space Administration
George C. Marshall Space Flight Center
Marshall Space Flight Center, AL 35812

By:

Ten-See Wang
Youssef Dakhoul

CONTINUUM, Inc.
4715 University Drive
Suite 118
Huntsville, AL 35816-3495

June 27, 1986

INTRODUCTION

The objective of this work is to collate and submit the HGM-CFD results obtained by Continuum (Ref. 1, 2) to NASA/MSFC for a comparative study. The results of the comparative study will be used to evaluate the role of CFD analysis in the future HGM design.

RESULTS NEEDED FOR COMPARATIVE STUDY OF HGM ANALYSES

1. System ΔP.

The pressure coefficient (C_p) is plotted in Figures 1 and 2 as a function of distance from HGM inlet along centerline of HGM. The 5.4 drop in C_p, for the laminar case (Fig. 1), is equivalent to a 48 psi total pressure drop. For the turbulent case (Fig. 2), the 1.65 drop in C_p is equivalent to a 20 psi total pressure drop.

2. Circumferential ΔP (outer wall).

a. Downstream of TAD (turnaround duct):

Figures 3 and 4 show the circumferential distribution of C_p for laminar and turbulent cases, respectively, at 1.028" from the TAD bend. The laminar case (Fig. 3) shows a 2.37 drop in C_p while the turbulent case (Fig. 4) shows a drop of 1.08.

b. At G-6 flange:

The G-6 flange is located at 5.4" from the TAD bend. Figure 5 shows a circumferential drop of 4.2 in C_p for the laminar case, while Figure 6 shows a drop of 2.36 for the turbulent case.

3. Gross Features of Flow.

As shown in Figures 7 through 10, separation takes place over the backstep at the exit of the struts region. Recirculation occurs in the fuel bowl. The top end of the fuel bowl is a stagnation region. No separation is observed in the 180° bend. It is postulated that the optimum geometric design of the TAD prevented separation. These observations are true for both the laminar and turbulent cases.

4. Swirl in Transfer Duct Midplane.

Figures 11 and 12 are velocity vector plots in transfer duct midplane for the laminar and turbulent cases respectively. For the laminar case a major counter-clockwise swirl is observed and a minor clockwise swirl is also seen in the lower right corner. For the turbulent case, the main swirl is in the clockwise direction. A minor counter-clockwise swirl is also observed at the upper left corner. The opposing directions of swirls is probably due to the different directions of recirculation in the fuel bowl near the transfer duct (see Figs. 8 , 10).

5. Mach Number Contours at Transfer Duct Midplane.

Figure 13 shows the laminar case Mach number contours at transfer duct midplane. The peak is between 0.25 and 0.3 and is located roughly in the upper right region. This is also true for the turbulent case as shown in Figure 14. Note also that the local minima in the turbulent Mach number distribution coincide with the centers of the swirls shown in Figure 12.

6. Swirl in Transfer Duct Exit Plane.

Figures 15 and 16 show the velocity vectors in the transfer duct exit plane for the laminar and turbulent cases respectively. The swirls are similar to those observed at the duct's midplane.

7. Mach Number Contours at Transfer Duct Exit Plane.

For both the laminar and turbulent case (see Figures 17 and 18), the peak mach number is between 0.25 and 0.3 and is located in the upper right region.

8. Static Pressure Coefficient Profile at Transfer Duct Exit Plane.

The static pressure coefficient profile at transfer duct exit is plotted against centerline distance from duct inner wall to outer wall as shown in Figure 19. The view is in right hand transfer duct looking toward main injectors. The results showed almost constant static pressures at the exit of the transfer duct for both the laminar and turbulent cases.

BACKGROUND DATA

1. Boundary Conditions.

a. Upstream at TAD entrance/turbine exit:

The flow conditions at TAD entrance/turbine exit were specified by the customer. The fluid in the system is air at 530 °R flowing at 72 lbm/sec. The pressure across the inlet is described by the equation:

$$P = 190.0\left[0.98 + 0.0441\ \mathrm{Sin}^2\left(\frac{\phi}{2}\right)\right] \mathrm{psia}\ (\mathrm{lbf/in^2})$$

where ϕ is the angular location which ranges from 0° between the transfer tubes and 180° on the plane of symmetry on the side fartherest from the transfer tubes. The velocity profile in the TAD inlet is defined by the equation:

$$V = \bar{V}(1.0 + 0.04\ \mathrm{Cos}\phi)\ (\mathrm{ft/sec})$$

where V is the average velocity at any angle ϕ and $\bar{V}$ is the average velocity over the entire inlet which is equal to the mass flow rate divided by ρA .

These inlet conditions are applied to the artifically displaced inlet (3.75" upstream of real inlet) of TAD. In laminar flow case, a laminar parabolic velocity profile is superimposed on the average velocity (V) defined above. The total conditions at the inlet are held fixed, there by allowing spurious signals to pass through upstream boundary and out of the problem.

b. Downstream at transfer duct exit:

The mass flow rate in the exit plane of the transfer tube is held fixed at 72 lbm/sec.

c. Inlet swirl specification:

The inlet velocity has no cross flow component due to the assumption of no turbine-induced swirl.

2. Initial Conditions.

For the laminar case, the initial velocity profile throughout the domain is a laminar parabolic profile superimposed on the inlet's average velocity V. The pressure is described by the same equation given in the preceding section. The fluid is air at 530 °R flowing at 72 lbm/sec. The turbulent calculation is started by using the laminar solution as the initial condition.

3. Problem Parameters.

a. $\dot{M}$ at turbine exit/TAD inlet:

72 lbm/sec

b. Reynolds number:

2.35×10^6 for turbulent calculation and 235 for the laminar case. These values are based on an average velocity of 351.26 ft/sec at the TAD inlet.

c. Mach Number:

The sound speed in air at 530 °R is 1128.6 ft/sec. This corresponds to a Mach number of 0.3 based on a velocity of 351.26 ft/sec.

4. Turbulence Model.

An algebraic turbulence model is used to calculate an eddy viscosity which increases with distance from the walls. The computational wall is slightly displaced away from the real wall and a wall function (based on the logarithmic velocity profile) is used to calculate the flow properties at the wall. Complete details are found in Refs. 2 and 3.

5. Geometry.

The geometry analyzed consists of the FMOF TAD, the "phase 3" manifold which includes a flow separator, and two "version B" transfer tubes. The struts region between TAD and BOWL is included. Its corners were not rounded off. The effects of turbine-induced swirl are neglected at the direction of the customer; hence, a plane of symmetry between the two transfer tubes is incorporated. The inlet to the TAD is artifically extended 3.75" upstream to avoid influencing the flow in the 180° bend by the prescribed inlet flow conditions.

6. Computational Grid.

a. Total number of nodes:

10,724

b. Number of nodes in each region:

TAD: 3059
Struts: 1554
Fuel bowl: 5121
Transfer duct: 990

c. Distribution of nodes:

The distributions of nodes are mostly uniform in each region, except that the nodal increment is decreasing axially in the extension of the TAD inlet and increasing axially toward the exit of the transfer duct.

7. Number of iterations to obtain a converged solution.

a. The numerical method used is a forward time marching explicit scheme. 11,000 iterations are used for the convergence of the laminar case and 8,000 additional iterations are required to achieve the convergence for the turbulent case.

b. The sum of squares of the time derivatives of the primitive variables are used as indicators for convergence. These quantities approach zero as the solution converges to the steady state.

8. Computer time used to obtain converged solutions.

a. Total CPU time:

Laminar case 49 hrs (11,000 iterations, Scalar VAST code)
Turbulent case 2.61 hrs (8,000 iterations, Vectorized VAST code)

Note that the total number of nodes, for both cases, is 10, 724.

b. Type of Computer:

CRAY 1 S at United Information Service

c. Total number of FLOPS to obtain convergence:

Laminar case: 1.4112×10^{13} (scalar)
Turbulent case: 7.525×10^{11} (vector)

d. FLOPS/node to obtain convergence:

Laminar case: 1.3159×10^{9} (scalar)
Turbulent case: 7.0171×10^{7} (vector)

9. Convergence Criteria.

The VAST convergence criteria is based on the fact that if the steady state was reached, the sum of the squares of the time derivative of the primitive variables, $\dot{U}_j$, should be very small and independent of time. Theoretically, it can approach zero:

$$\sum_{n=1}^{N} (\dot{U}_j)_n^2 \longrightarrow 0, \quad j=1,\ldots J$$

where N is the total number of nodes; J is the total number of primitive variables; and $\dot{U}_j$ is the time derivative of U_j.

Practically, the above quantity is plotted against the elapsed time for each variable. The steady solution is acheived when these quantities become, say, 10^5 times less than their initial values.

REFERENCES

1. Anderson, P.G., and R.C. Farmer, "Calculation of Flow About Posts and Powerhead Model", Interim Report, Contract NAS8-35506, Continuum, Inc., December 1984.

2. Anderson, P.G. and R.C. Farmer, "Calculation of Flow About Posts and Powerhead Model", Interim Report, Contract NAS8-35506, Continuum, Inc., December 1985.

3. Farmer, R.C., T.S. Wang, S.D. Smith and R.J. Prozan, "SSME Main Combustion Chamber and Nozzle Flowfield Analysis", Final Report, Contract NAS8-35510, Continuum, Inc., CI-FR-0085, March 1986.

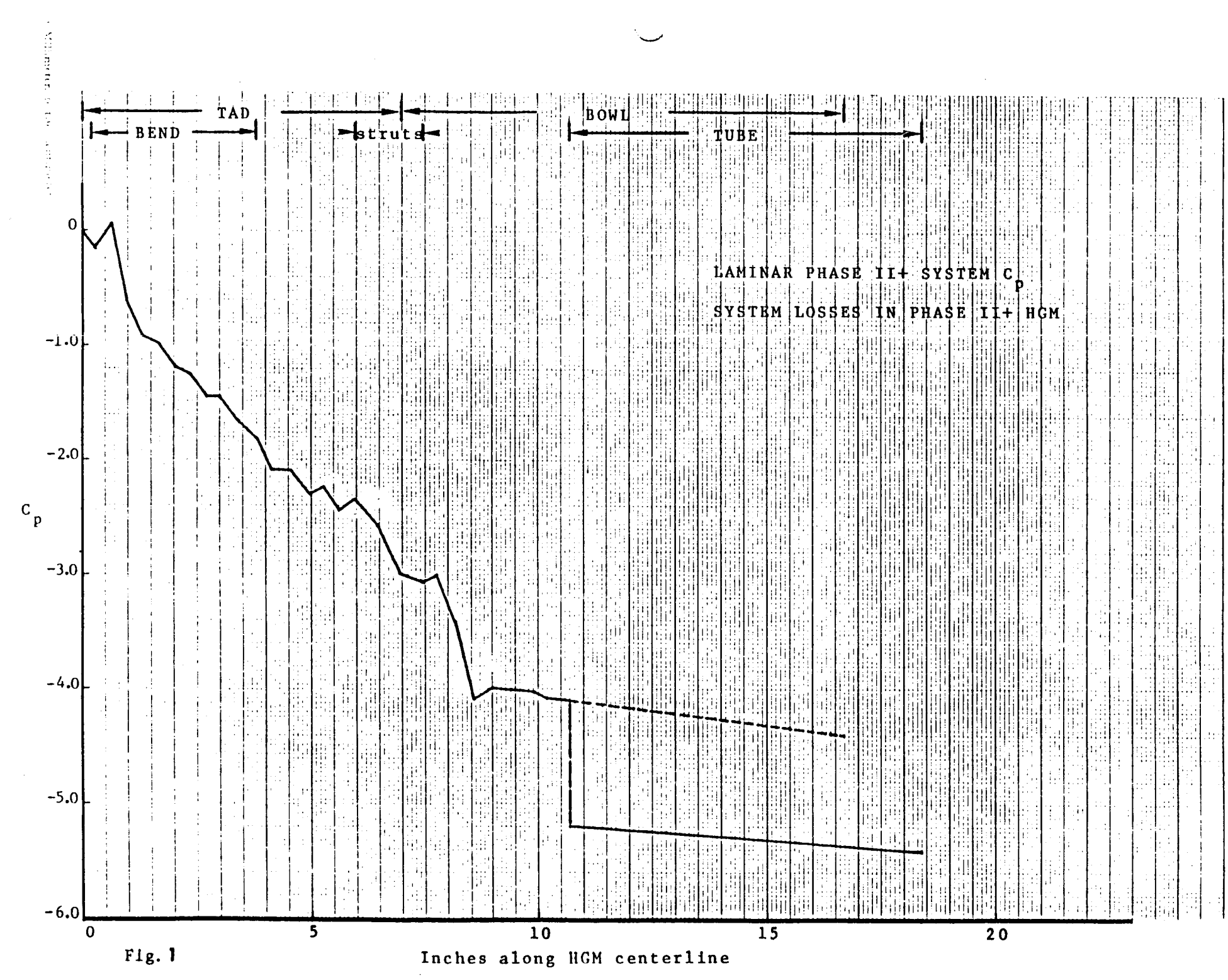
TAD
BEND
struts
BOWL
TUBE
LAMINAR PHASE II+ SYSTEM C_p
SYSTEM LOSSES IN PHASE II+ HGM
0
-1.0
-2.0
-3.0
-4.0
-5.0
-6.0
C_p
0
5
10
15
20
Inches along HGM centerline

Fig. 1

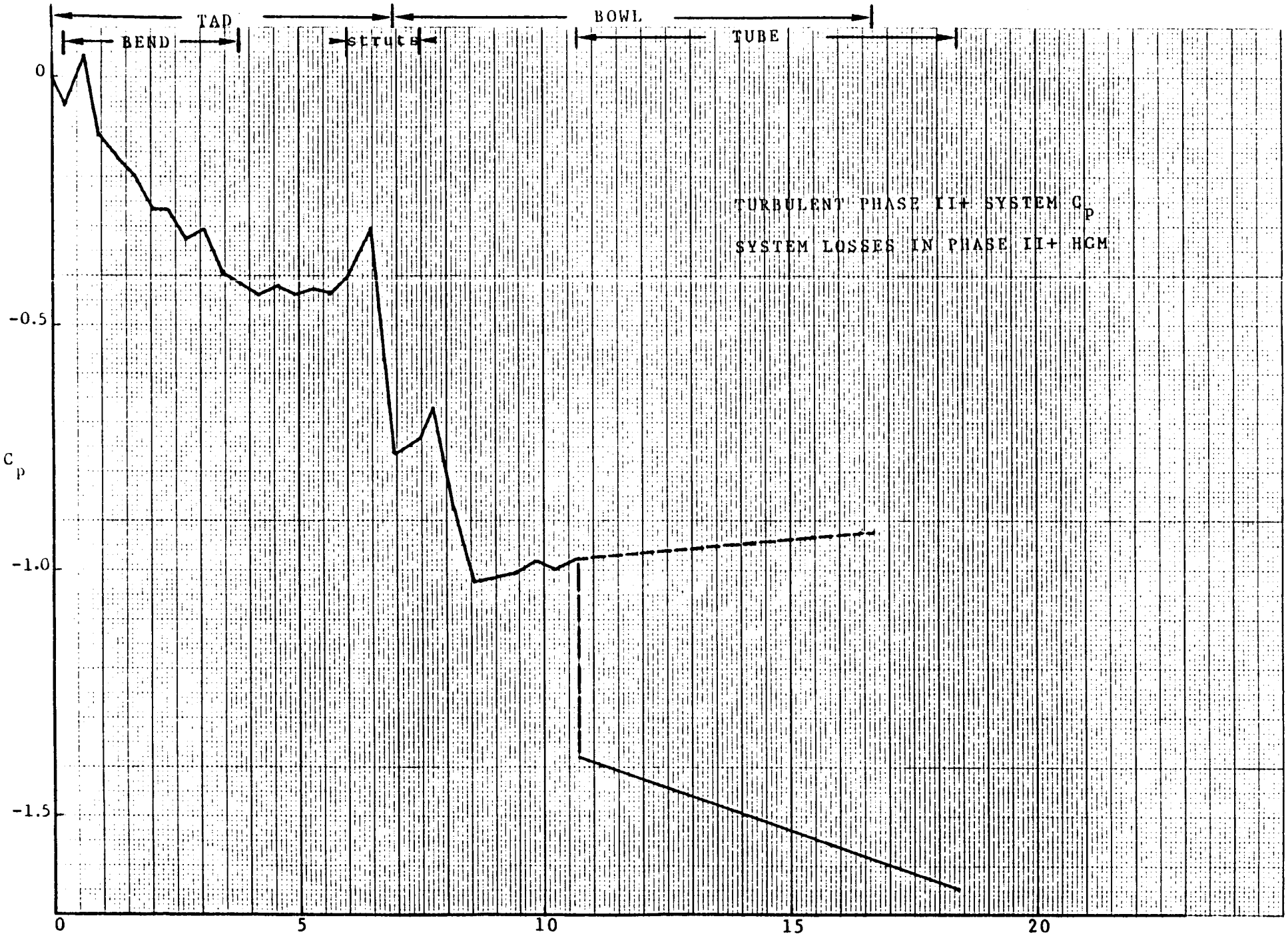

Fig. 2

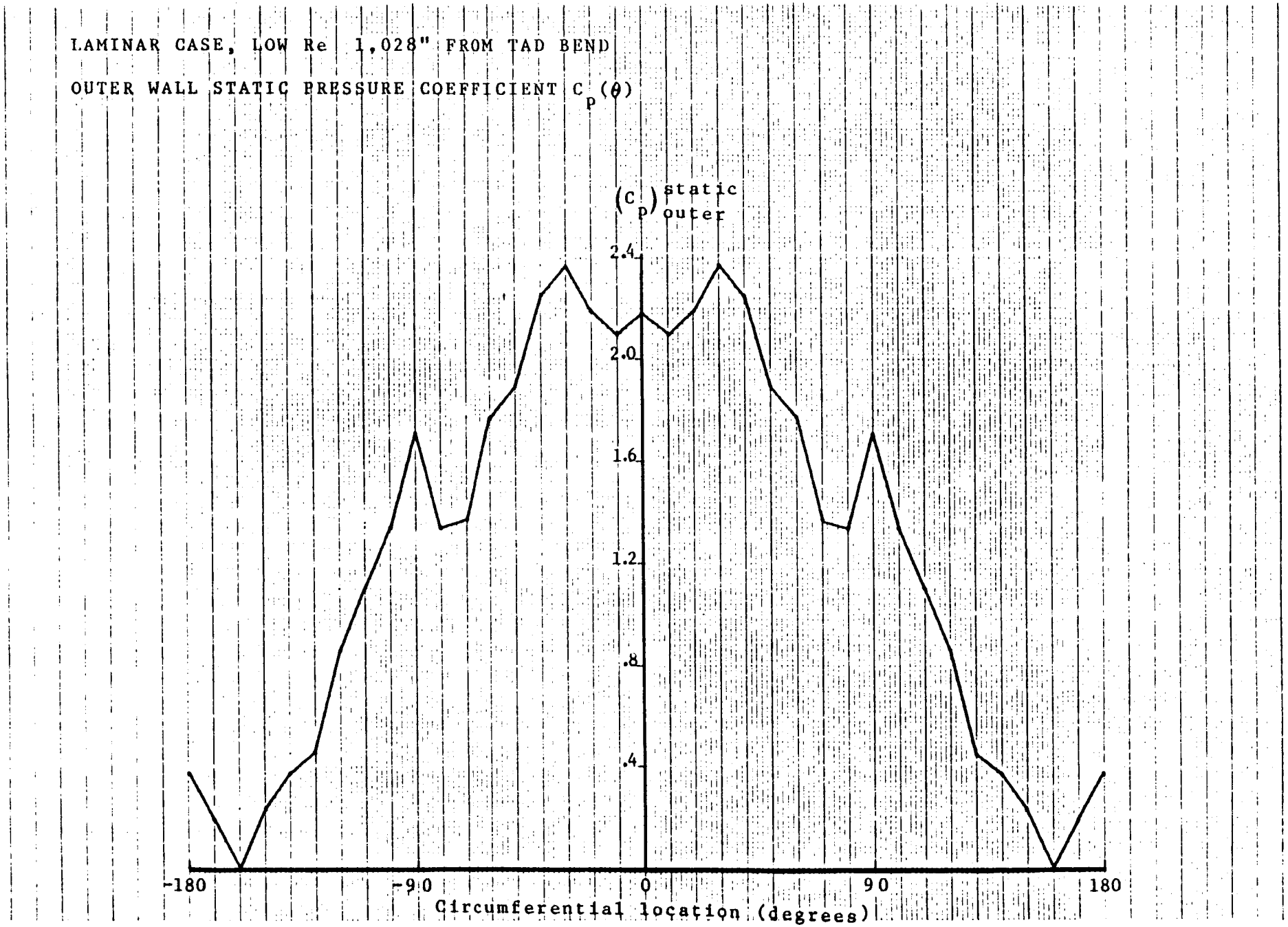
LAMINAR CASE, LOW Re 1,028" FROM TAD BEND
OUTER WALL STATIC PRESSURE COEFFICIENT $C_p(\theta)$
$(C_p)_{outer}^{static}$
2.4
2.0
1.6
1.2
.8
.4
-180
-90
0
90
180
Circumferential location (degrees)

Fig. 3

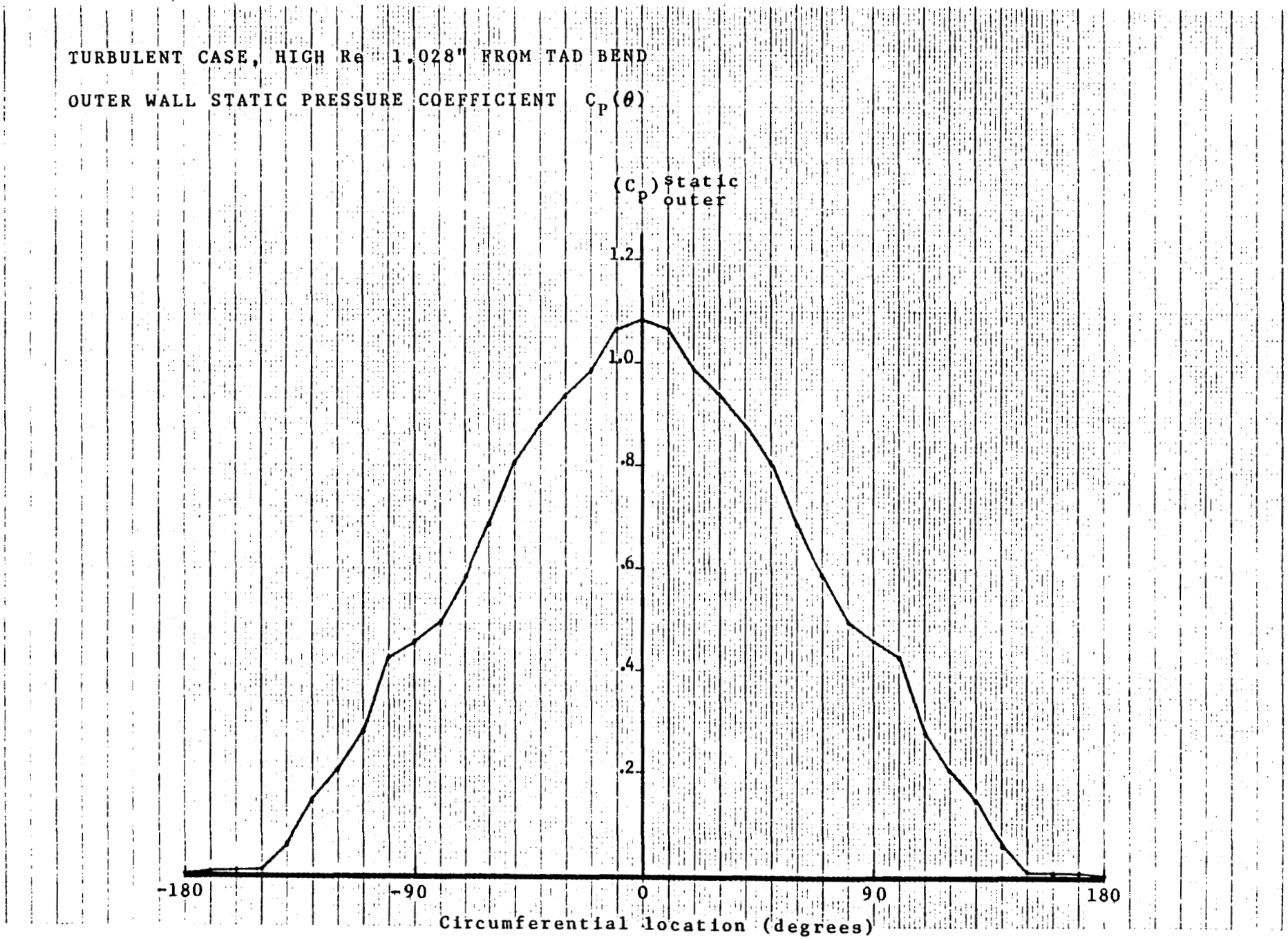
TURBULENT CASE, HIGH Re 1.028" FROM TAD BEND
OUTER WALL STATIC PRESSURE COEFFICIENT $C_P(\theta)$
$(C_P)_{static\ outer}$
1.2
1.0
.8
.6
.4
.2
-180
-90
0
90
180
Circumferential location (degrees)

Fig. 4

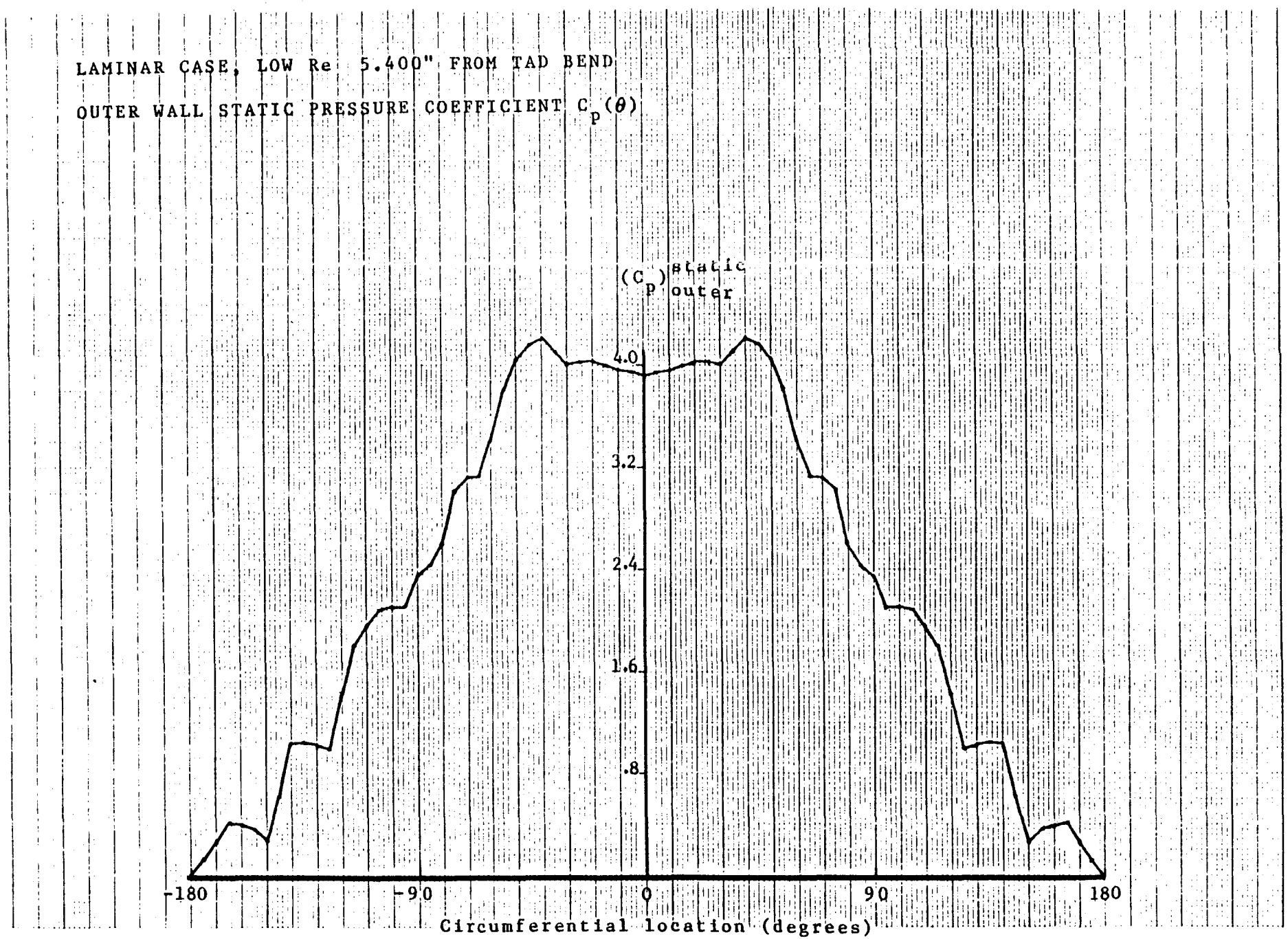
LAMINAR CASE, LOW Re 5.400" FROM TAD BEND
OUTER WALL STATIC PRESSURE COEFFICIENT $C_p(\theta)$
$(C_p)_{static\ outer}$
4.0
3.2
2.4
1.6
.8
-180
-90
0
90
180
Circumferential location (degrees)

Fig. 5

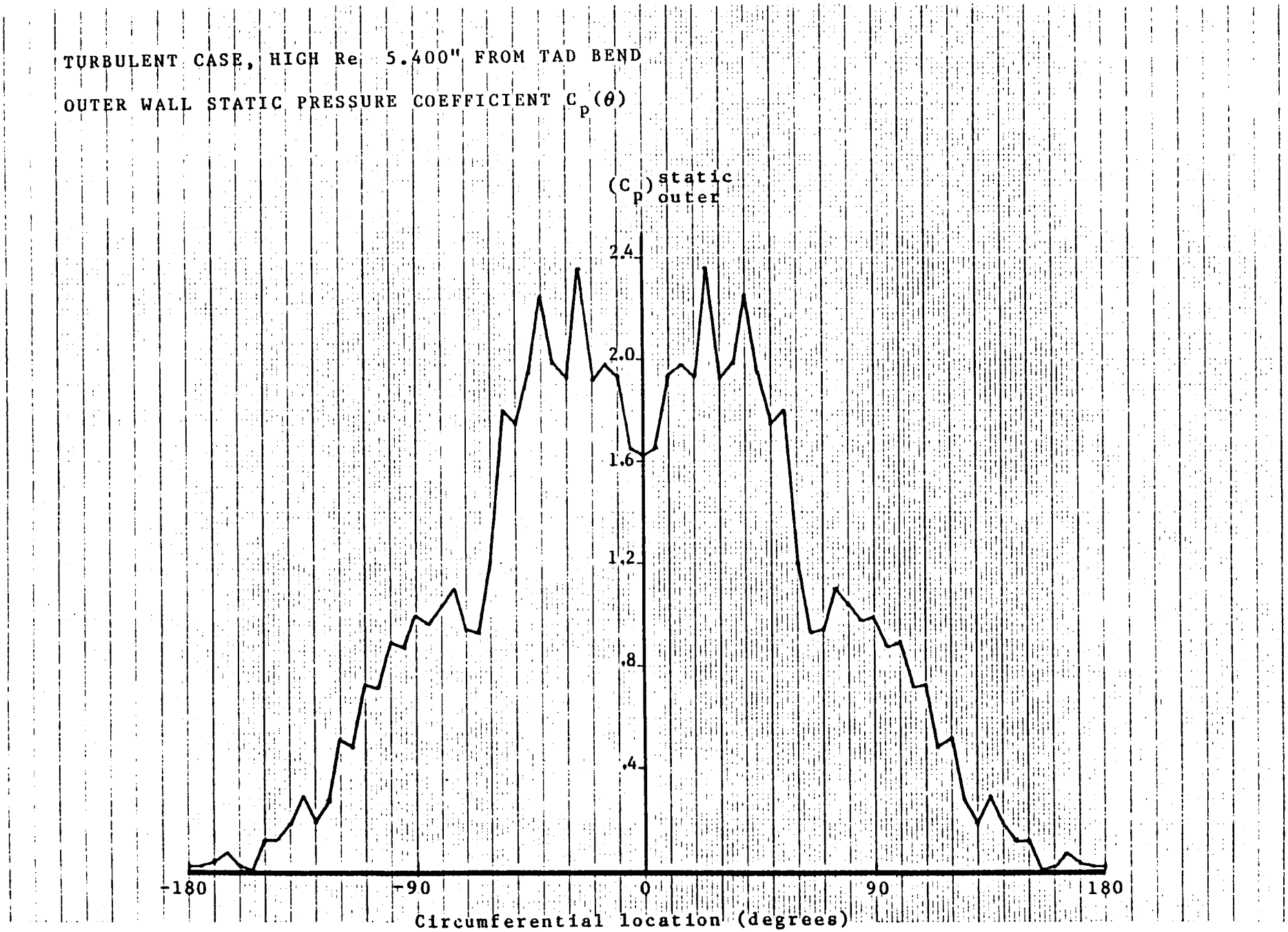
TURBULENT CASE, HIGH Re 5.400" FROM TAD BEND
OUTER WALL STATIC PRESSURE COEFFICIENT $C_p(\theta)$
$(C_p)_{static\ outer}$
2.4
2.0
1.6
1.2
.8
.4
-180
-90
0
90
180
Circumferential location (degrees)

Fig. 6

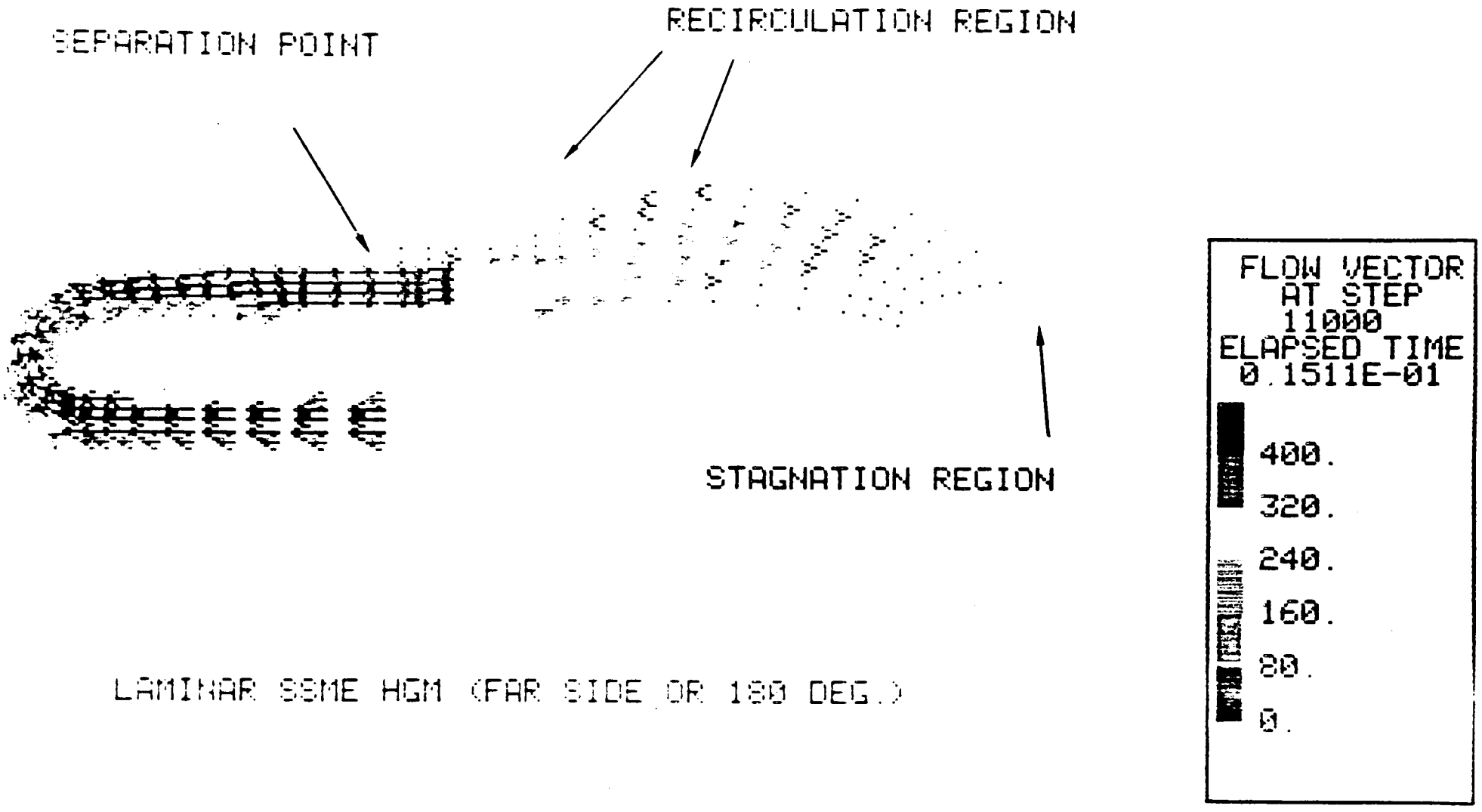

LAMINAR SAME MGM (FAR SIDE OR 180 DEG.)

Fig. 7

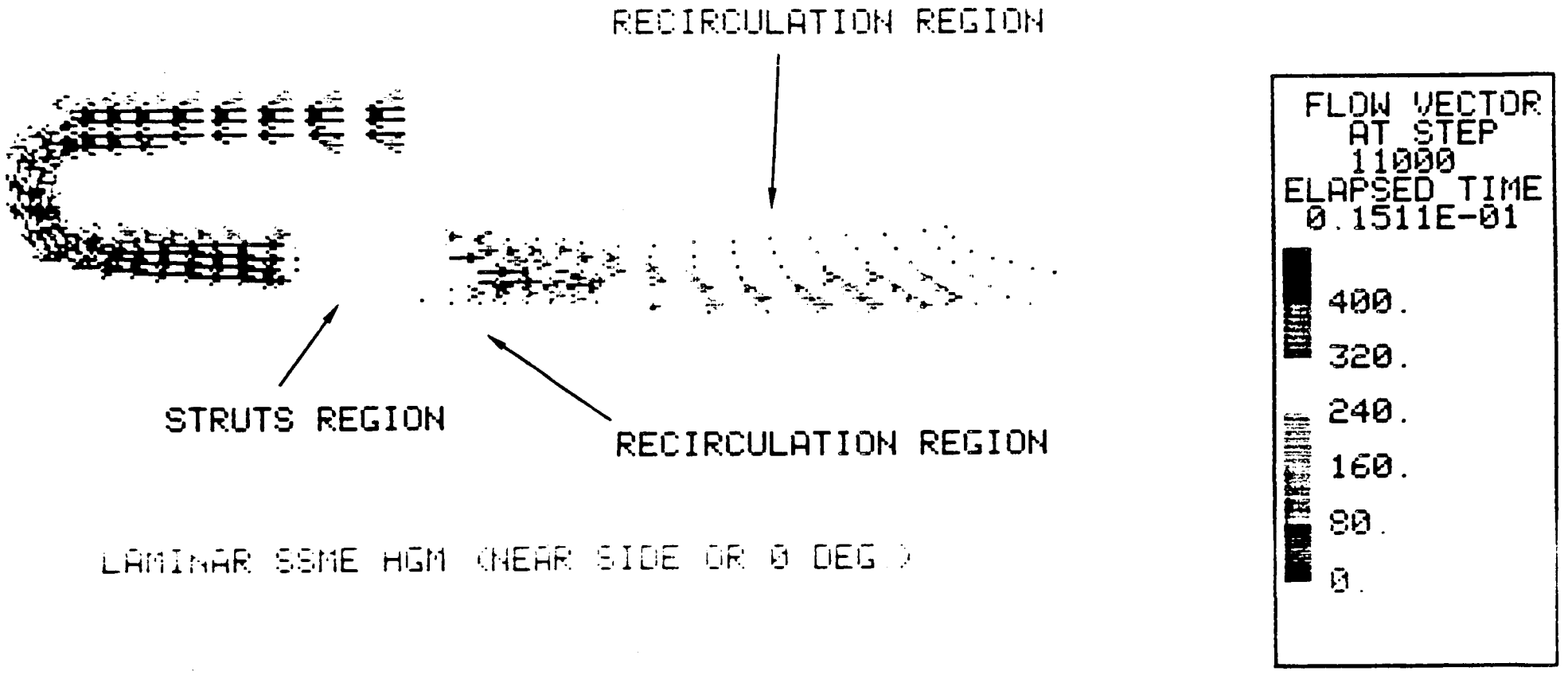
RECIRCULATION REGION
STRUTS REGION
RECIRCULATION REGION
LAMINAR SSME HGM (NEAR SIDE OR 0 DEG.)
FLOW VECTOR
AT STEP
11000
ELAPSED TIME
0.1511E-01
400.
320.
240.
160.
80.
0.

Fig. 8

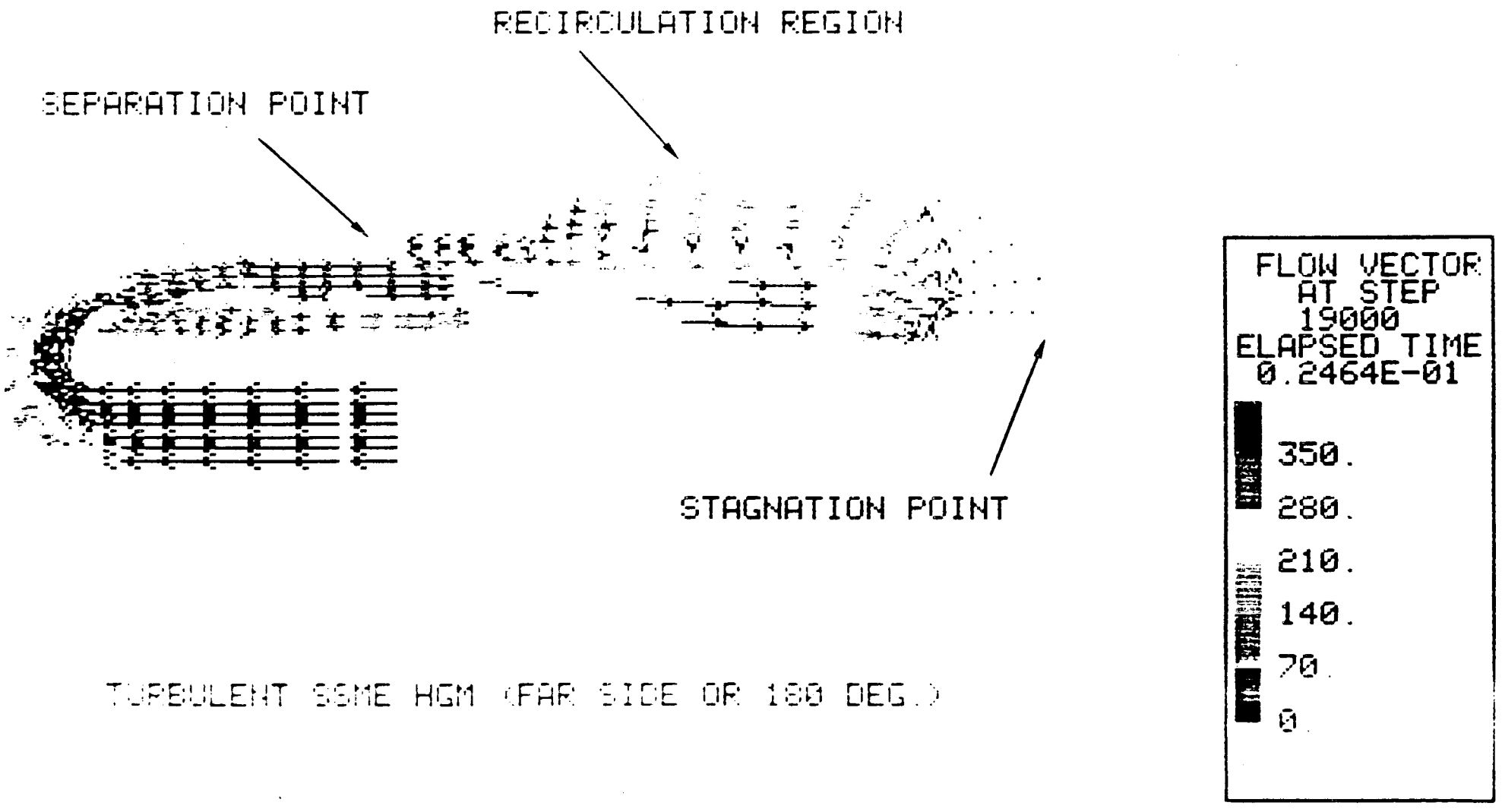
RECIRCULATION REGION
SEPARATION POINT
STAGNATION POINT
FLOW VECTOR
AT STEP
19000
ELAPSED TIME
0.2464E-01
350.
280.
210.
140.
70.
0.
TURBULENT SAME HGM (FAR SIDE OR 180 DEG.)

Fig. 9

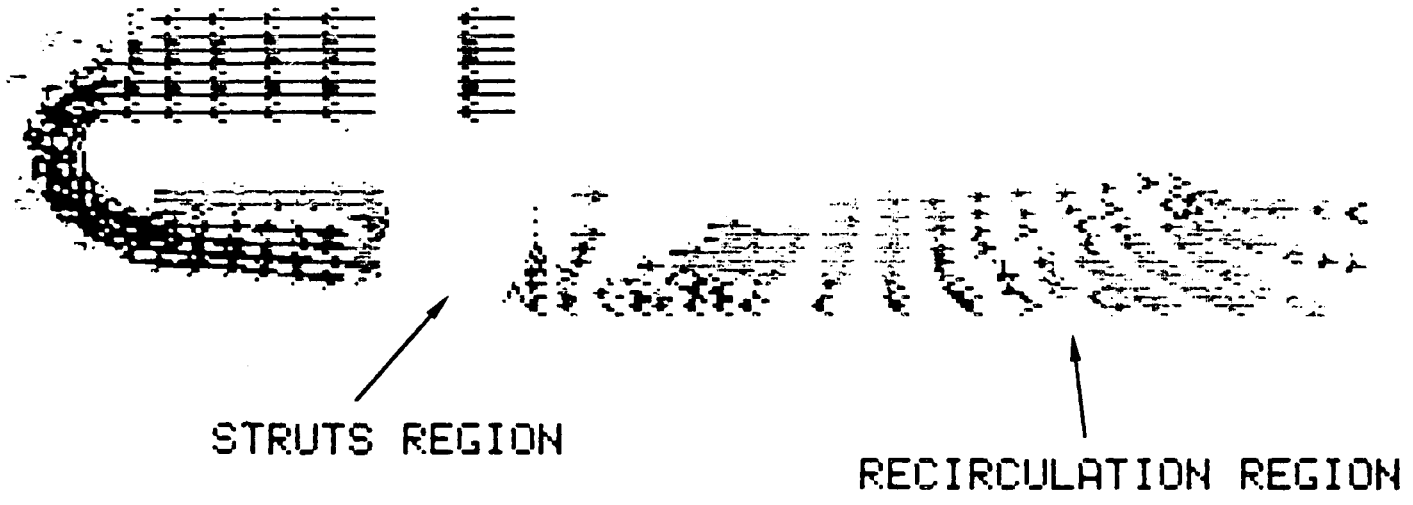

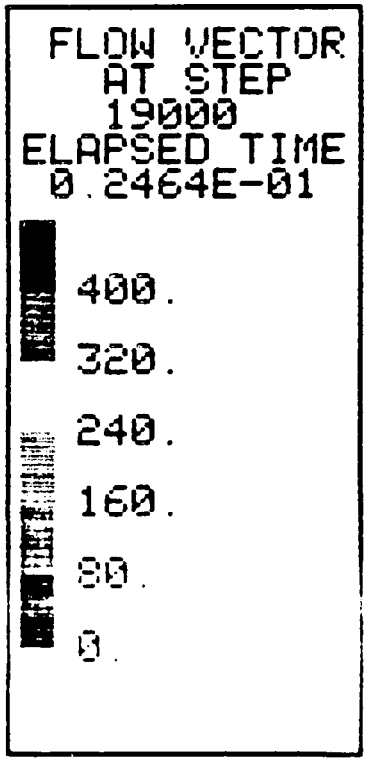

TURBULENT SSME HGM (NEAR SIDE OR 0 DEG.)

Fig. 10

LAMINAR SSME HGM TRANSFER DUCT MIDPLANE

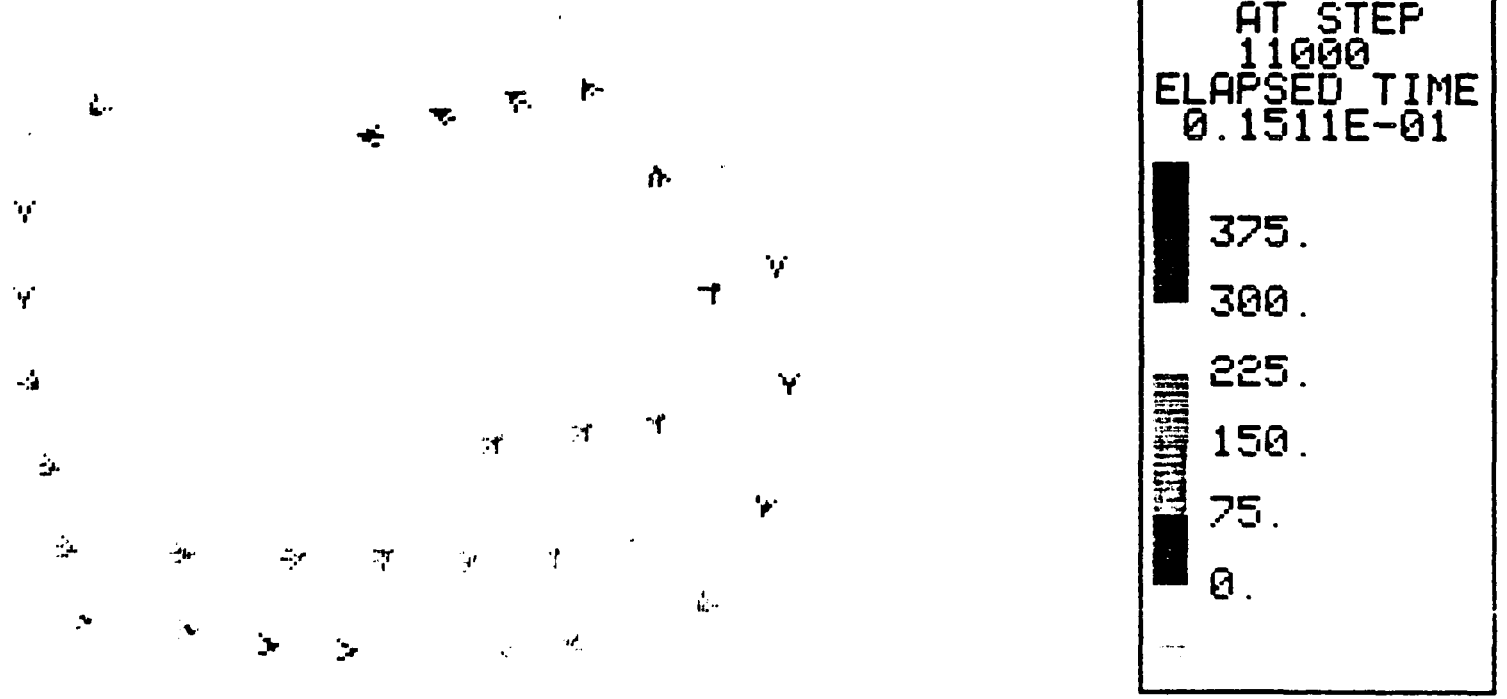

Fig. 11

TURBULENT SSME HGM TRANSFER DUCT MIDPLANE

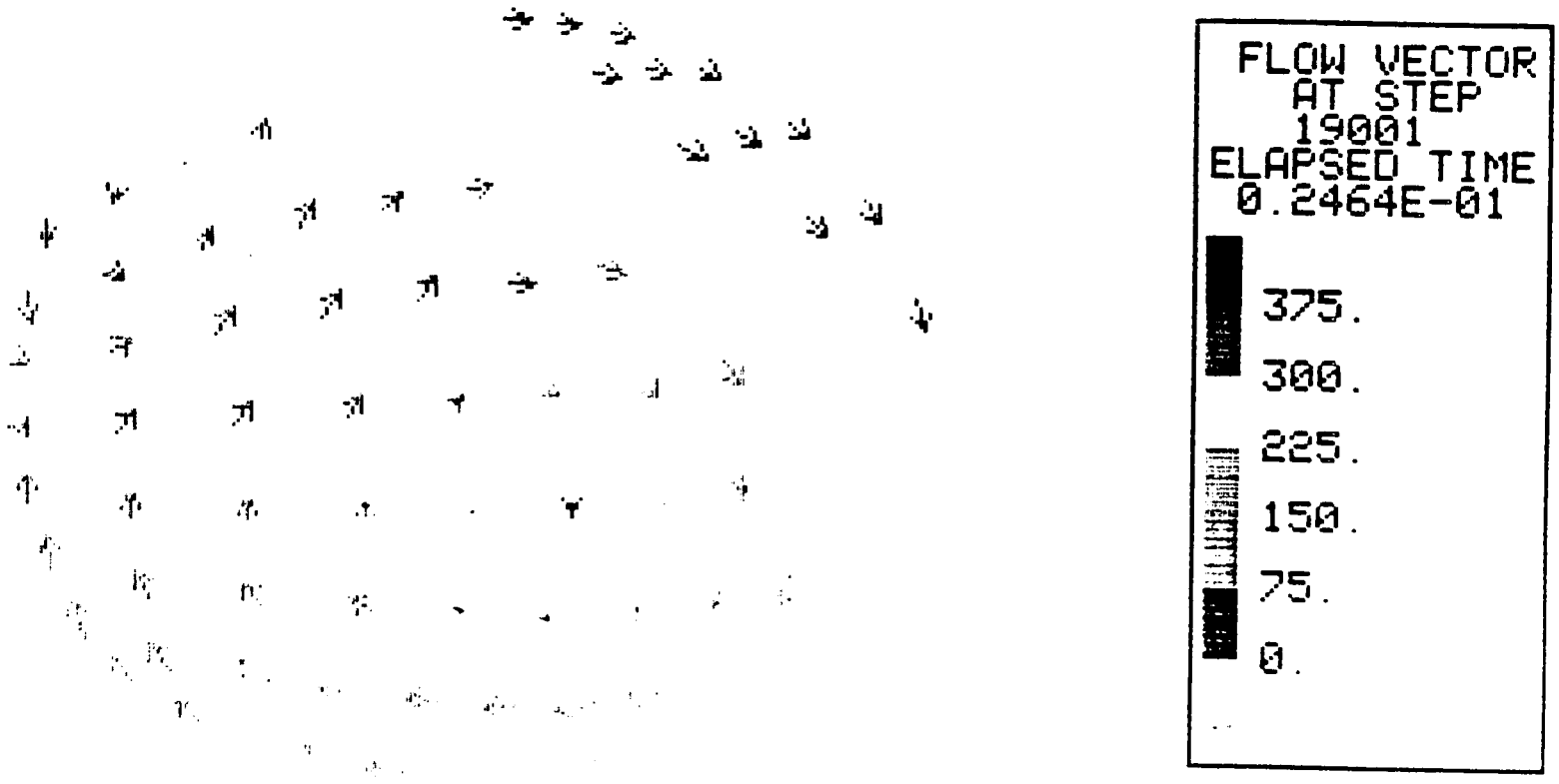

Fig. 12

LAMINAR SSME HGM TRANSFER DUCT MIDPLANE

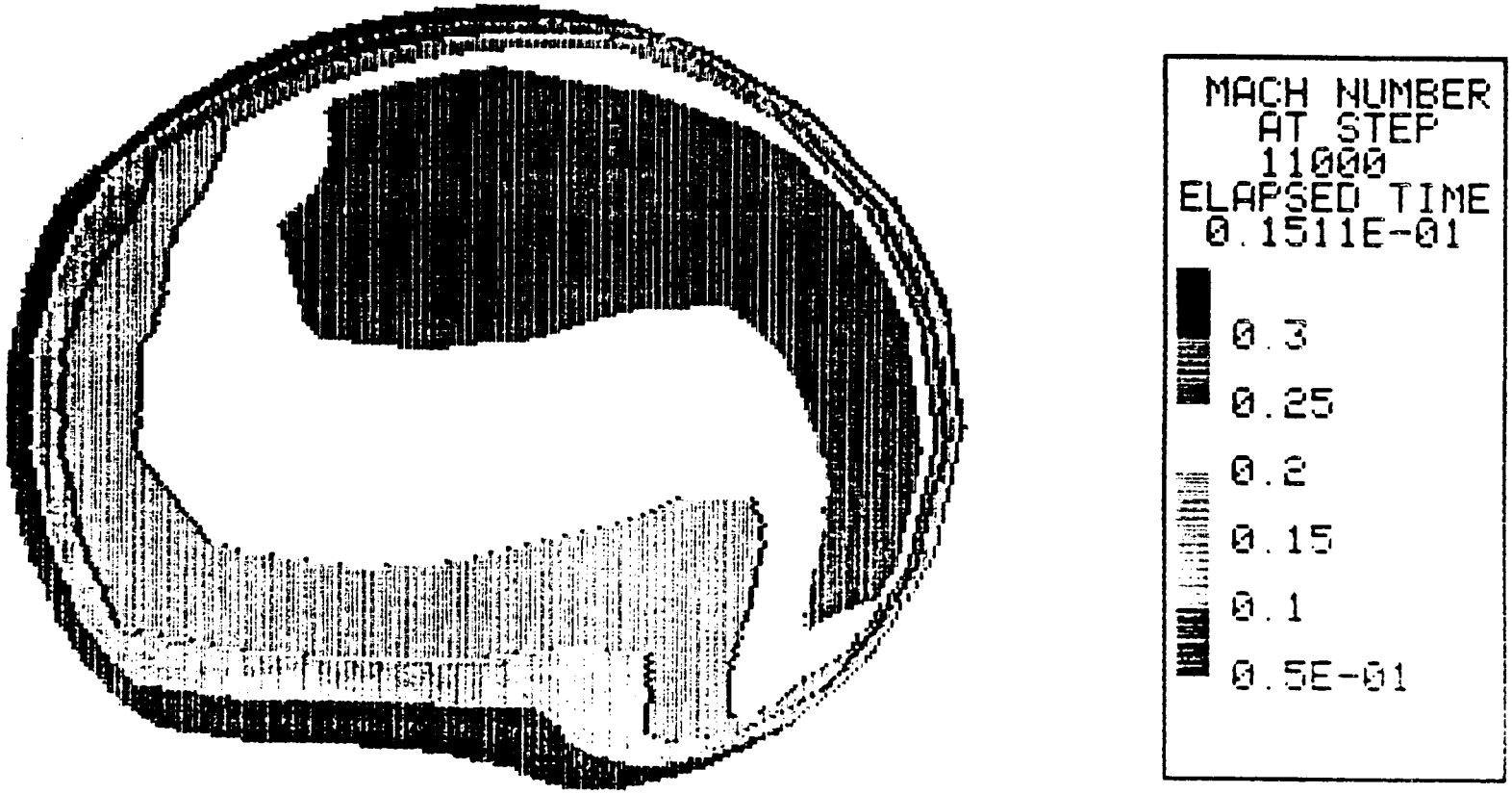

Fig. 13

TURBULENT SSME HGM TRANSFER DUCT MIDPLANE

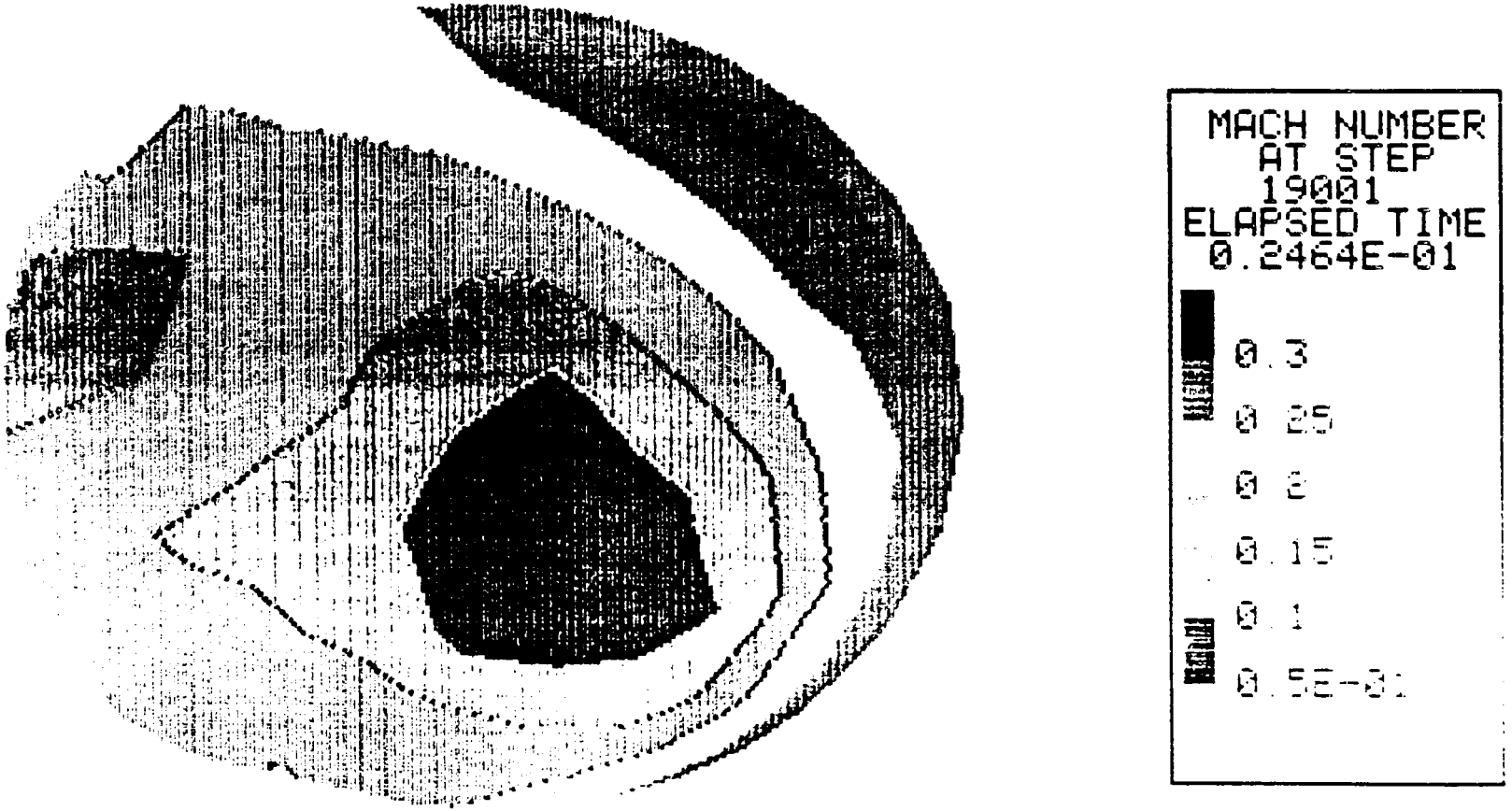

Fig. 14

LAMINAR SSME HGM TRANSFER DUCT EXIT PLANE

Fig. 15

TURBULENT SSME HGM TRANSFER DUCT EXIT PLANE

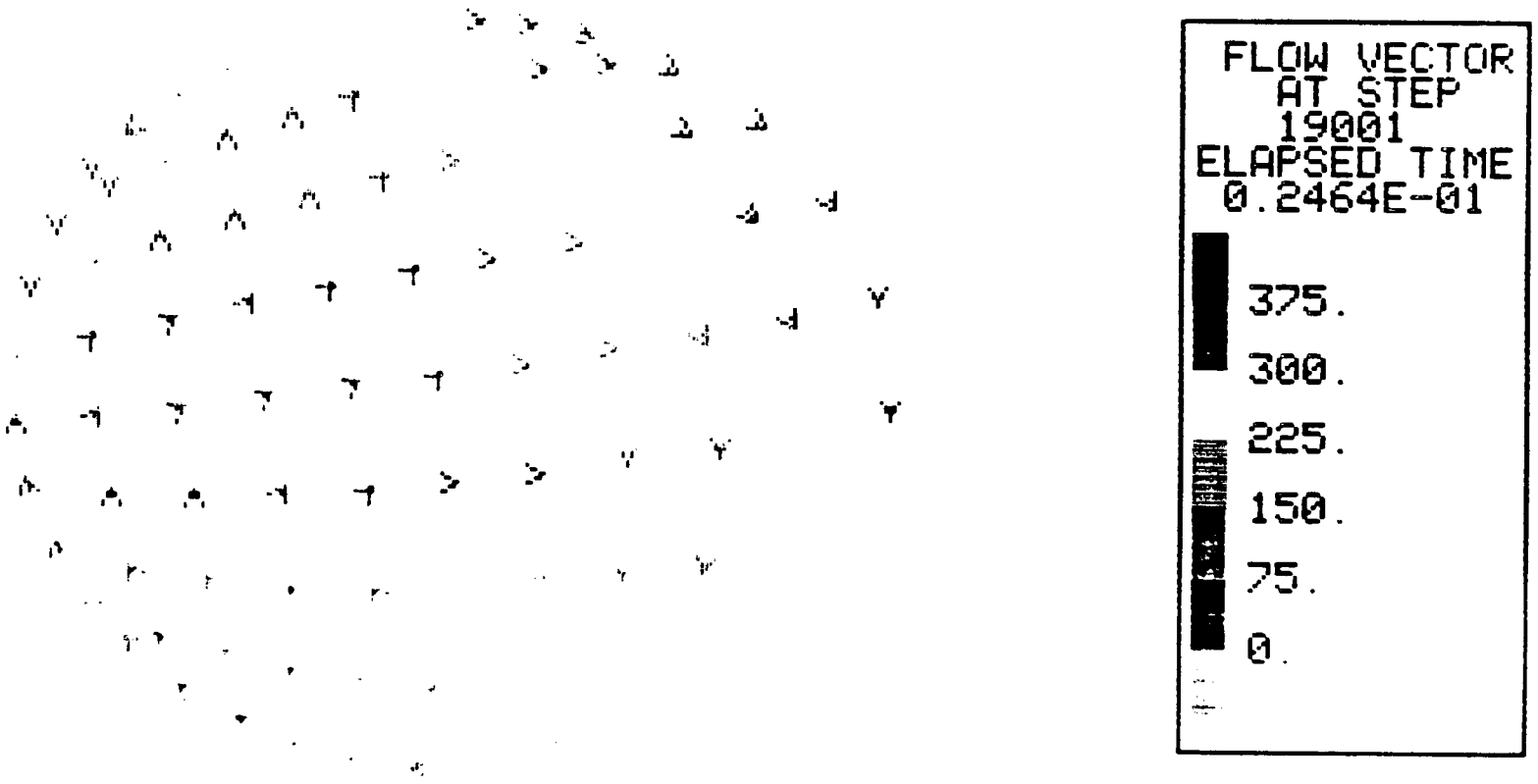

Fig. 16

LAMINAR SSME HGM TRANSFER DUCT EXIT PLANE

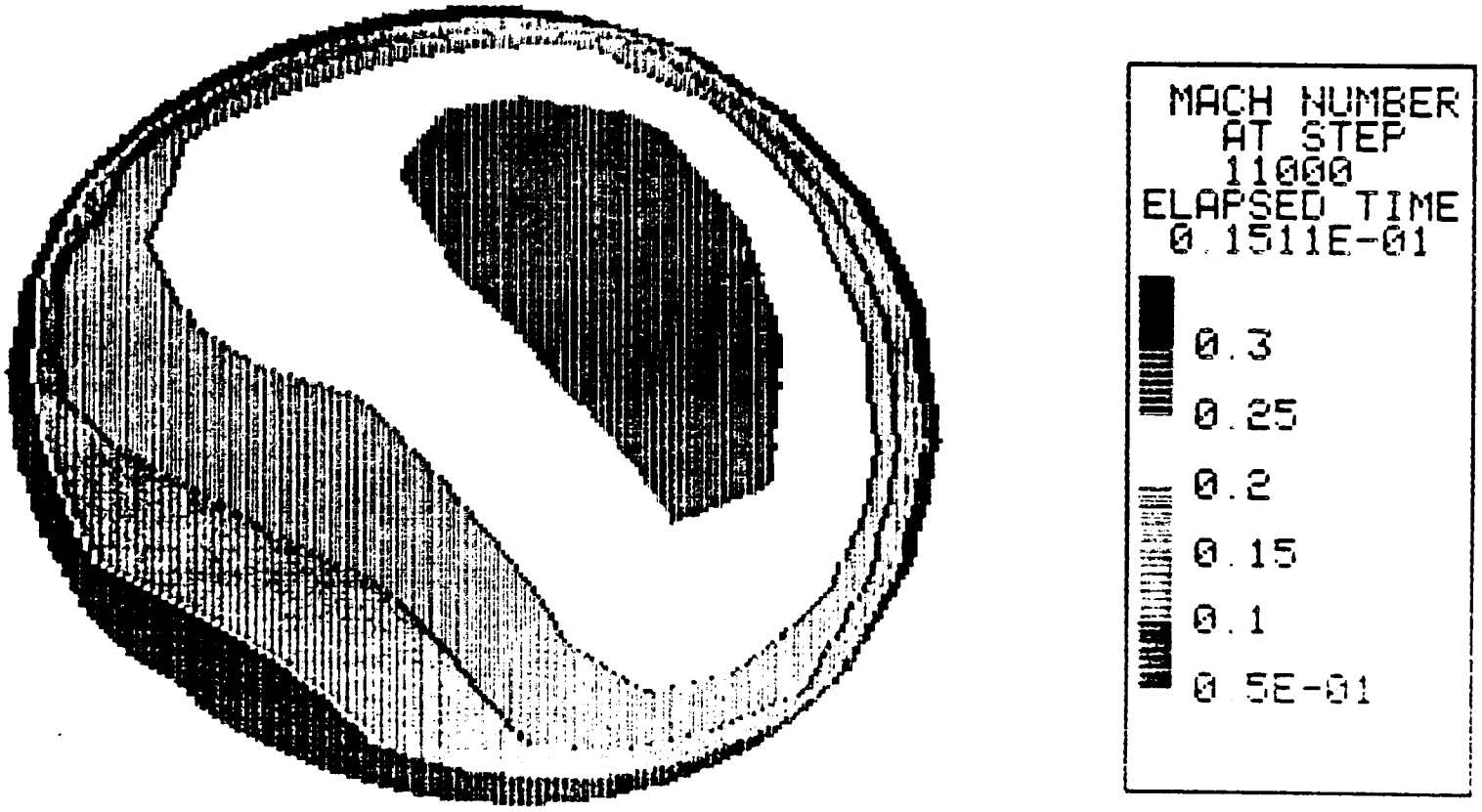

Fig. 17

TURBULENT SSME HGM TRANSFER DUCT EXIT PLANE

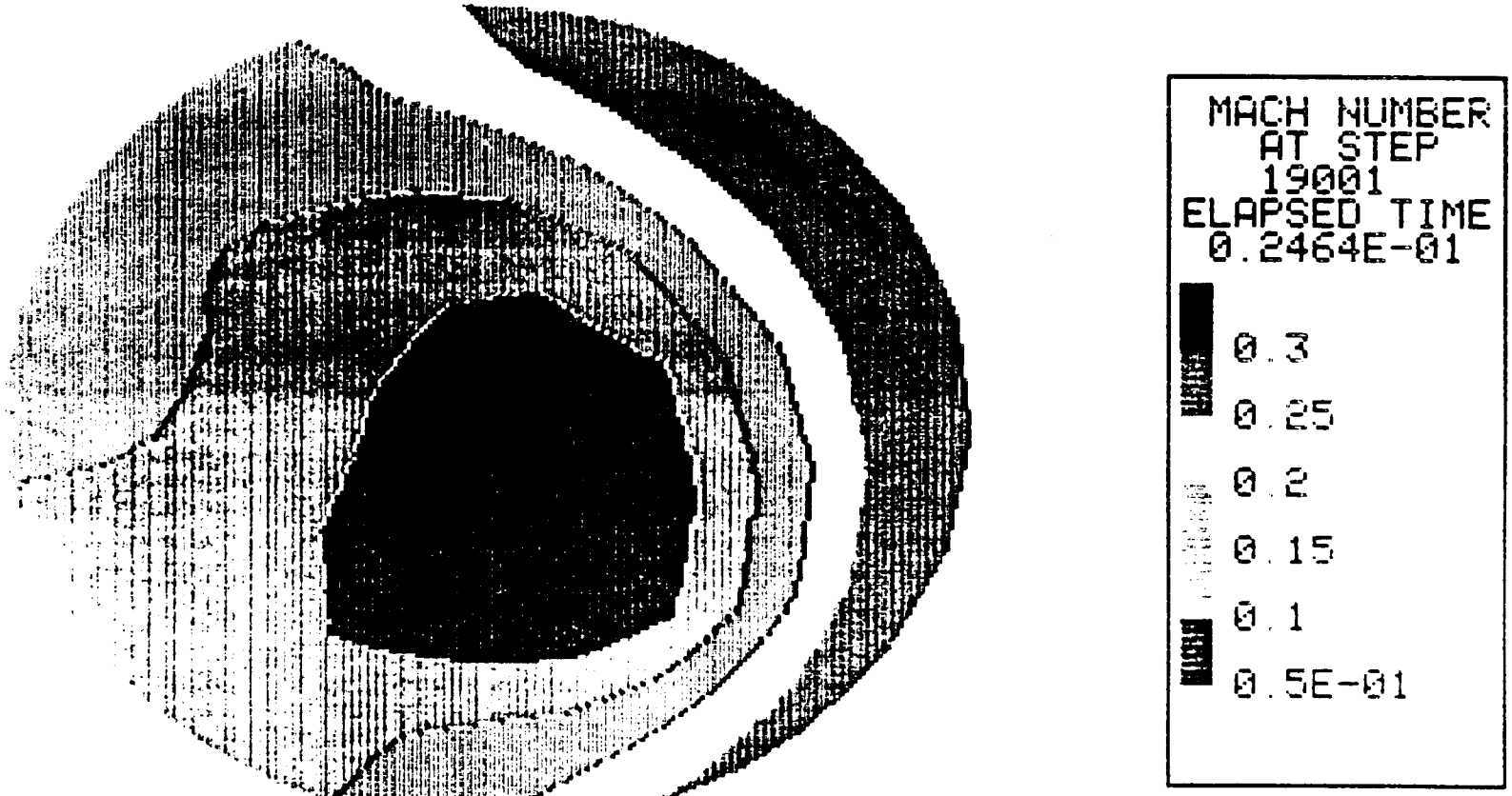

Fig. 18

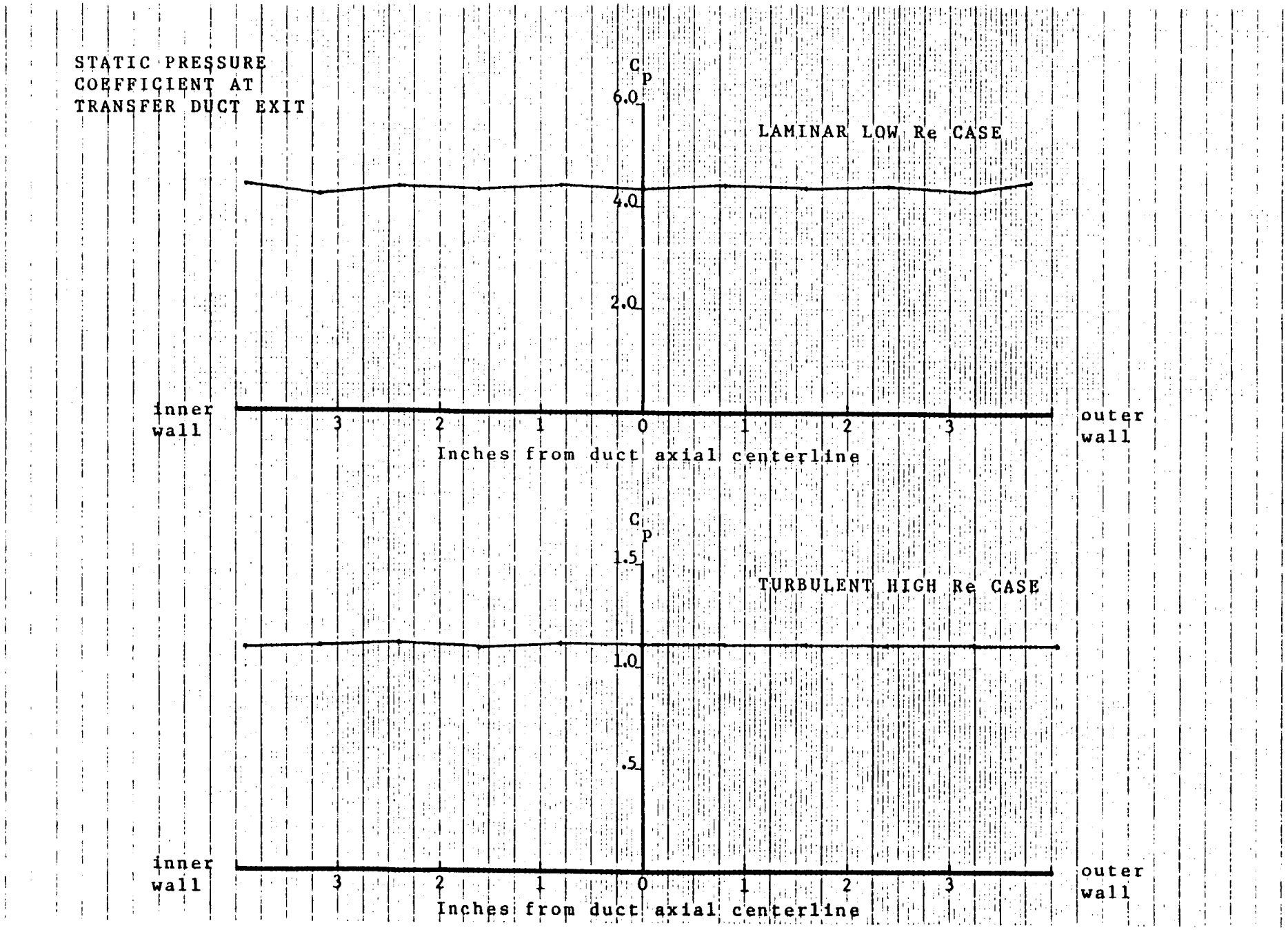
STATIC PRESSURE
COEFFICIENT AT
TRANSFER DUCT EXIT
C_p
6.0
4.0
2.0
LAMINAR LOW Re CASE
inner wall
3
2
1
0
1
2
3
outer wall
Inches from duct axial centerline
C_p
1.5
1.0
.5
TURBULENT HIGH Re CASE
inner wall
3
2
1
0
1
2
3
outer wall
Inches from duct axial centerline

Fig. 19

APPENDIX D

TURBULENT FLOW IN THE TURNAROUND DUCT, HOT GAS MANIFOLD, AND TRANSFER TUBES

R.C. FARMER & P.G. ANDERSON

CONTINUUM, INC.

JUNE 11, 1985

STATUS OF TAD/LOX POSTS STUDY

- VAST CODE WAS VECTORIZED
  - BOTH CYBER 205 (AMES) AND CRAY (UIS)
  - APPROXIMATELY 20 TIMES FASTER THAN OLD VERSION
- EDDY VISCOSITY TURBULENCE MODEL WAS IMPLEMENTED
  - ALEGRAIC MODEL WITH SPECIAL WALL ELEMENT TREATMENT
- TAD/HGM/TRANSFER DUCT CALCULATION IN PROGRESS

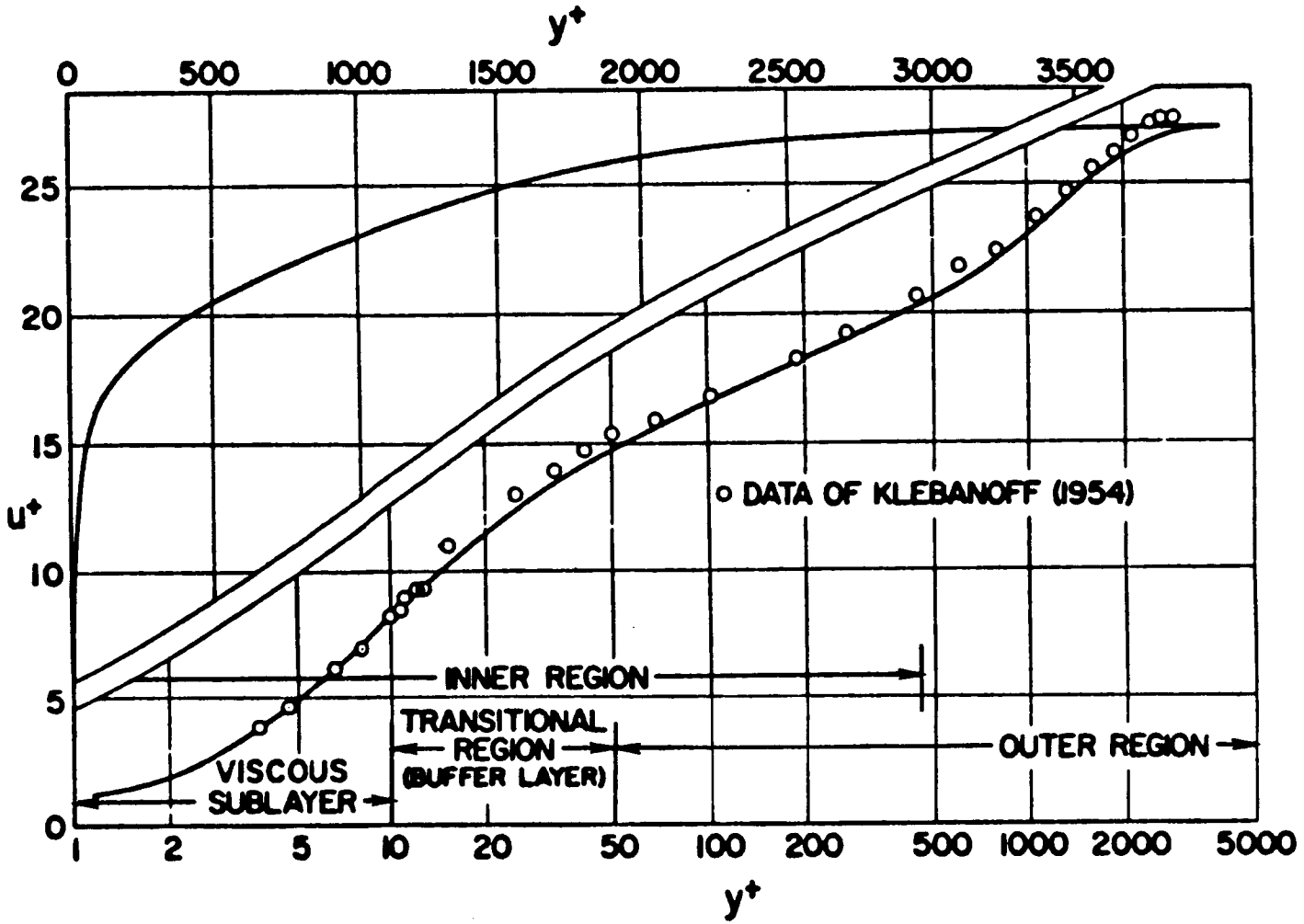

Semilogarithmic and linear plots of mean velocity distribution across a turbulent boundary layer with zero pressure gradient.

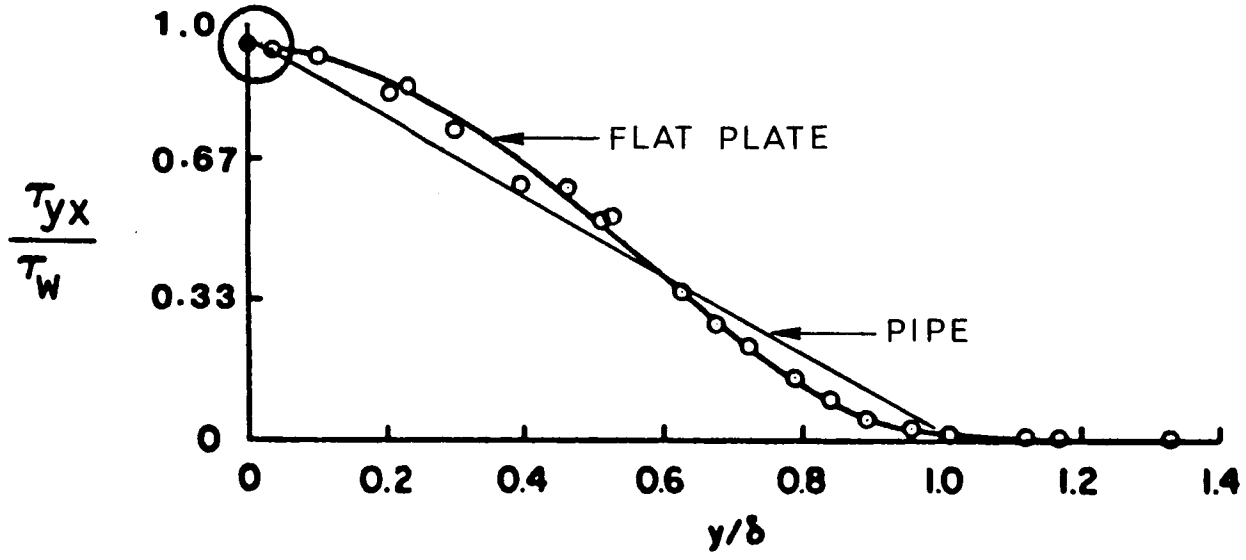

Dimensionless shear-stress distribution across the boundary layer at zero pressure gradient, according to the data of Klebanoff (1954).

VELOCITY PROFILES FOR PIPES & FLAT PLATES

Empirical.

$$u^+ = u/u_\tau = y\, u_\tau/\nu \equiv y^+ \qquad 0 < y^+ < 5$$

$$u^+ = (2/\kappa)\, \ln(y^+) - 3.05 \qquad 5 < y^+ < 30$$

$$u^+ = (1/\kappa)\, \ln(y^+) + B \qquad 30 < y^+ < 500$$

$$(\kappa,\ B) = (0.4,\ 5.5)_N = (0.41,\ 5.0)_C \text{ for plates \& pipes}$$

$$\frac{U_e - u}{u_\tau} = -(1/\kappa)\, \ln(y/\delta) + A \qquad 50 < y^+$$

A varies for pipes, flat plates & flows w/pressure gradients

Musker's Eq.

$$(u/u_\tau) = 5.424 \tan^{-1}(0.1198\ y^+ - 0.4880) - 3.52$$

$$+ 4.168 \ln(y^+ + 10.6) - 0.8684 \ln(y^{+2} - 8.15\ y^+ + 86)$$

$$+ (14.64\ \Pi + 2.44)(y/\delta)^2 - (9.76\ \Pi + 2.44)(y/\delta)^3$$

when $u_\tau = (\tau_w/\rho)^{0.5}$

$\Pi = \kappa\ A/2$, A = 2.35 flat plate

A = 0.65 pipes

$$\Pi = 0.8\ (\beta + 0.5)^{0.75}$$

$$\beta = (\delta^*/\tau_w)(dP/dx)$$

EDDY VISCOSITY

$$\varepsilon_e \equiv \tau_{yx} / (du/dy)$$

$$\tau_{yx} = (1 - y/R)\, \tau_w$$

$$(du/dy) = (u_\tau / \kappa\, y) \qquad \text{for } y^+ > 30$$

$$\varepsilon_e = (1 - y/R)(\kappa\, y/R)(u_\tau\, R)$$

$$(\varepsilon_e / \nu) = (\kappa\, y/R)(1 - y/R)(0.5\, Re)(0.125\, f_m)^{0.5}$$

$\varepsilon_{e,max}$ from experiment

for pipes

$$(\varepsilon_{e,max} / \nu) = 0.07\, (u_\tau\, R/\nu) = 0.07(R\, U_e/\nu)(0.125\, f_m)^{0.5}$$

for flat plates

$$\varepsilon_{e,max}/\nu = 0.07(u_\tau \delta/\nu) = 0.07(\delta U_e/\nu)(C_f/2)^{0.5}$$

$$\varepsilon_{e,max}/\nu = 0.016\, U_e\, \delta^*/\nu \qquad \text{as } R_e \rightarrow \infty$$

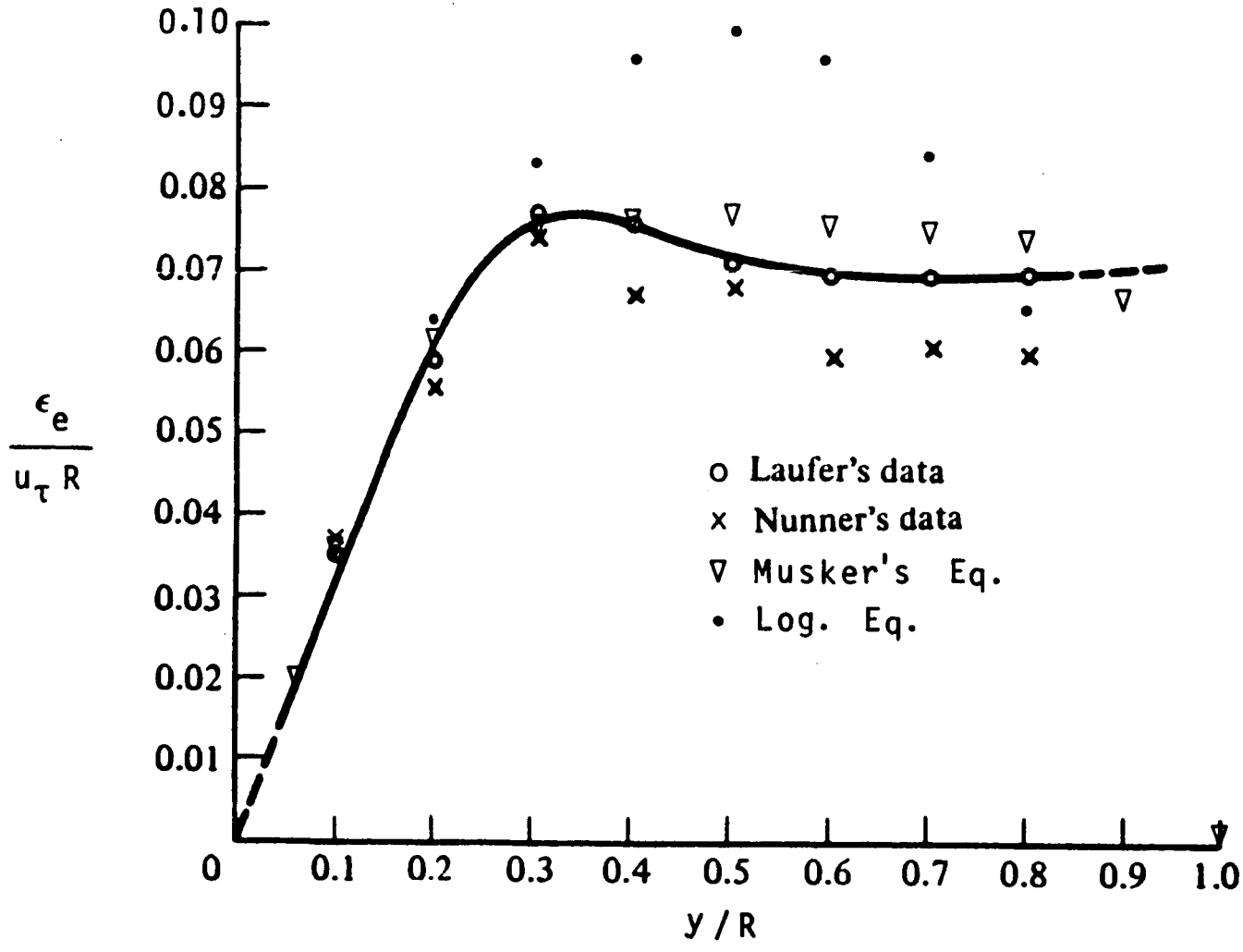

eddy viscosity in pipe flow

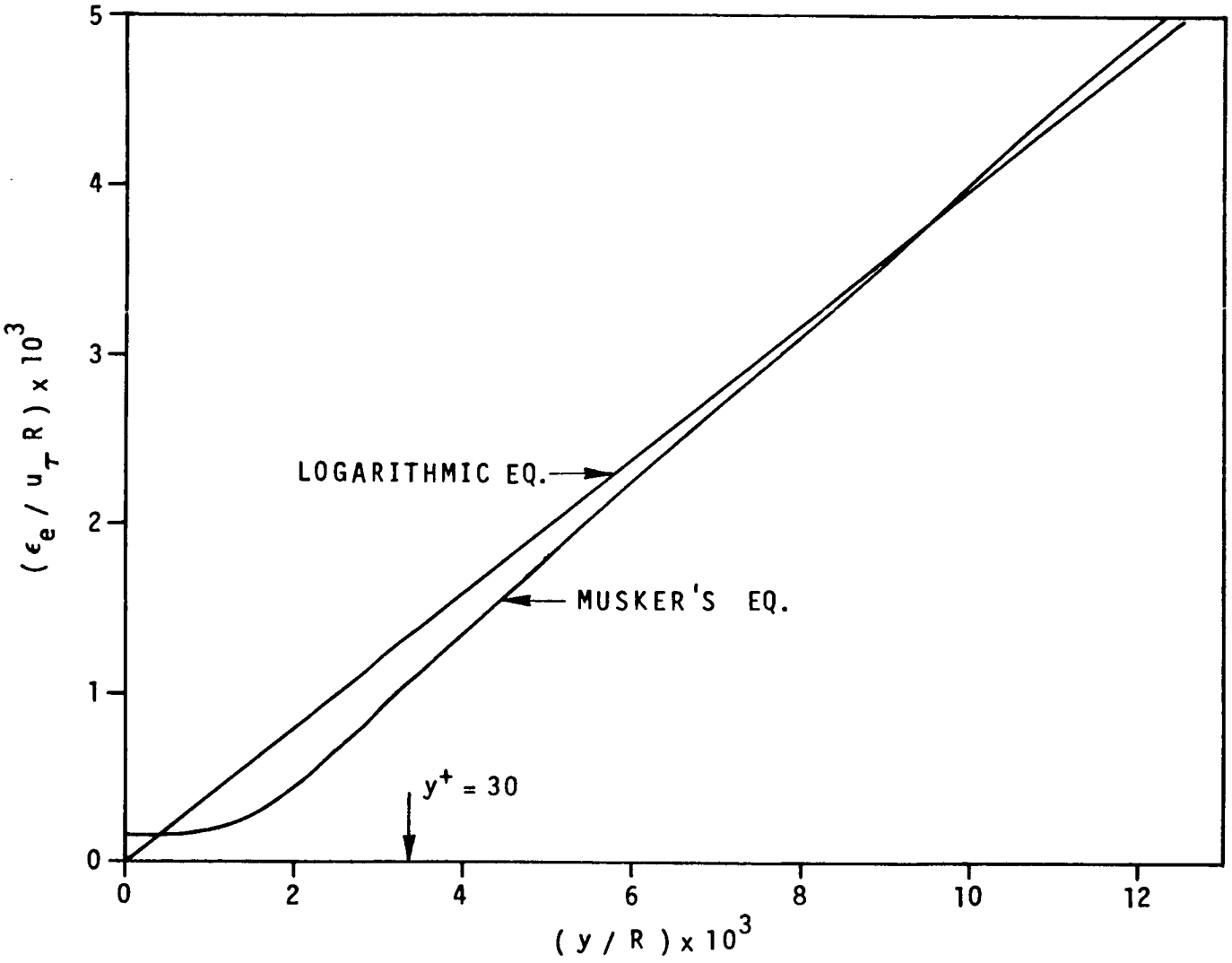
5
4
3
2
1
0
0
2
4
6
8
10
12
$(\epsilon_e / u_\tau R) \times 10^3$
$(y / R) \times 10^3$
LOGARITHMIC EQ.
MUSKER'S EQ.
$y^+ = 30$

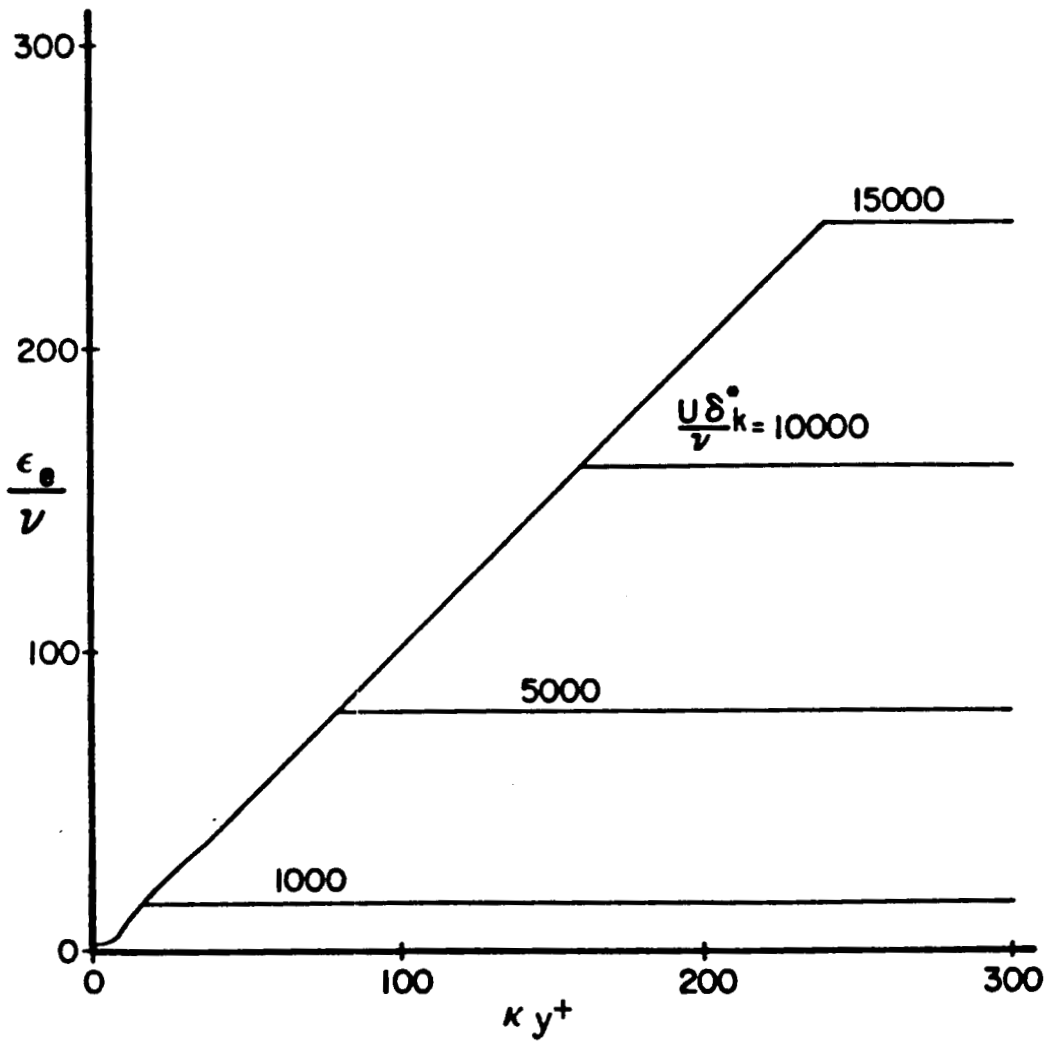

Illustrations of the composite effective viscosity function for an incompressible flow.

TEMPERATURE PROFILES

$$\theta\ (\kappa/u_\tau) = \ln\left\{\frac{2\ y^+\ Pr^{0.5}}{\theta\ (T_r - 1) + 2}\right\} + 9.3027\ Pr^{0.5}\ \kappa_\theta$$

$$- 1.7556 - \exp(-(9.737\ Pr^{0.5}\ \kappa_\theta + 0.6807))$$

where $\theta = (T - T_w)/(T_e - T_w)$

$$T_r = T_e\ /\ T_w$$

$$\kappa_\theta = \kappa\ St\ /\ (u_\tau^2\ T_e\ /\ T_w)$$

$$St = q_w\ /\ \rho_e\ C_p\ U_e\ (T_w - T_e)$$

$$q_w = -\ k_w\ (\partial T/\partial y)_w$$

Note: The denominator of the ln term is a density correction to y^+; such a correction also applies to the compressible velocity correlation equations.

APPLICATION TO VAST CODES

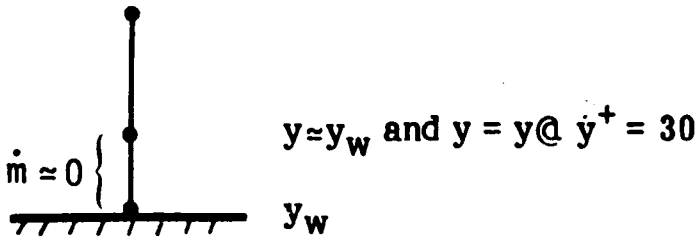

1. $\left(\frac{\partial u}{\partial y}\right)_{30}$, $\left(\frac{\partial T}{\partial y}\right)_{30}$, u_τ, q_w

   are calculated from inner (wall) functions using $y^+ = 30$, for u & T at the nearest nodes to the wall.

2. 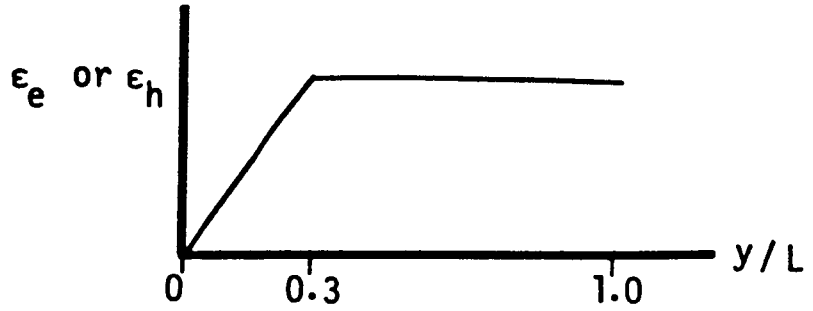

$$\varepsilon_{e,max} = (2.06\ E\ -3)(U_e\ L)(C_f\ /\ C_{f,e})^{0.5}$$

$$\varepsilon_{h,max} = (3.15\ E\ -3)(U_e\ L)(C_f\ /\ C_{f,e})^{0.5}$$

$$L = R_h \text{ or } \delta$$

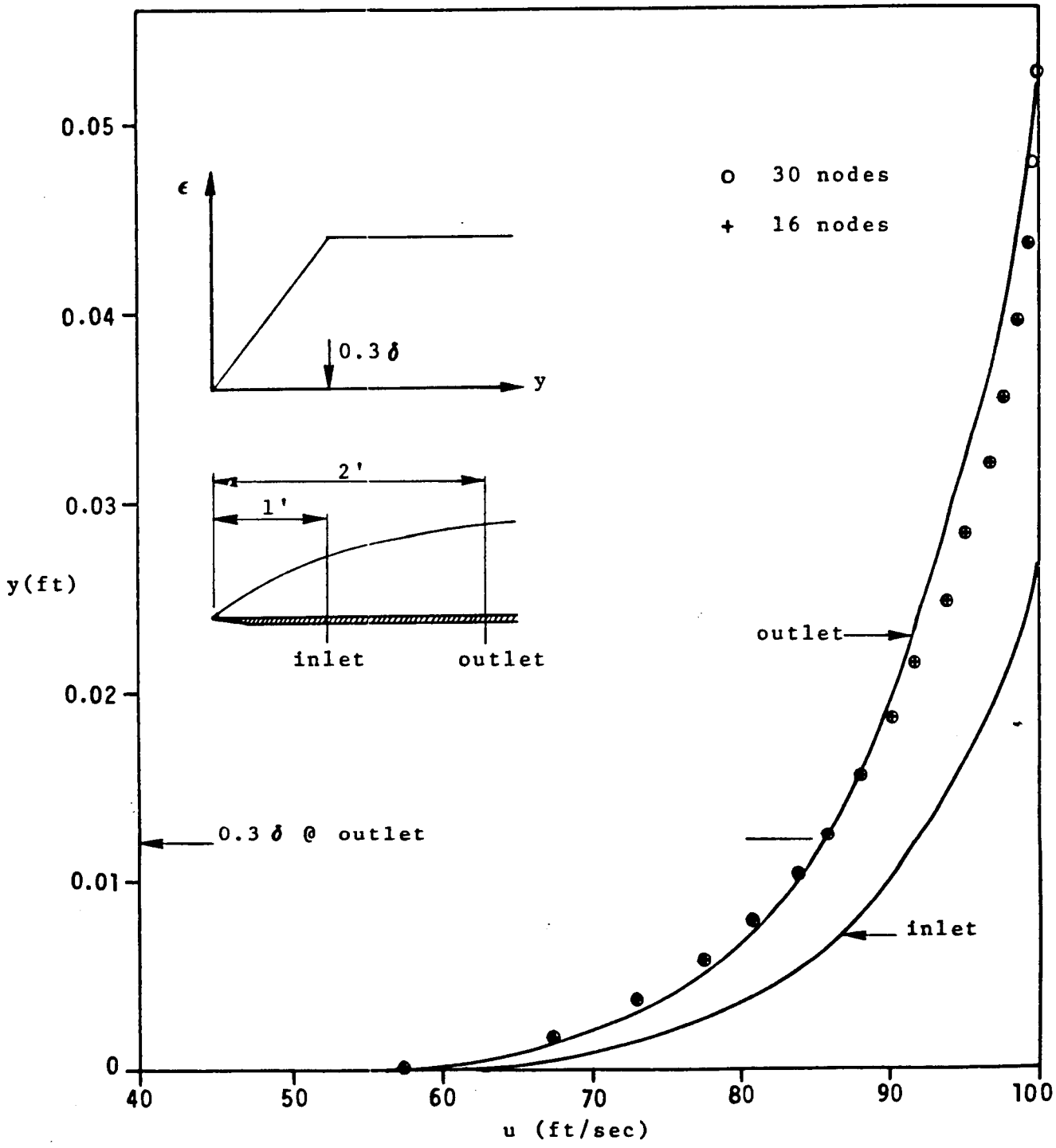

TURBULENT BOUNDARY LAYER ON A SMOOTH FLAT PLATE

TAD/HGM/TRANSFER TUBE FLOW ANALYSIS

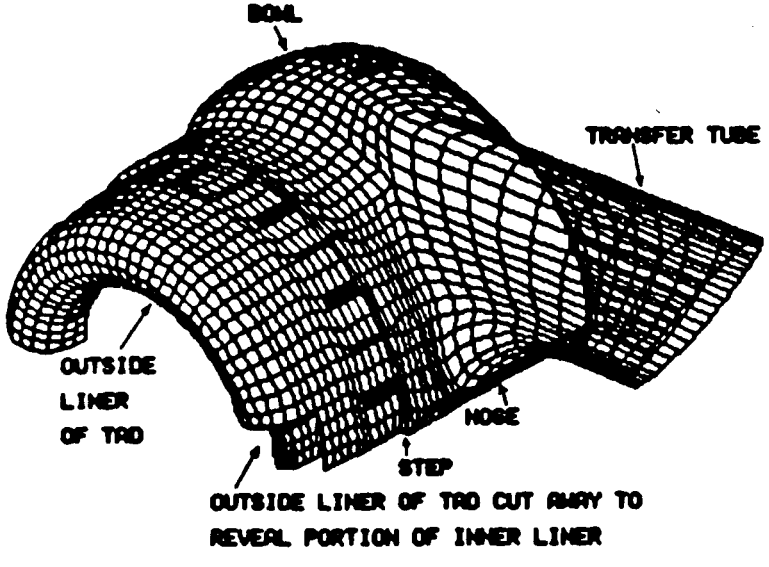

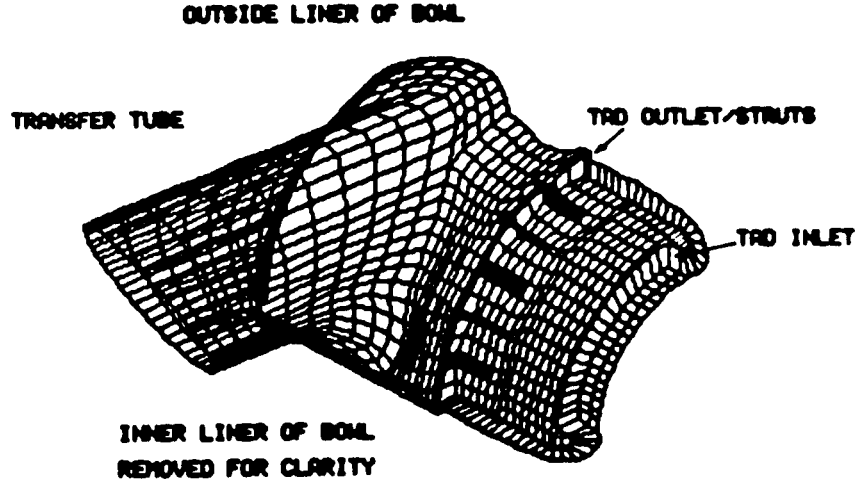

APPENDIX E

FLOW ANALYSIS OF SSME HPFTP EXHAUST SYSTEM

PETER G. ANDERSON
CONTINUUM, INC.

NOVEMBER 28, 1984

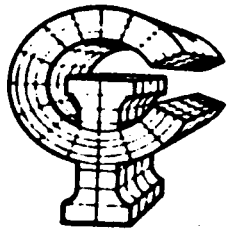

Continuum, Inc.
4715 University Dr.
Suite 118
Huntsville, Al. 35805

TAD/HGM/TRANSFER TUBE FLOW ANALYSIS

- CONFIGURATION
  - FMOF TURN AROUND DUCT
  - PHASE 3 TWO-DUCT HGM
  - "VERSION B" TRANSFER TUBE WITH FLOW SEPARATOR
- SPECIFIED CONDITIONS
  - AIR AT 530 DEG. R
  - PRESSURE AND VELOCITY DISTRIBUTIONS SPECIFIED AT TAD INLET
  - FLOW RATE OF 72.0 LBM/SEC
  - NO TURBINE INDUCED SWIRL
  - TURBULENT VISCOSITY = 10^4 X LAMINAR VISCOSITY
    (RESULTS IN REYNOLDS NUMBER OF ABOUT 400)
- COMPUTATIONAL MODEL
  - 10724 NODES USING CONTINUUM'S VAST CODE
  - PLANE OF SYMMETRY BETWEEN TRANSFER TUBES (180 DEG.)
  - STRUTS AND POSTS MODELLED VIA "NULL" ELEMENTS
  - PARABOLIC VELOCITY DISTRIBUTION IN RADIAL DIRECTION AT TAD INLET
- RESULTS
  - 11000 ITERATIONS
  - TOTAL PRESSURE DROP THROUGH SYSTEM OF 48 PSI

TURN AROUND DUCT CONFIGURATION

INSIDE LINER

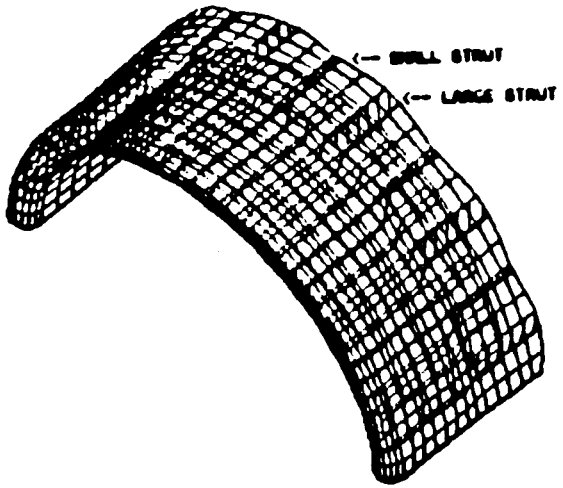

OUTSIDE LINER

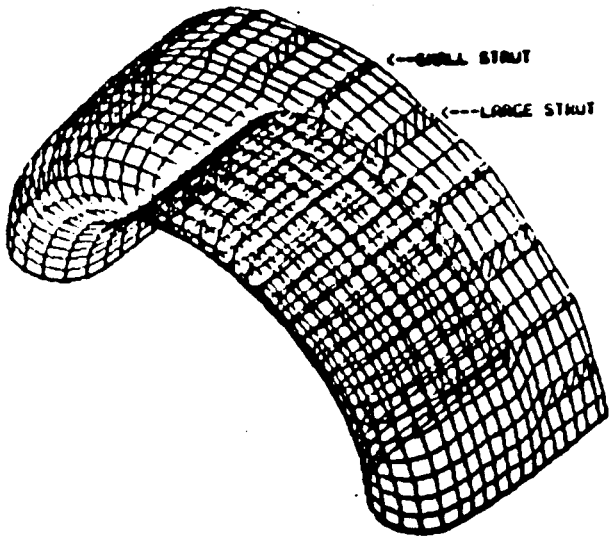

HOT GAS MANIFOLD CONFIGURATION

INSIDE LINER

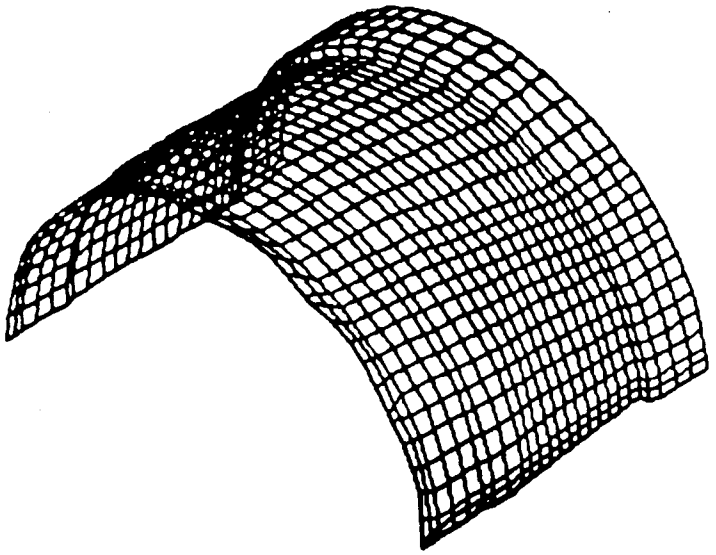

OUTSIDE LINER

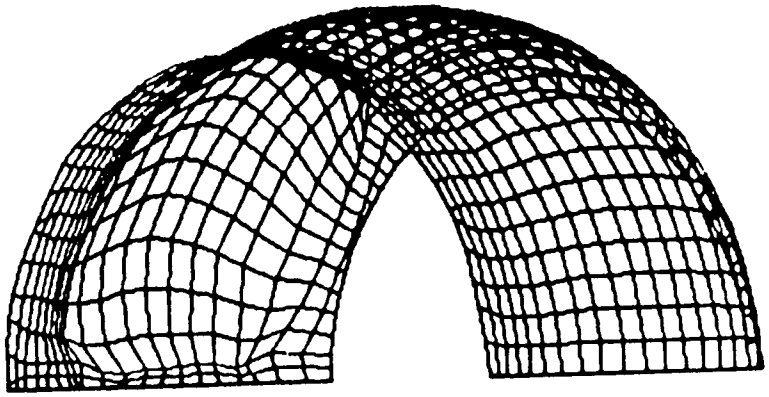

BOWL OUTER LINER AND TUBE INLET

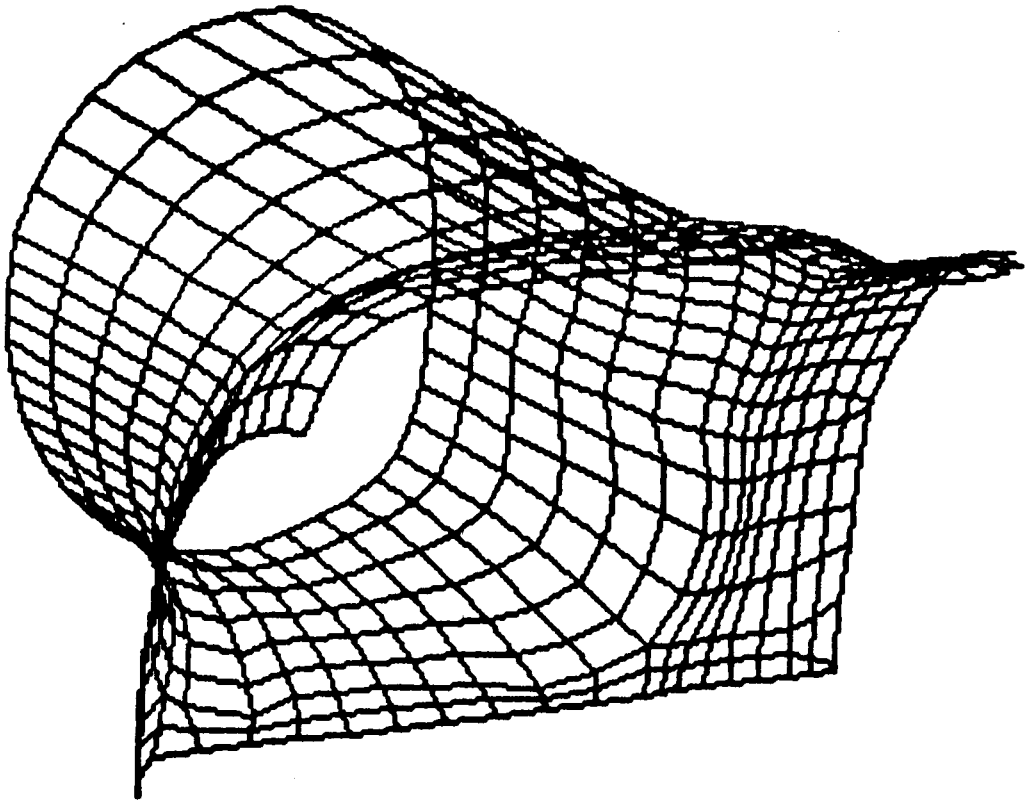

GRID FOR OUTSIDE LINER OF TAD, BOWL AND TUBE

(PORTIONS DELETED FOR CLARITY)

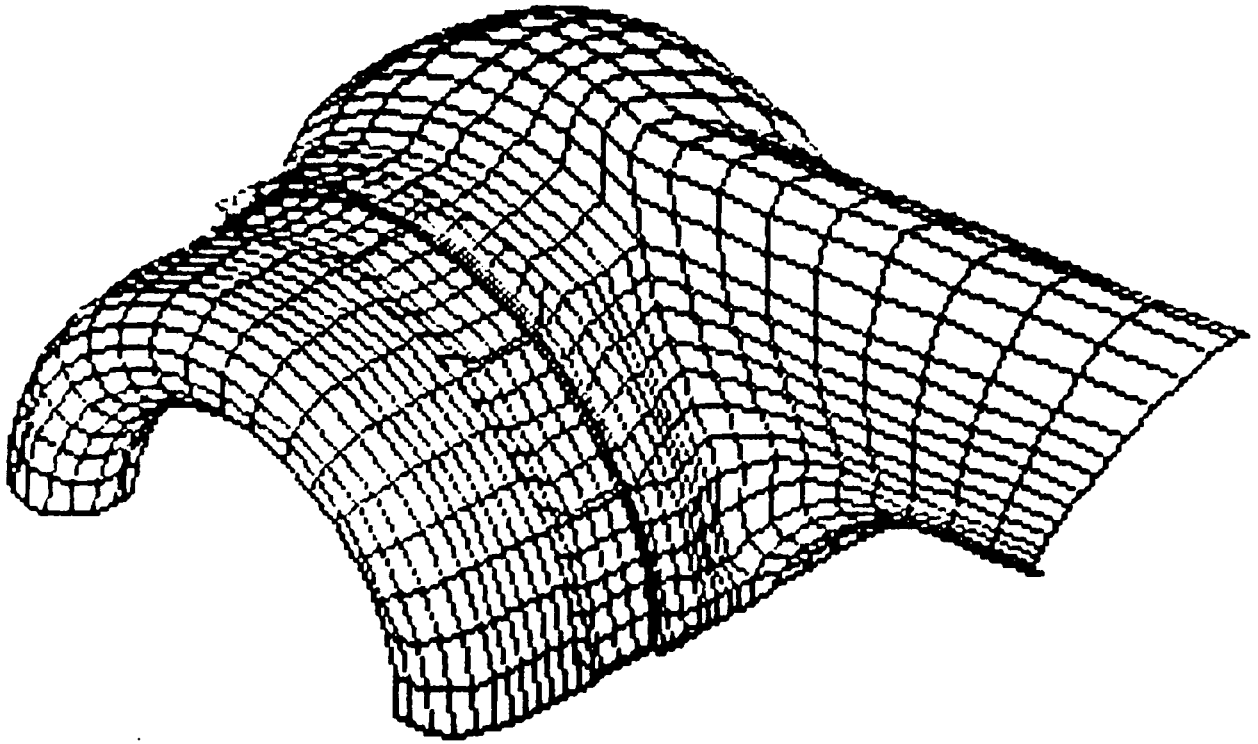

PRESSURE DISTRIBUTION IN 180 DEG PLANE OF SYMMETRY

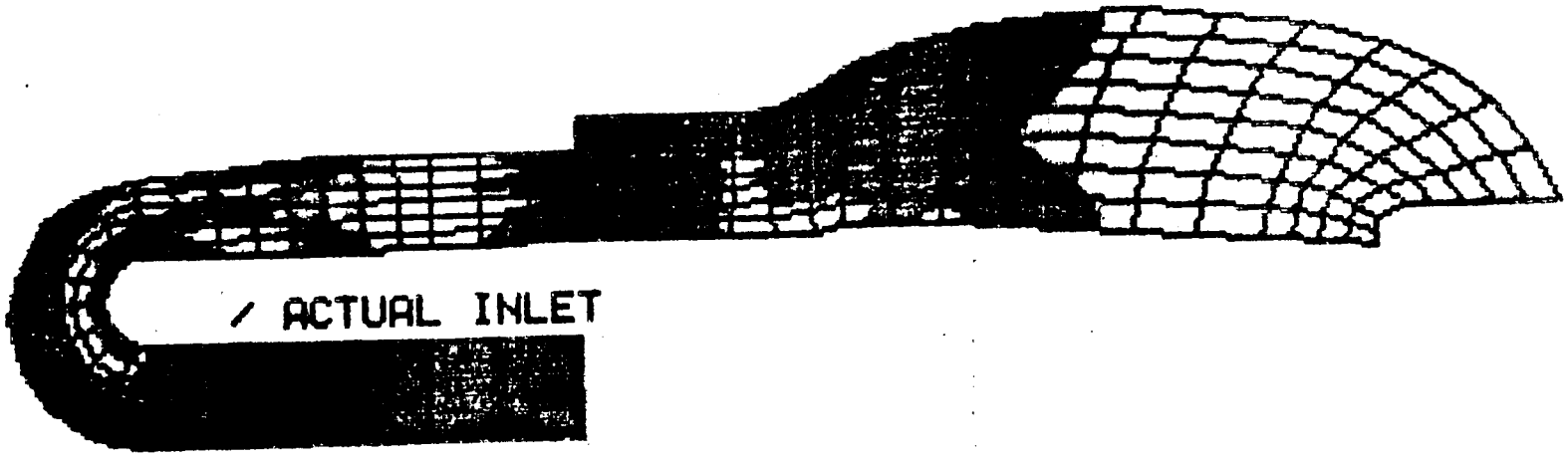

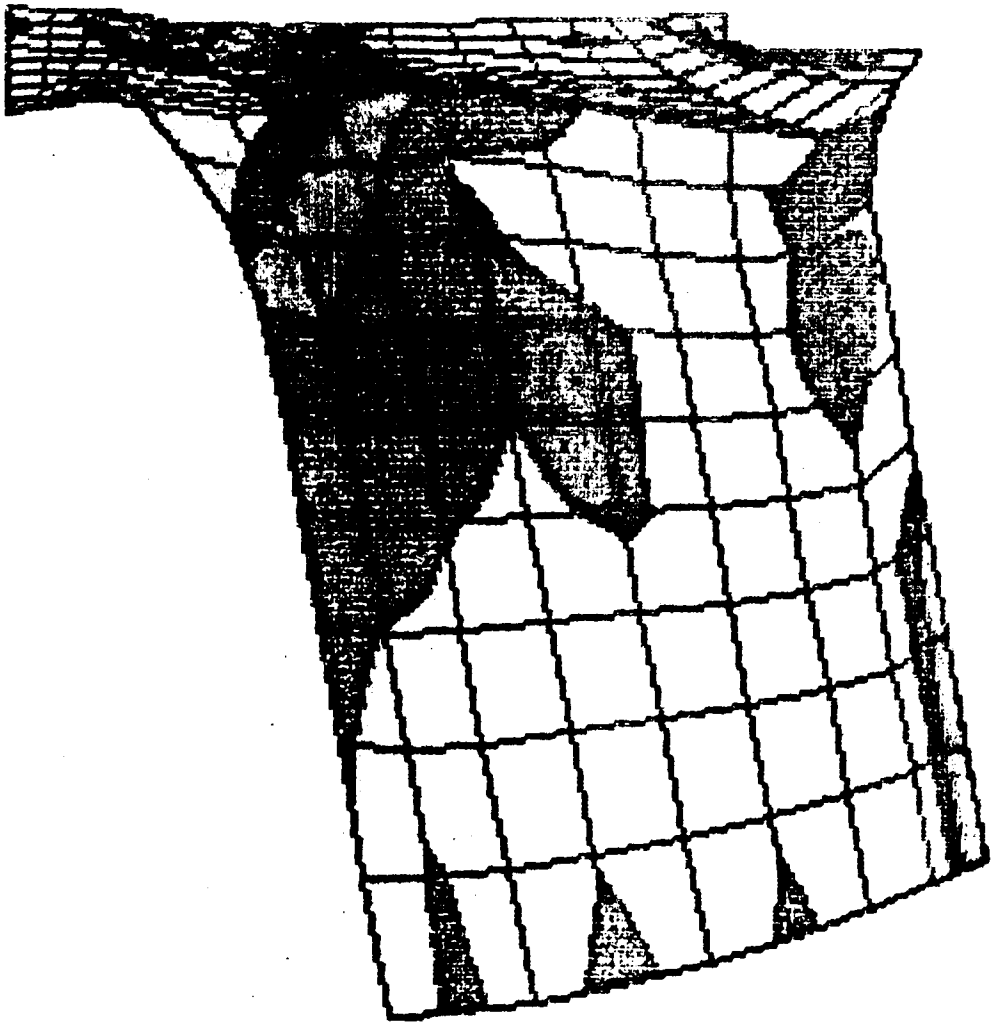

PRESSURE IN HGM

BOWL AND MID PLANE

(APPROX.) OF TUBE

(148-154 PSIA)

PRESSURE DISTRIBUTION IN 0 DEG. PLANE OF SYMMETRY

(153-198 PSIA)

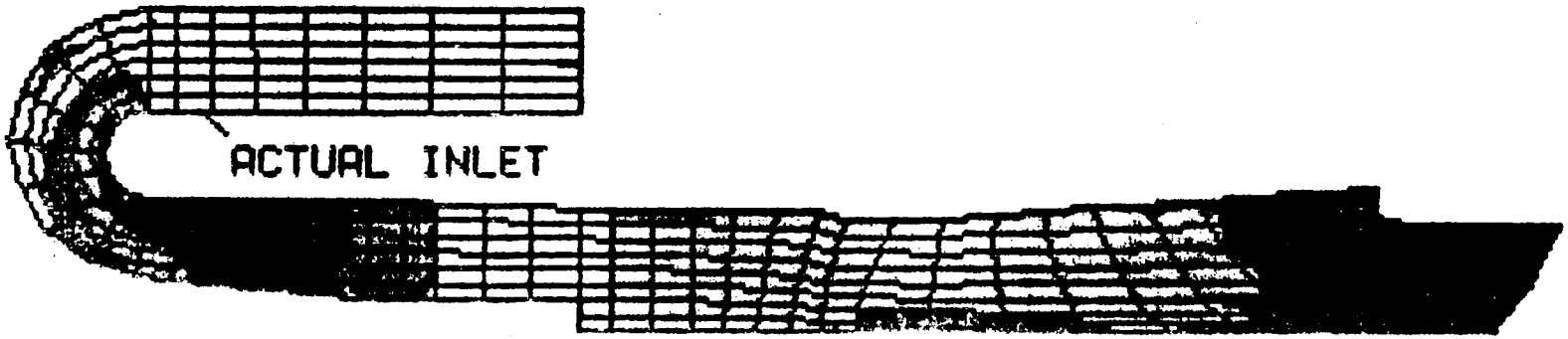

PRESSURE IN HGM BOWL CROSS SECTION AND MID PLANE
OF TRANSFER TUBE (152-184 PSIA)

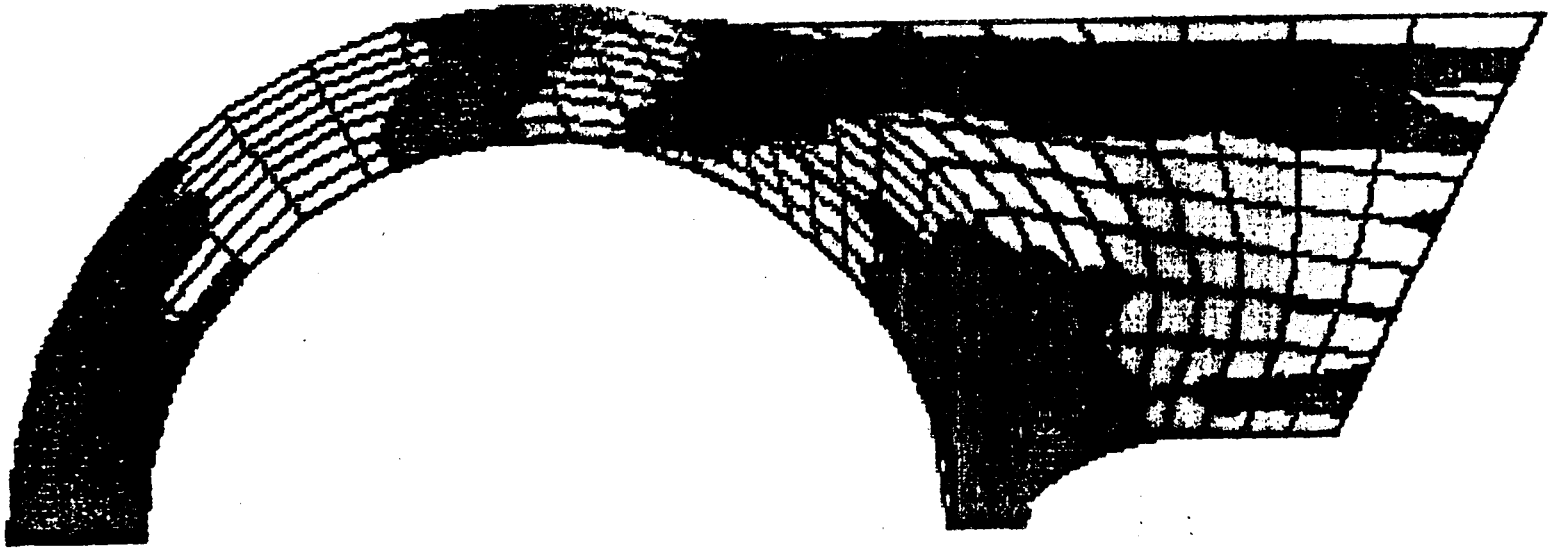

PRESSURE DISTRIBUTION ON OUTSIDE SURFACE

(153 -198 PSIA)

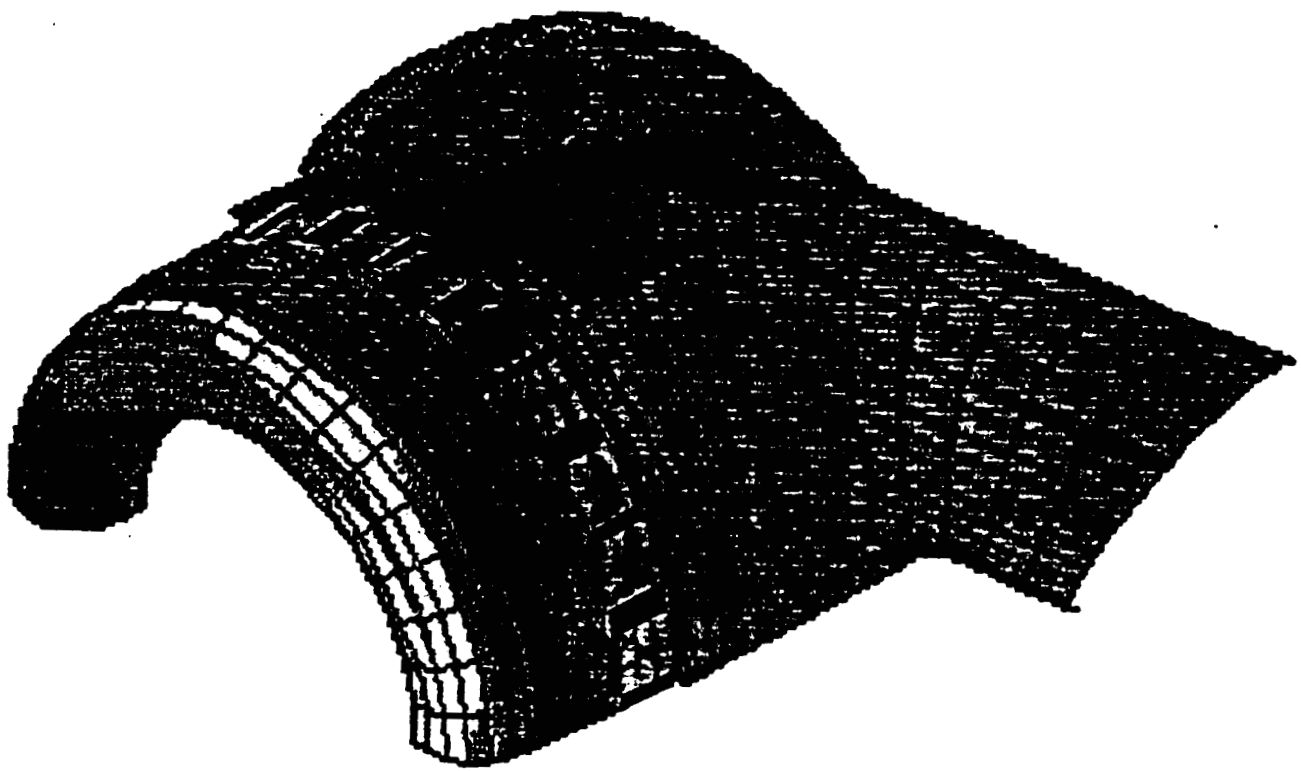

VELOCITY VECTORS IN TAD AND BOWL

(0-480 FPS)

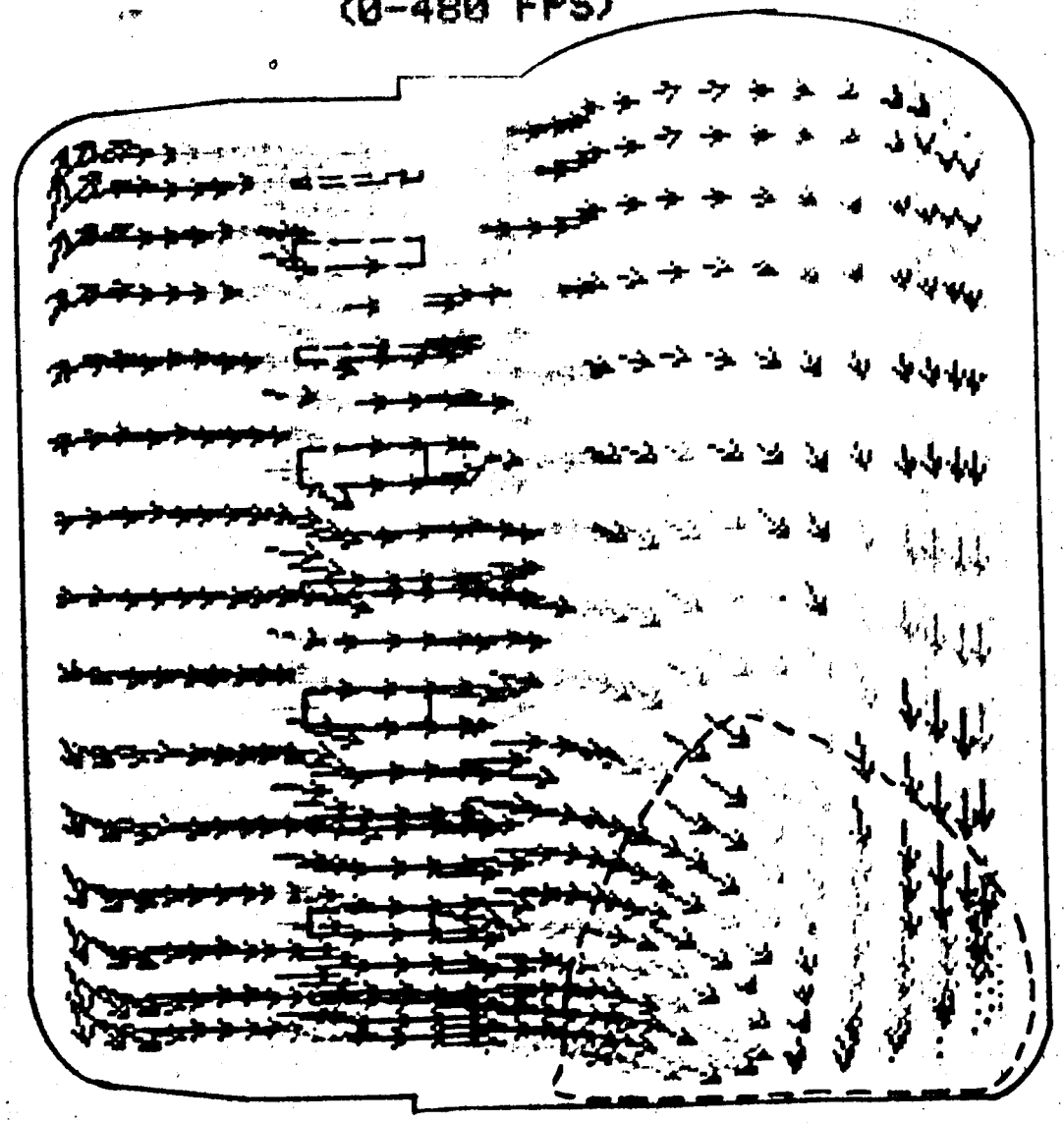

VELOCITY VECTORS IN
COMPUTATIONAL PLANE
IN HGM BOWL AND
MID PLANE THROUGH
TRANSFER TUBE
(0 - 360 FPS)

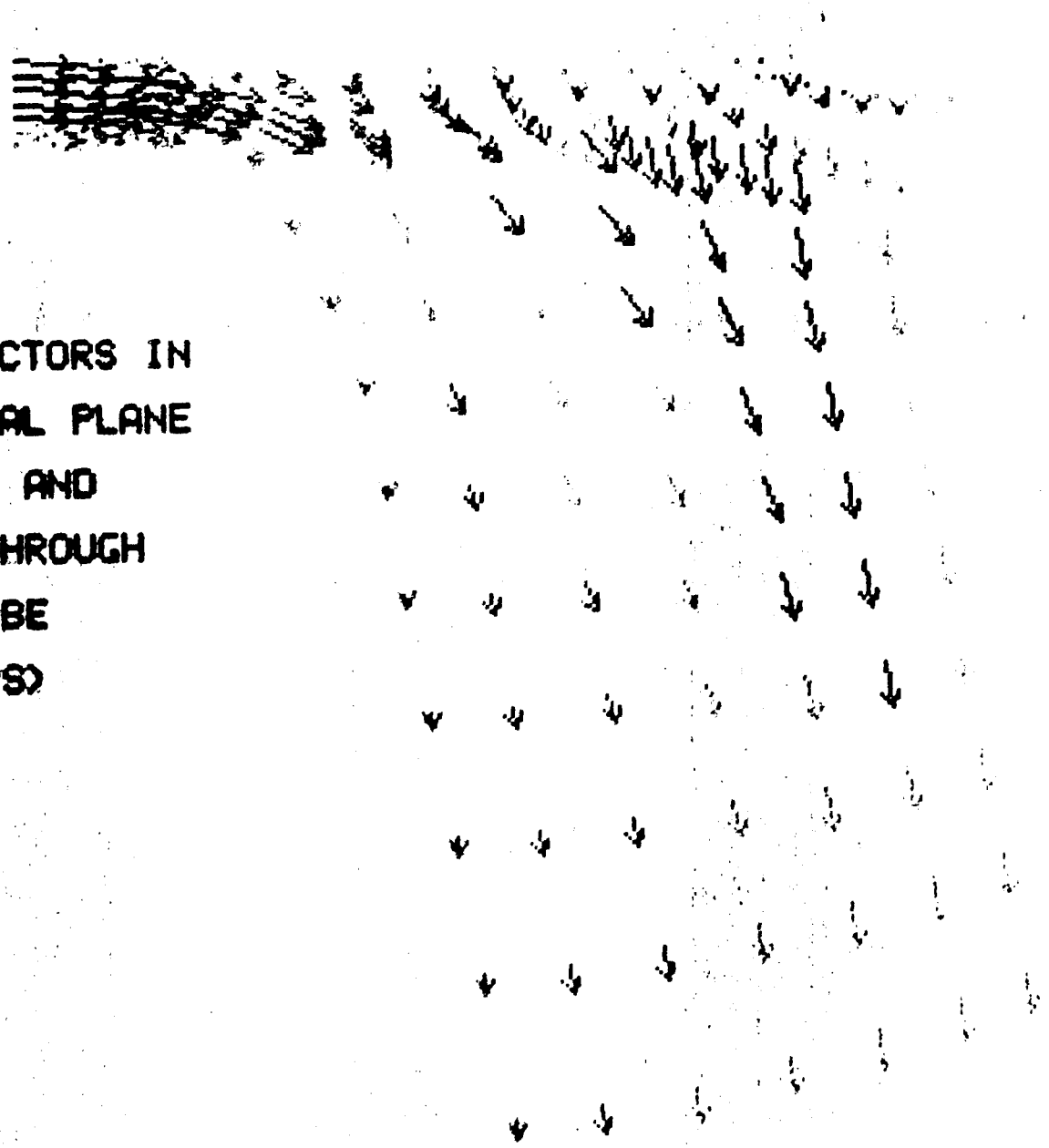

VELOCITY VECTORS IN CROSS SECTION OF BOWL AND MID PLANE OF TRANSFER TUBE (0 - 360 FPS)

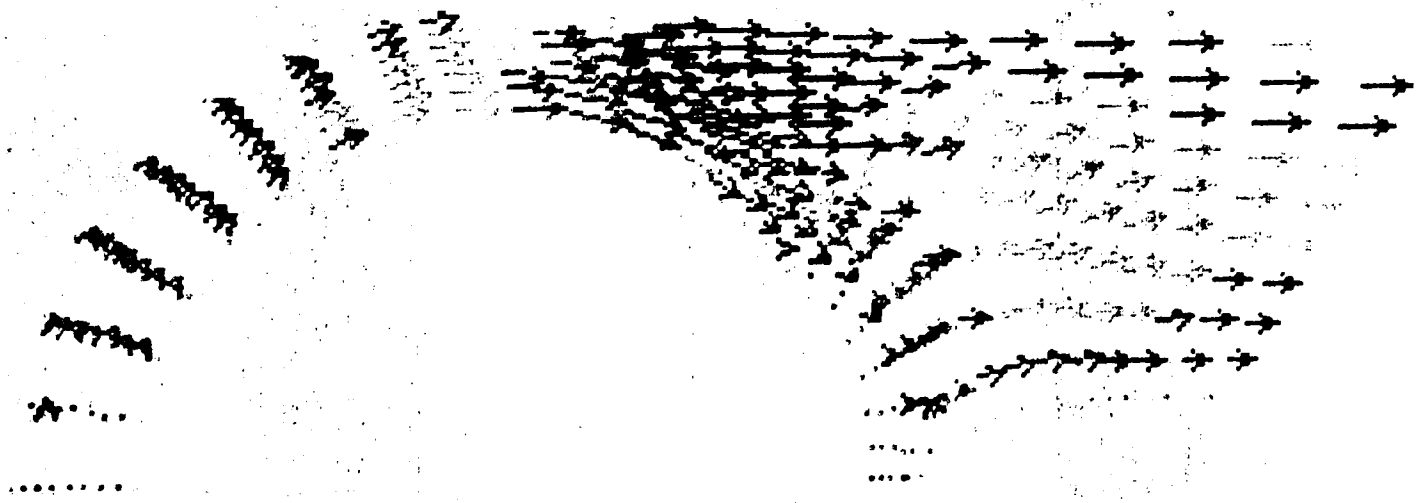

VELOCITY VECTORS IN BOWL BETWEEN TRANSFER TUBES (0 DEG.)

(0 - 400 FPS)

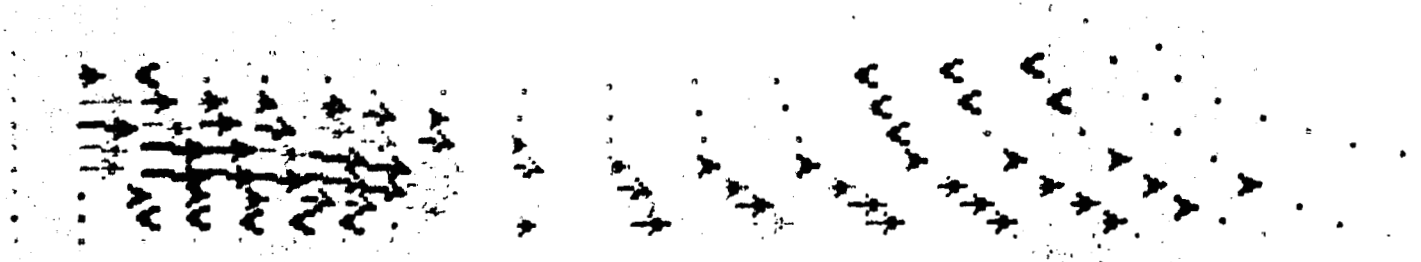

FLOW SEPARATOR

VELOCITY VECTORS IN TAD (NEAR SIDE OR 0 DEG.)

(0 - 400 FPS)

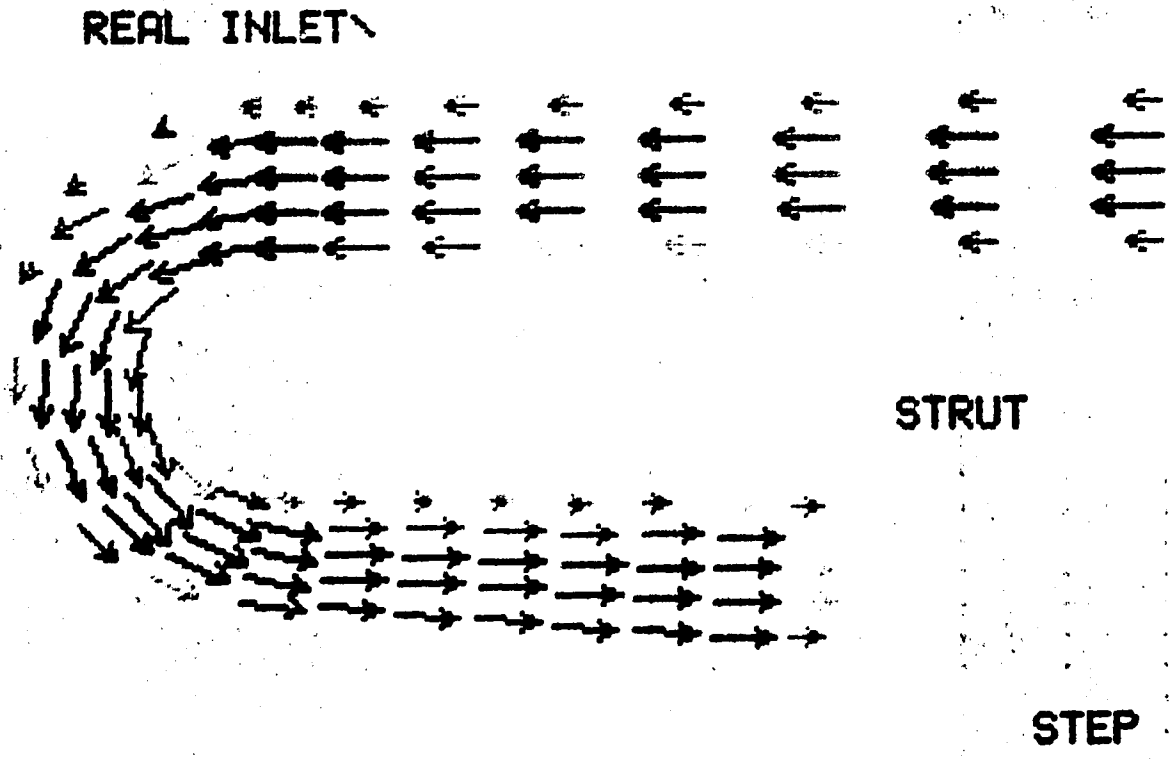

VELOCITY VECTORS IN BOWL (FAR SIDE OR 180 DEG.)

(0 - 400 FPS)

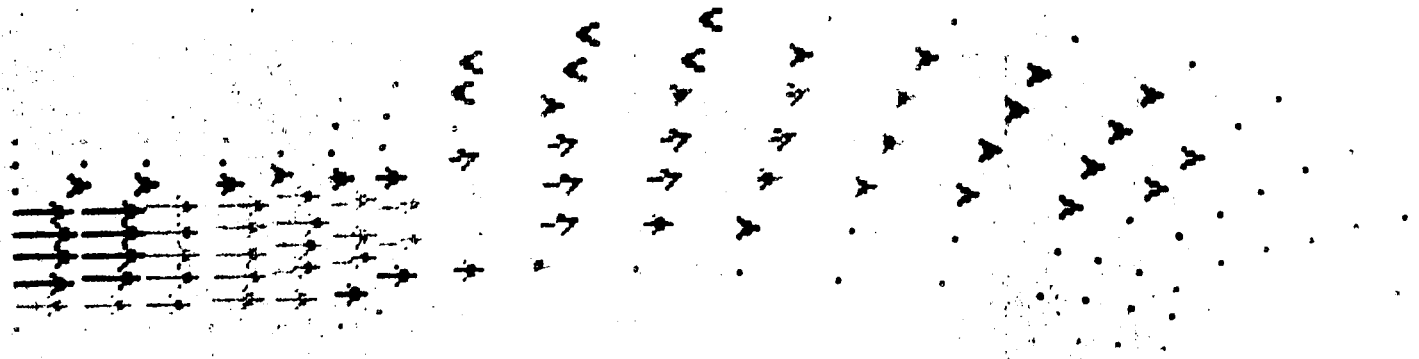

VELOCITY VECTORS IN TAD (FAR SIDE OR 180 DEG.)

(0 - 400 FPS)

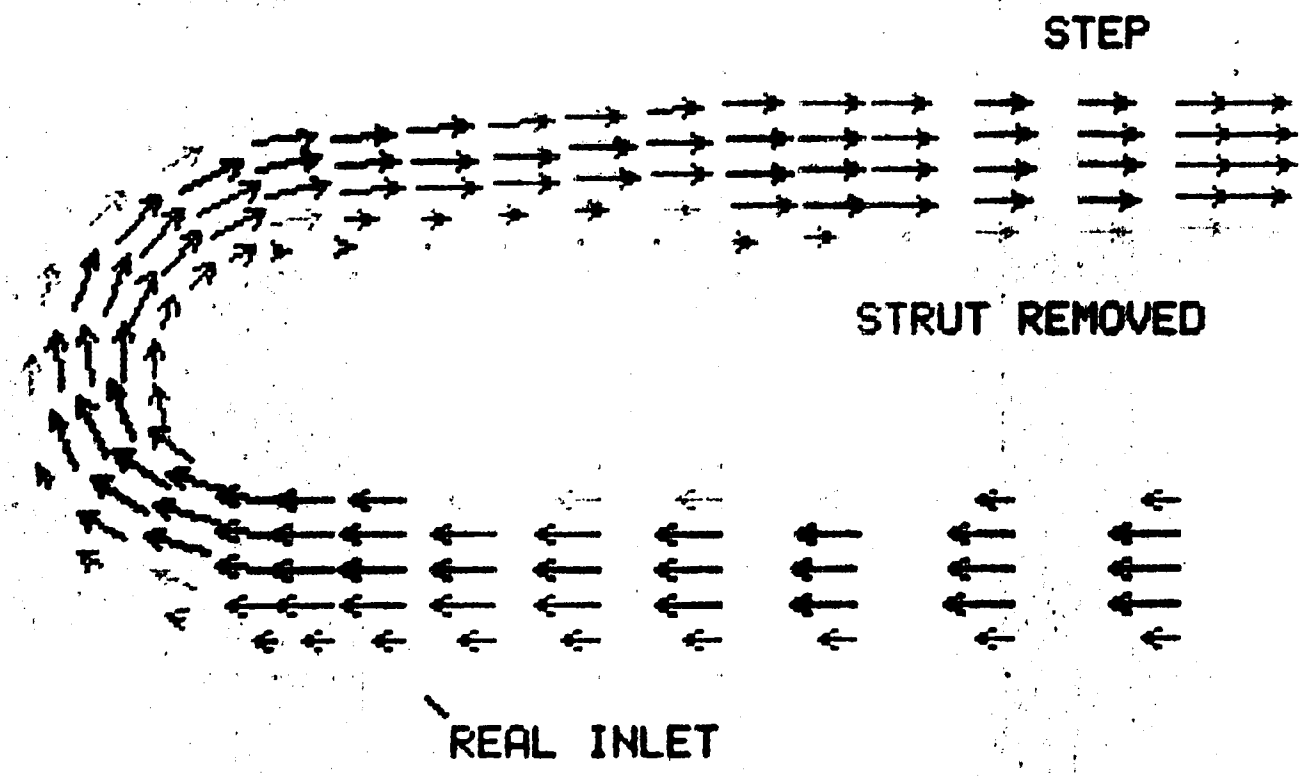

RESULTS

- PRESSURE DROP
  - 48 PSI
  - COMPUTED PRESSURE DROP BETWEEN THEORETICAL LAMINAR AND TURBULENT VALUES (CRANE HANDBOOK)
- CONVERGENCE
  - 11000 ITERATIONS
  - SUM OF SQUARES OF TIME DERIVATIVES DECREASED 2-3 ORDERS OF MAGNITUDE
  - CHANGES IN SELECTED PARAMETERS BECAME MINIMAL
- COMMENT
  - REYNOLDS NUMBER 0F 400 RENDERS COMPARISON OF RESULTS OF COMPUTATION TO TURBULENT TEST DATA UNREALISTIC

APPENDIX F

FLOW ANALYSIS OF SSME LOX MANIFOLD

Y. M. DAKHOUL
CONTINUUM, INC

C. M. SEAFORD
NASA/MSFC

SSME CFD FOURTH ANNUAL WORKING GROUP MEETING

NASA/MSFC APRIL 8-11, 1986

FLOW ANALYSIS OF SSME LOX MANIFOLD

Continuum, Inc.

OBJECTIVES

- CALCULATE MAIN FEATURES OF FLOW
- REVEAL ANY POSSIBLE CAUSES FOR VIBRATION
- PROVIDE DATA FOR FLUTTER ANALYSIS OF VANES

APPROACH

- 2-D APPROXIMATION OF THE 3-D CONFIGURATION
- SOLVE COMPRESSIBLE NAVIER-STOKES EQUATIONS
- PRESSURE SOLUTION $P = \rho R T$
- INVISCID FLOW
- SLIP WALLS
- LARGE NUMBER OF NODES, NO TURBULENCE MODEL

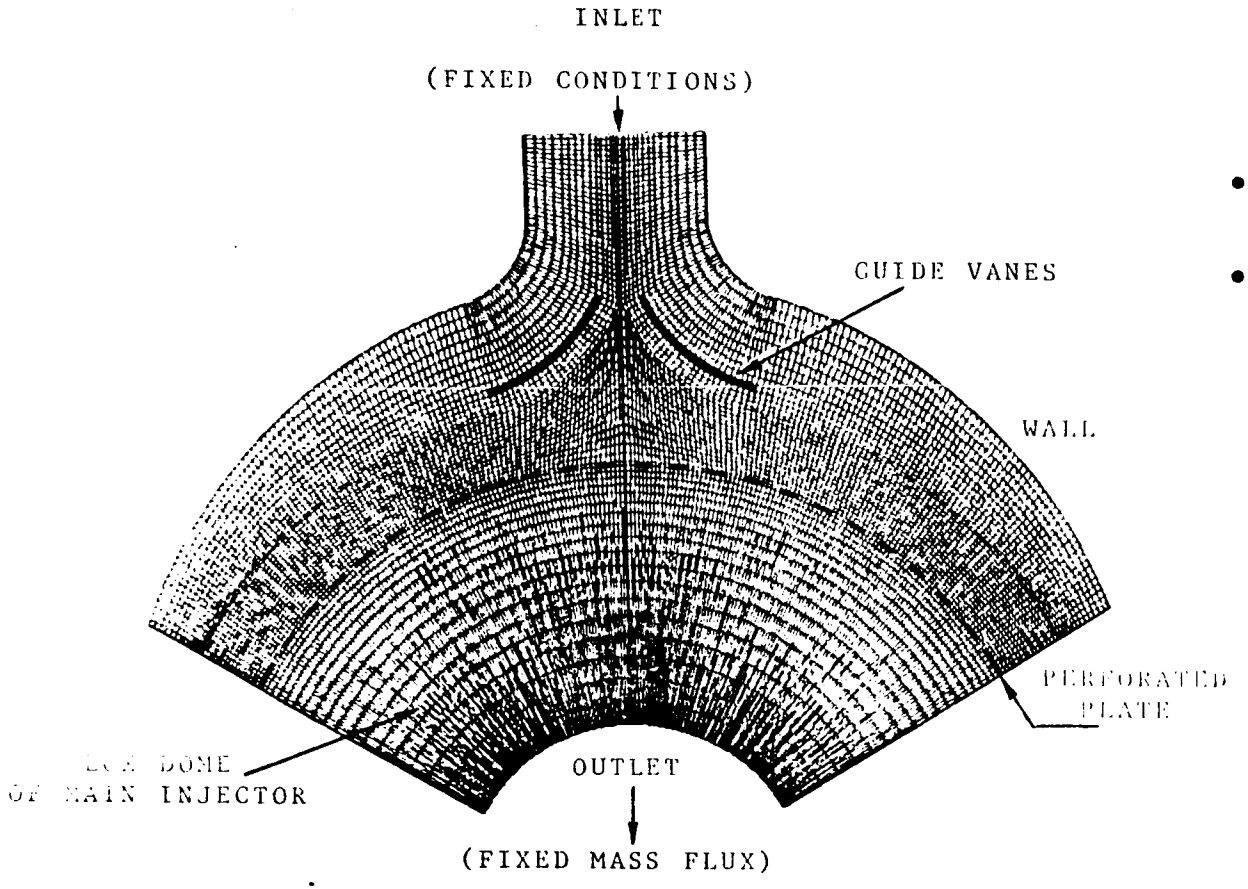

- TOTAL NUMBER OF NODES = 10,000
- INLET CONDITIONS:

  Q = 853 lb_m/sec

  ρ = 64.2 lb_m/ft

  P = 4120 psi

  T = 1960 °R

  V = 2428 ft/sec

Continuum, Inc.

GRID LAYOUT AND BOUNDARY CONDITIONS

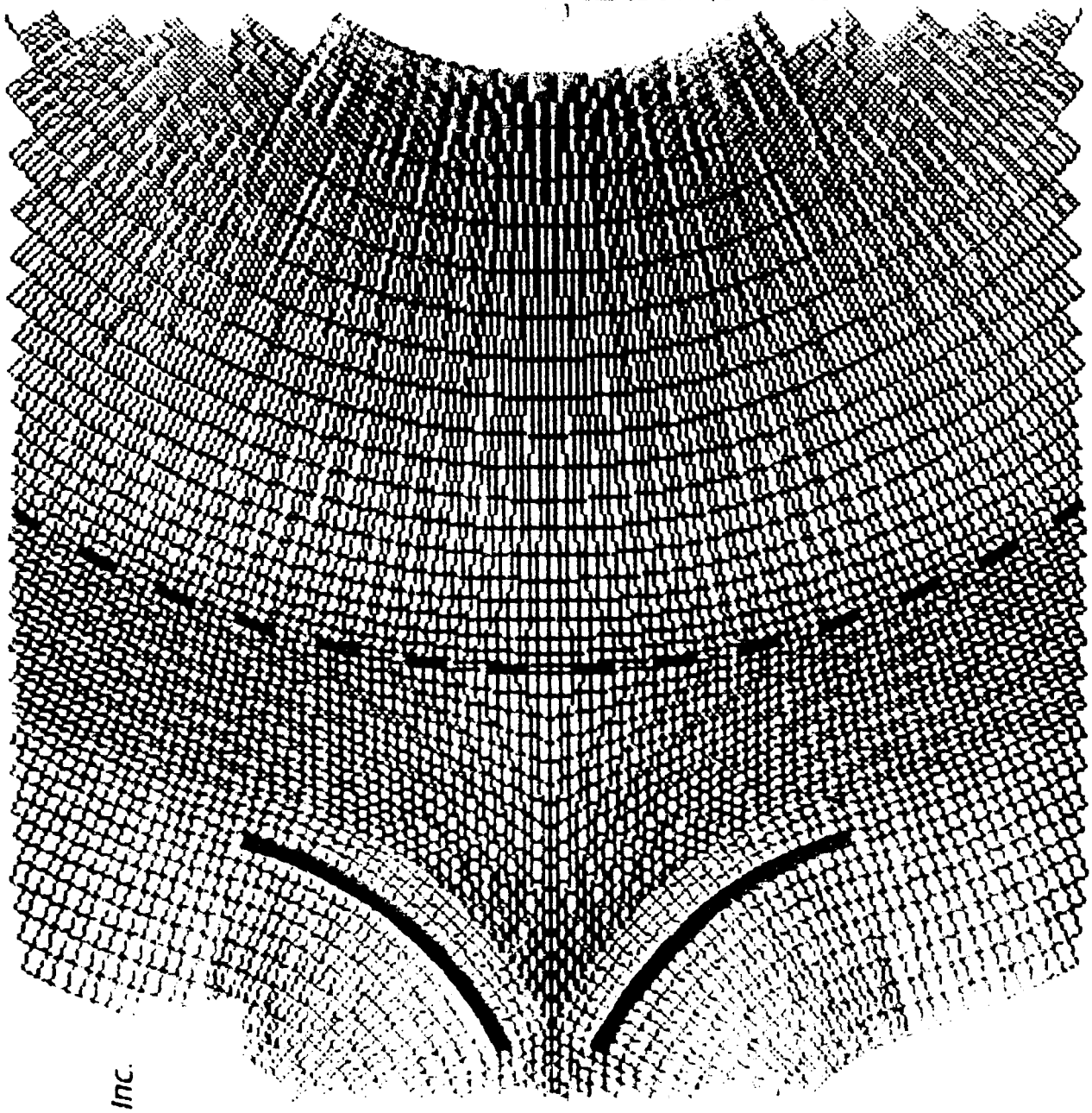

Continuum, Inc.

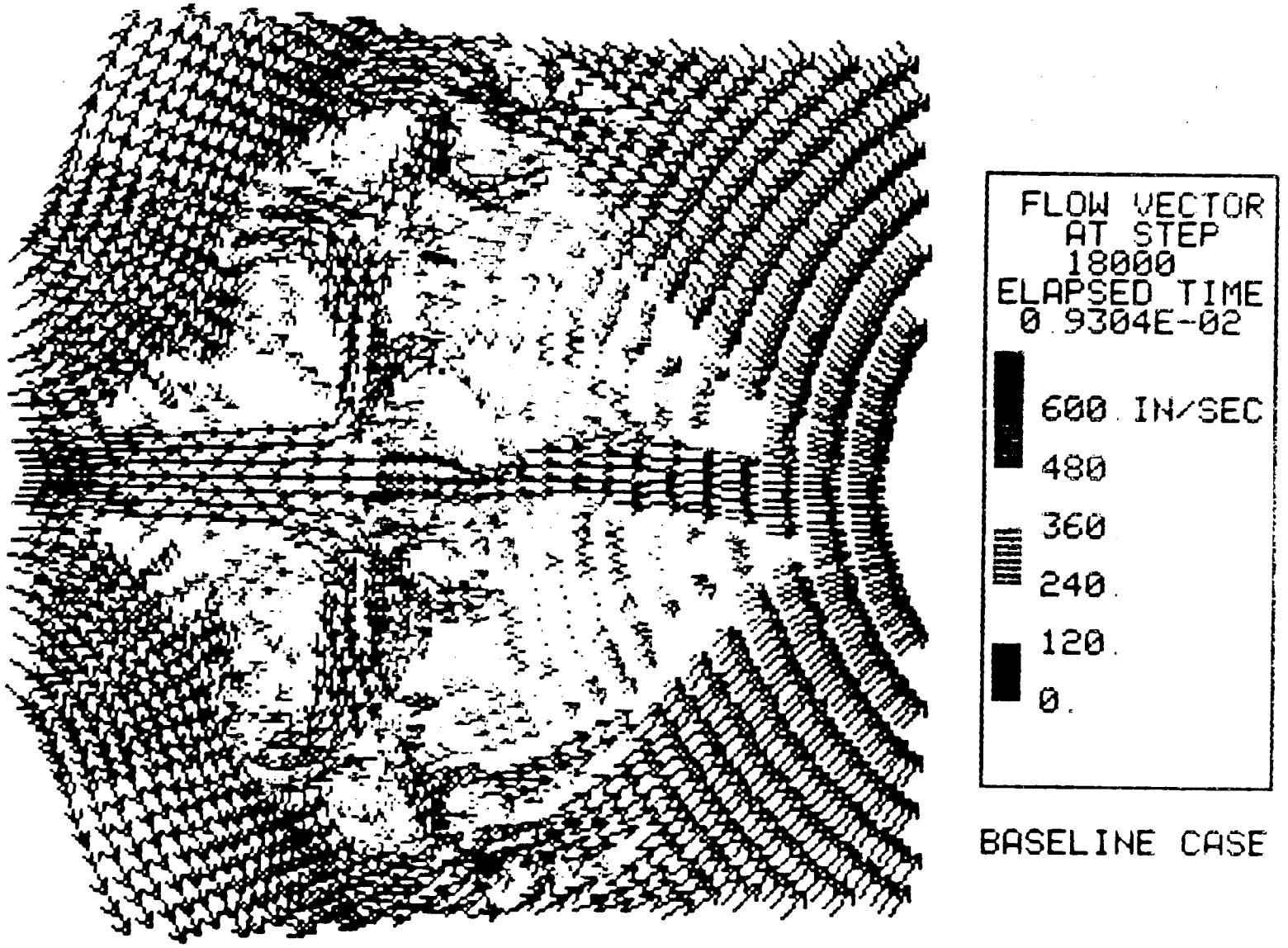

FLOW VECTORS _ BASELINE CASE

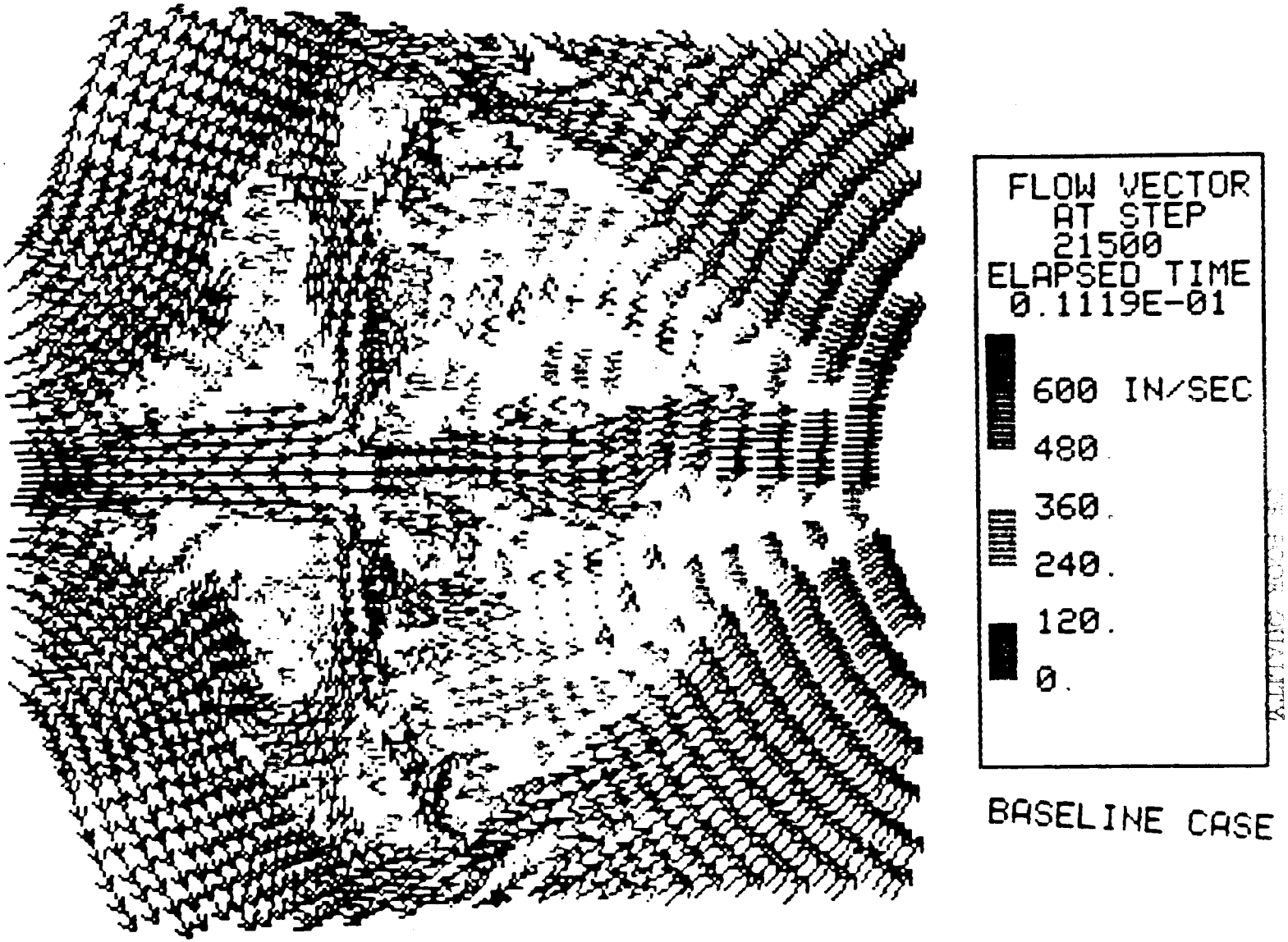

BASELINE CASE

FLOW VECTORS - BASELINE CASE

FLOW VECTOR
AT STEP
26000
ELAPSED TIME
0.98456E-02
600 IN/SEC
480
360
240.
120.
0.
THREE HOLES
IN EACH VANE

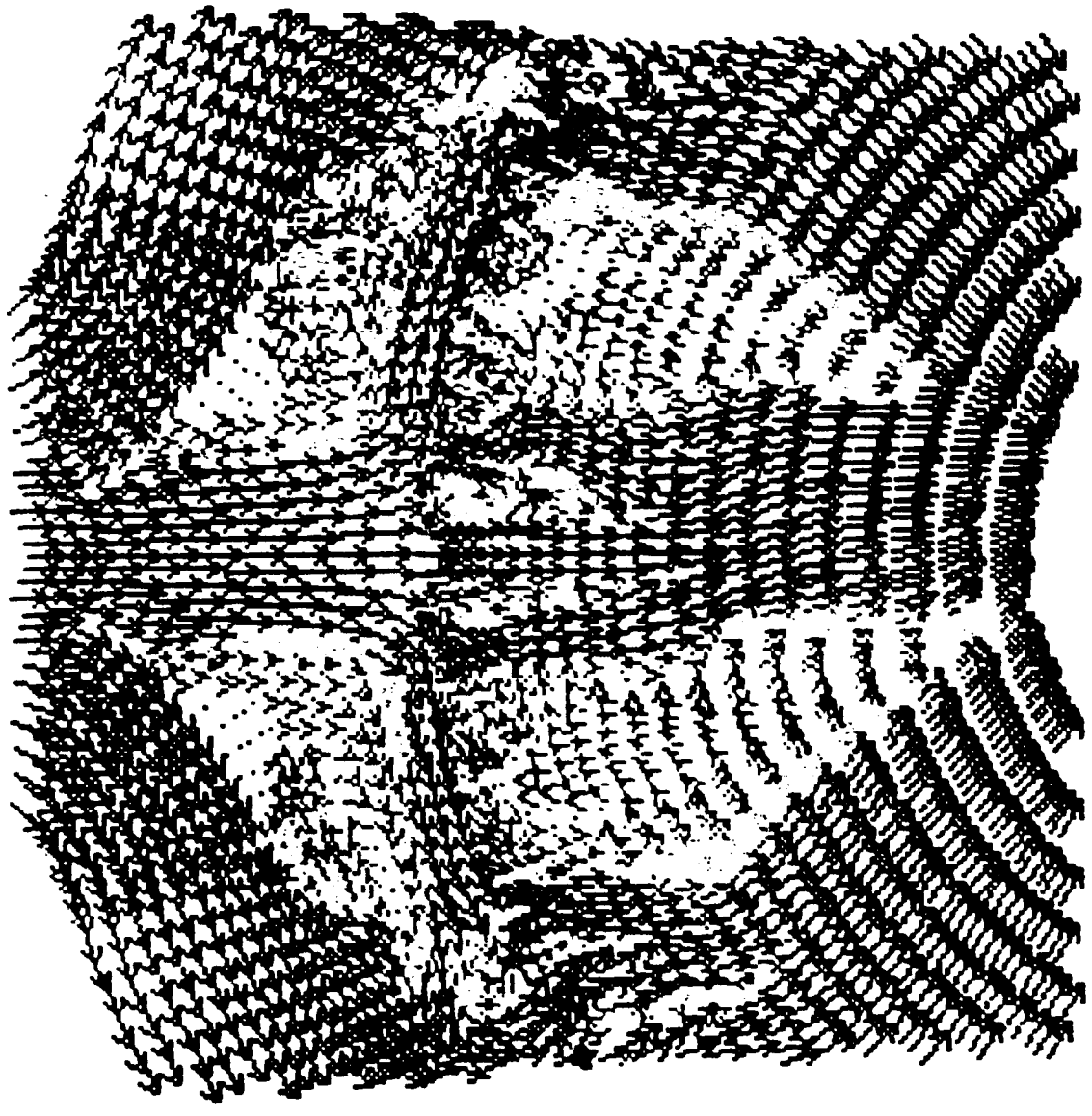

CONTINUUM

FLOW VECTOR
AT STEP
40000
ELAPSED TIME
0.2154E-01

600. IN/SEC
480.
360.
240.
120.
0.

VANES ROTATED
+5 DEGREES

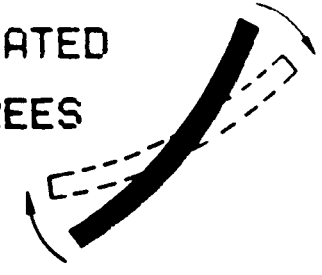

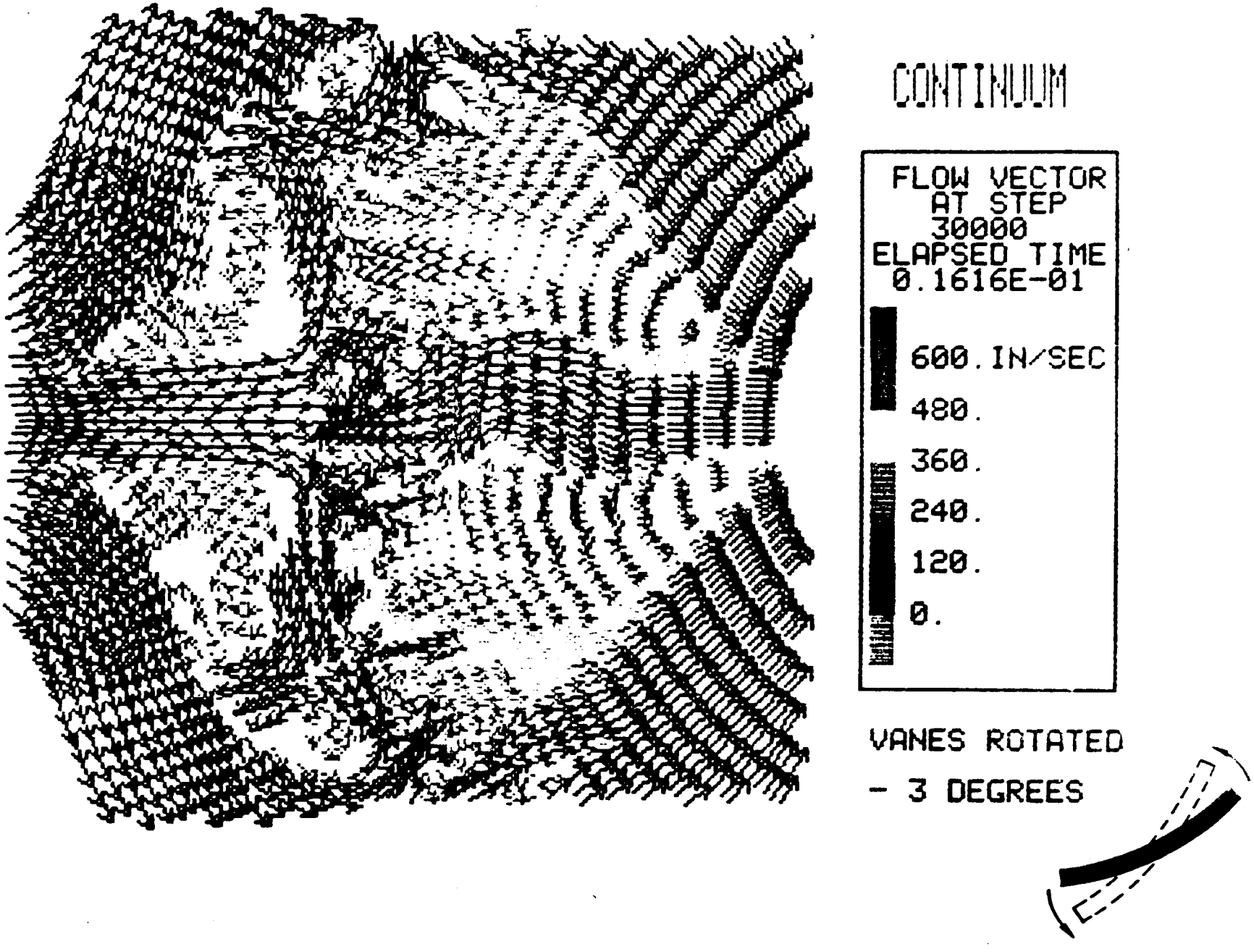
CONTINUUM
FLOW VECTOR
AT STEP
30000
ELAPSED TIME
0.1616E-01
600. IN/SEC
480.
360.
240.
120.
0.
VANES ROTATED
- 3 DEGREES

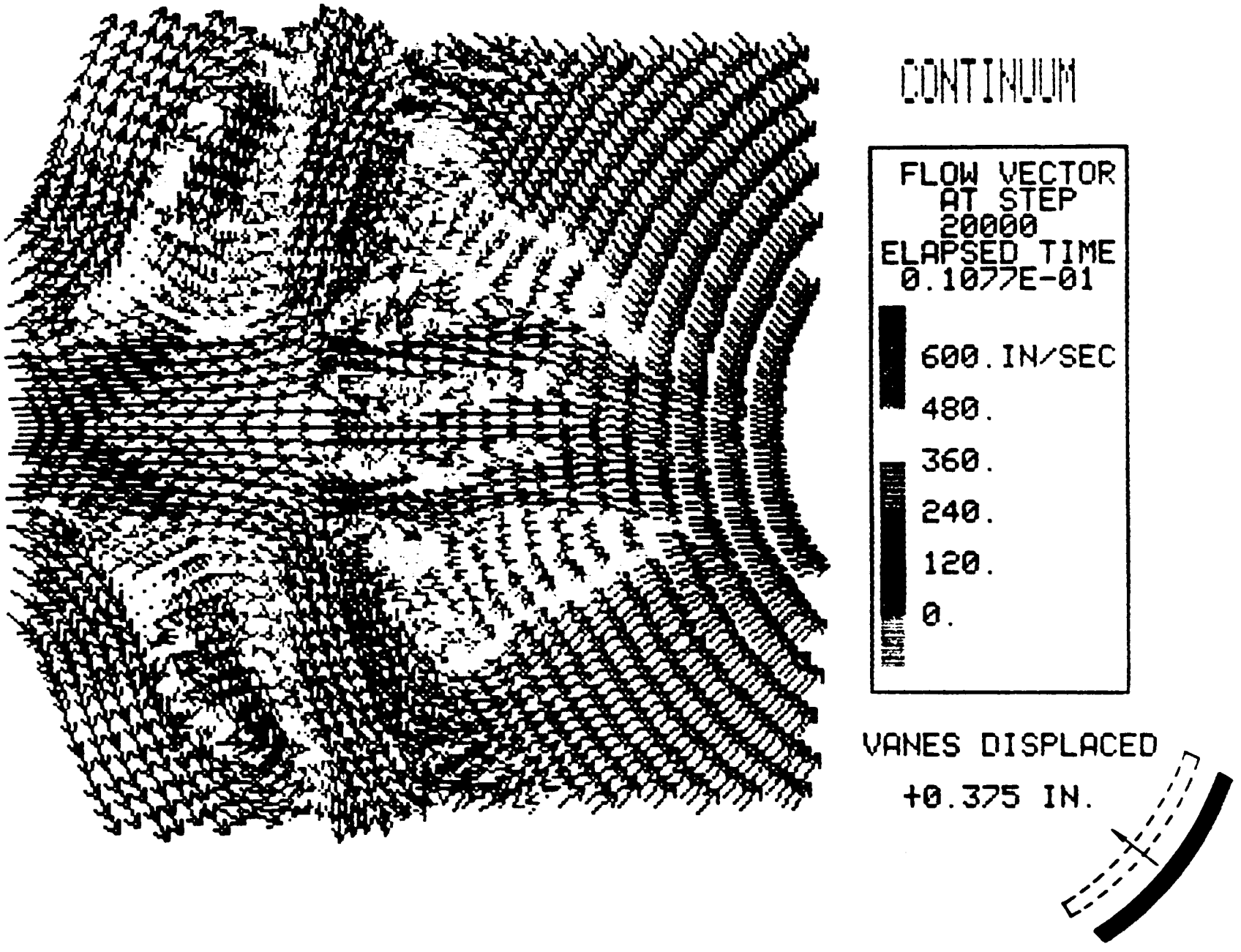
CONTINUUM
FLOW VECTOR
AT STEP
20000
ELAPSED TIME
0.1077E-01
600. IN/SEC
480.
360.
240.
120.
0.
VANES DISPLACED
+0.375 IN.

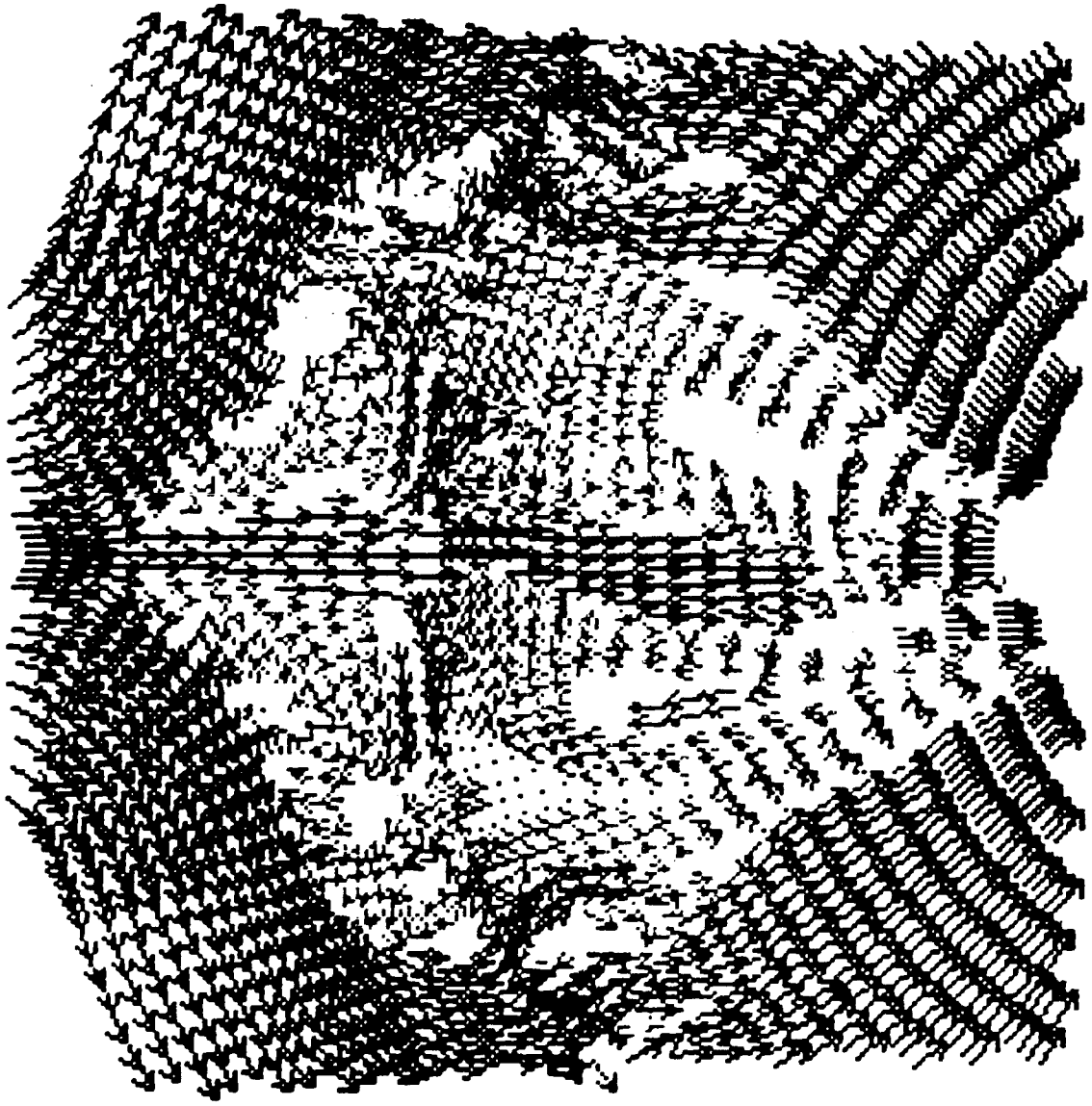

CONTINUUM

FLOW VECTOR
AT STEP
30000
ELAPSED TIME
0.1615E-01

600. IN/SEC
480.
360.
240.
120.
0.

VANES DISPLACED
-0.125 IN.

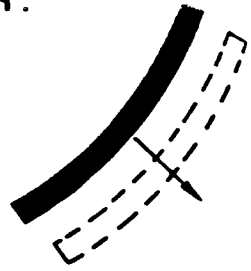

EXPERIMENTAL VERIFICATION (ROCKWELL INTERNATIONAL)

RESULTS

- TWO STRONG EDDIES BEHIND EACH VANE
- TWO LARGE CIRCULATION AREAS BEHIND THE INJECTOR PLATE
- STRONG CENTRAL STREAM WHICH MAY BE A SOURCE OF VIBRATION IN THE LOX DOME
- GOOD AGREEMENT WITH TEST DATA
- DATA PROVIDED FOR FLUTTER ANALYSIS

APPENDIX G

TWO-DIMENSIONAL FLAME TRENCH SIMULATION DURING ENGINE SHUT OFF

T. S. WANG

CONTINUUM, INC.

HELEN MCCONNAUGHEY

NASA/MSFC

APRIL 11, 1986

OBJECTIVES

- TO SIMULATE THE VAFB FLAME TRENCH FLOWFIELD DURING A SSME ENGINE SHUT DOWN
- TO ESTIMATE THE AMOUNT OF HYDROGEN AND AIR WHICH COULD BE TRAPPED IN THE TRENCH
- TO ASSESS THE POTENTIAL OF HAZARDOUS ENGINE CUT OFF

APPROACH

- THE PLUME WAS ALLOWED TO FLOW INTO THE TRENCH FOR ONE SECOND WITH A 34 KNOTS WIND BLEW FROM THE RIGHT HAND SIDE
- THE PLUME WAS THEN TURNED OFF TO ALLOW HYDROGEN TO BLEED FOR ANOTHER 1.5 SECONDS

FLOW VECTOR IN THE FLAME TRENCH

121

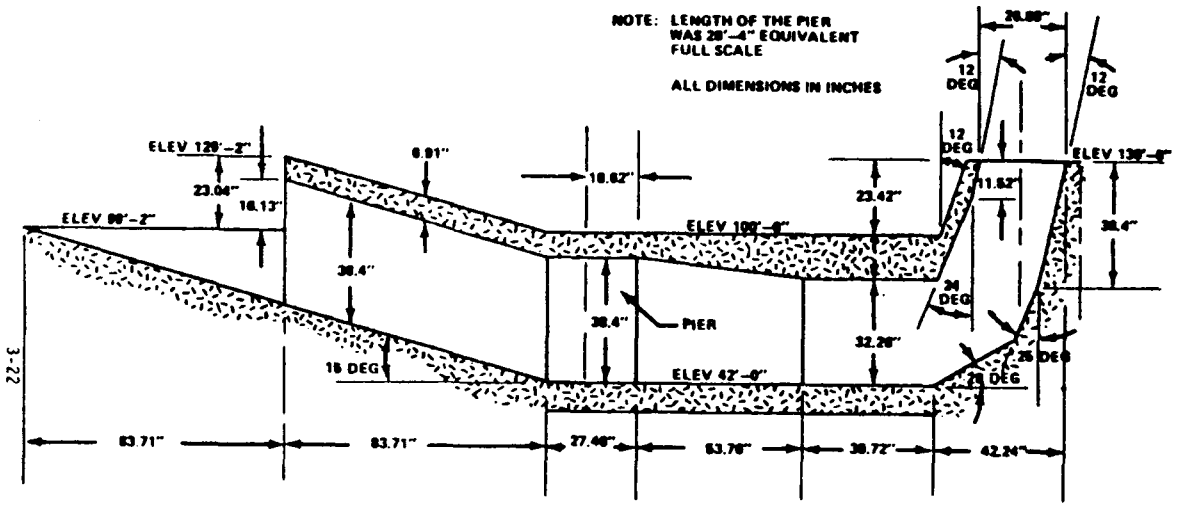

a. DUCT ELEVATION
FIGURE 3.4-4 MODEL SSME EXHAUST
PRESENT DUCT CONFIGURATION

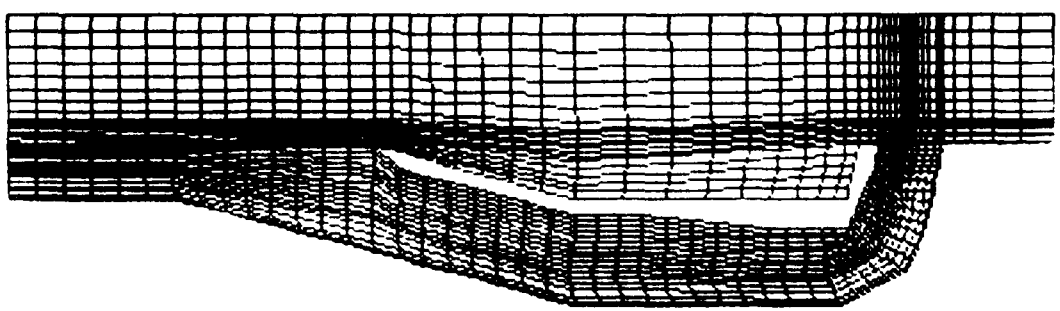

2D FLAME TRENCH GRID DEFINITION

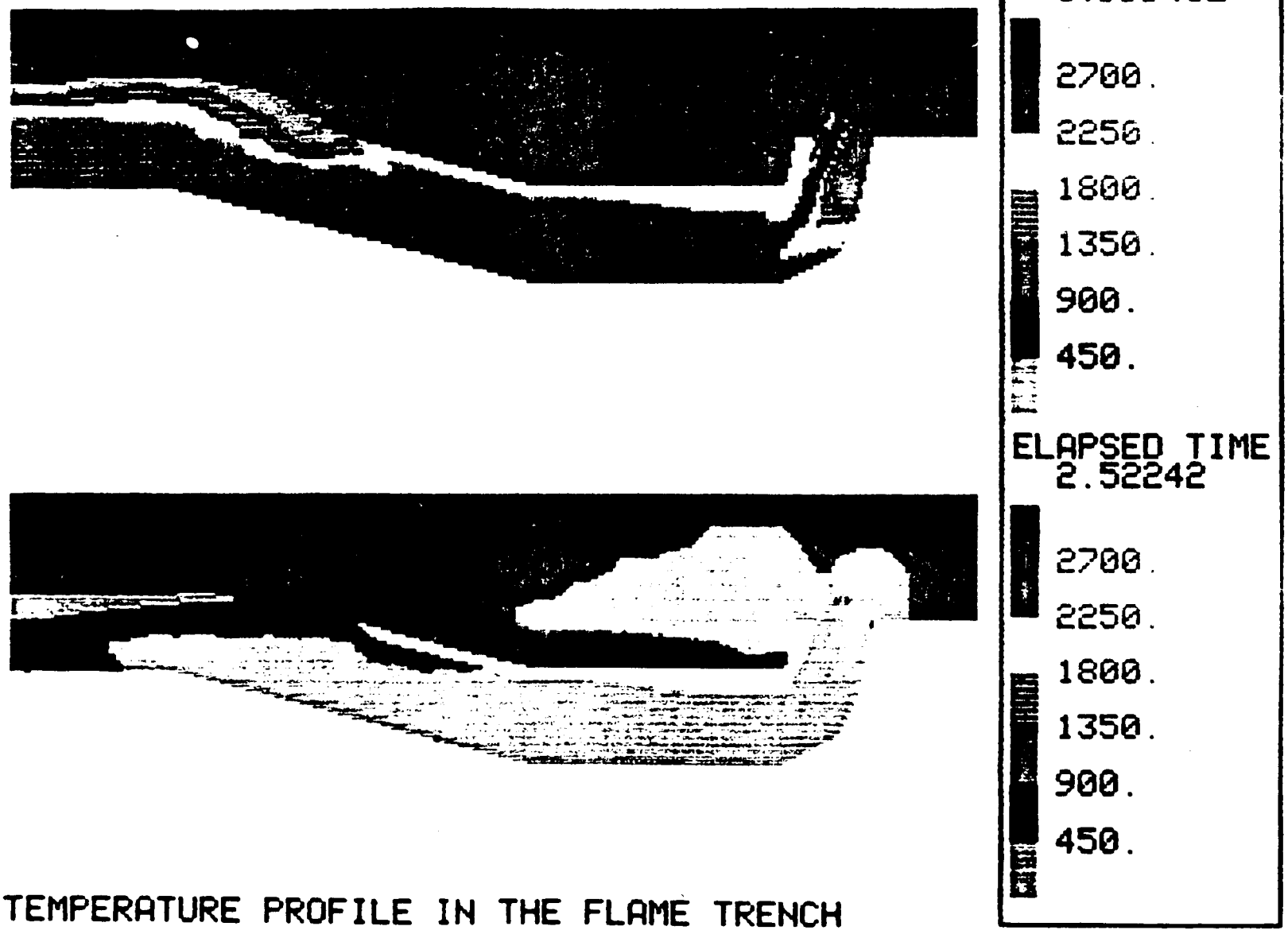

TEMPERATURE PROFILE IN THE FLAME TRENCH

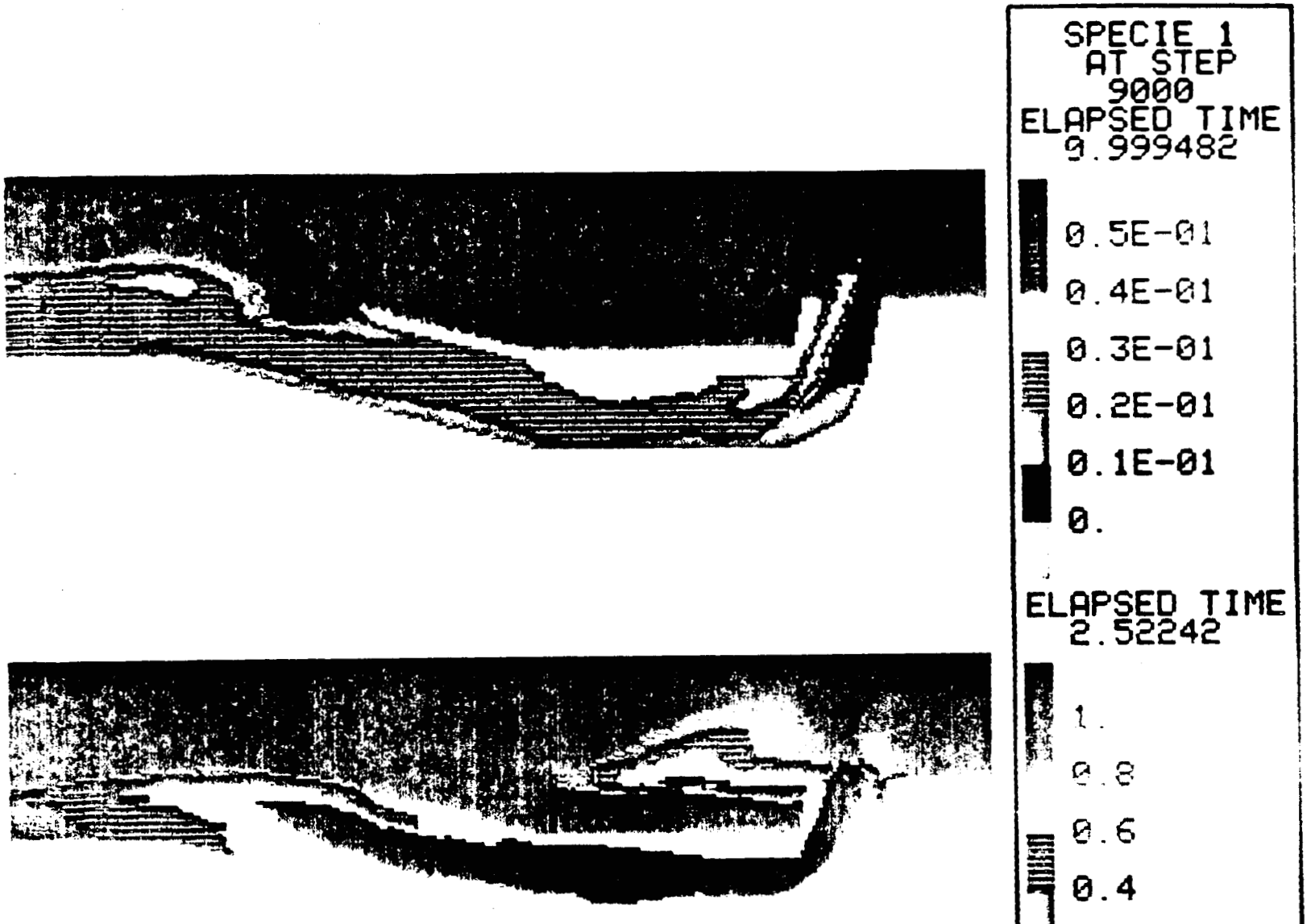

H2 MASS FRACTION PROFILE IN THE FLAME TRENCH

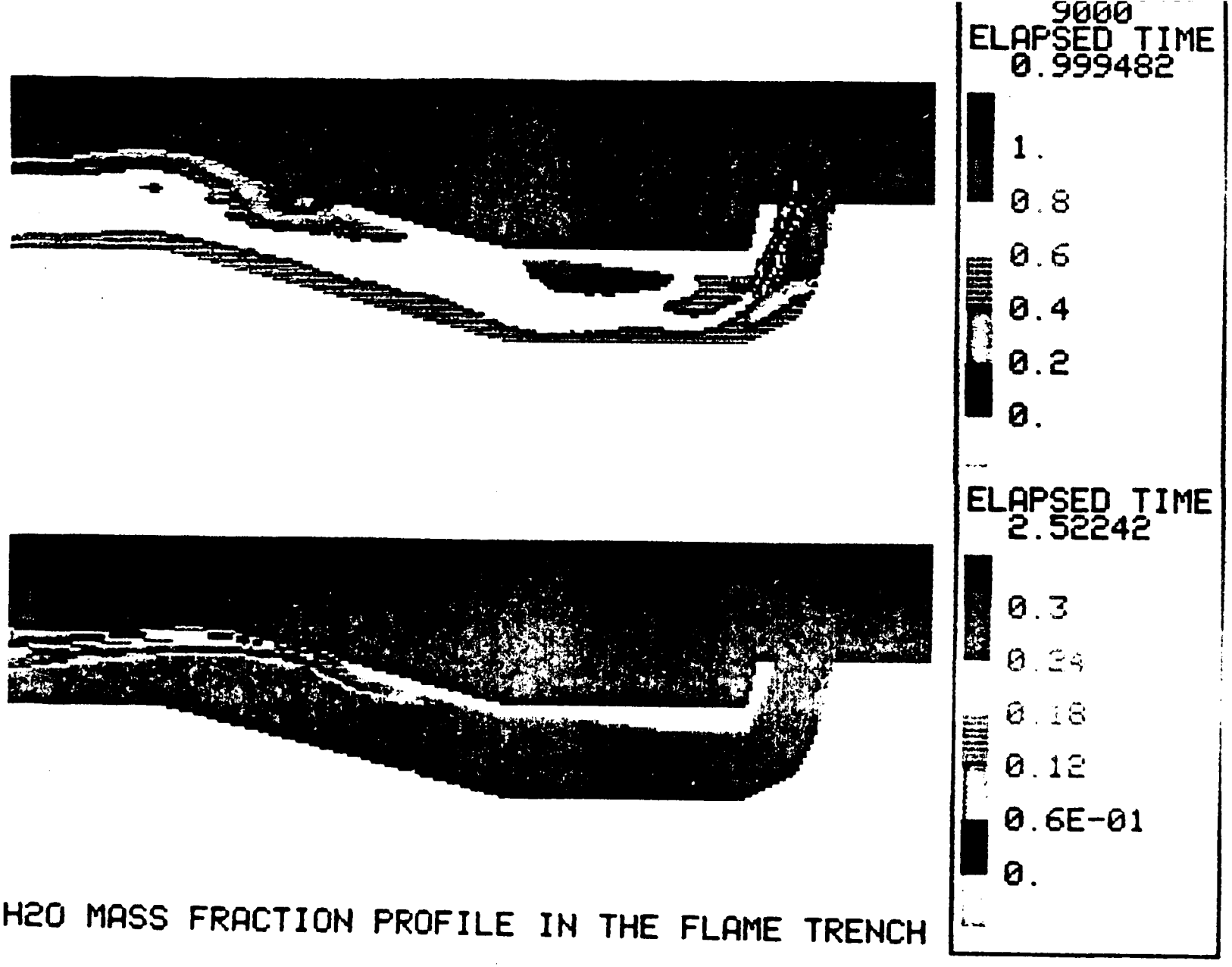

H2O MASS FRACTION PROFILE IN THE FLAME TRENCH

AIR MASS FRACTION PROFILE IN THE FLAME TRENCH

RESULTS

- THERE IS ENOUGH HYDROGEN AND AIR TRAPPED IN THE TRENCH DURING 2.5 SECONDS ENGINE CUT OFF TO POSE A PROBLEM
- THE ENTRAPPED HYDROGEN AND AIR COULD EXPLODE PROVIDED THERE IS AN IGNITION SOURCE

CONCLUSION

- A 3D SIMULATION IS RECOMMENDED FOR MORE ACCURATE ASSESSMENT. IF MORE DEFINITE MEASURES LIKE REMOVING THE DUCT COVER ARE NOT EMPLOYED